Design of Electromyogram and Electrocardiogram Acquisition Systems

A Major Qualifying Project submitted to the Faculty of WORCESTER POLYTECHNIC INSTITUTE in partial fulfillment of the requirements for the Degree of Bachelor of Science

Submitted by:
Khadijah Ibrahim
Athina Katsoula
Alexandra Meraz
Nghia Nguyen Trong

Advised by: Professor Edward A. Clancy

March 2021

Acknowledgements

We would like to thank the following individuals for their contributions towards our project's success: Professor Edward Clancy, He Wang, Jianan Li, and Ziling Zhu.

We would like to thank He Wang for his valuable input regarding the algorithms and for developing the code used for the TI microcontrollers and for spending time debugging the system.

Jianin Li and Ziling Zhu's contributions helped connect the wired EMG system to a prosthetic hand-wirst system that allowed us to control the hand and record valuable footage of a working device.

Lastly, we would like to thank Professor Clancy, our MQP advisor, for his guidance and support in all aspects of the project including components, technical explanations, understanding EMG and ECG, MATLAB functions, and other resources that helped develop the project.

Abstract

This report focuses on the design and implementation of both wired and wireless systems to detect and analyze electromyography (EMG) and electrocardiogram (ECG) signals. The wired and wireless EMG systems were connected to a set of electrodes enclosures. The input signal is then processed through the front end of the system where it is amplified with a 50 V/V gain. The front end also delivers a common mode rejection ratio (CMRR) of 80–100 dB at 60 Hz, and 1 uV(rms) of noise over the passband. Similarly, the wireless ECG system followed the same design approach but had a gain of 25.7 V/V. The signal for the wired and wireless EMG is filtered at a passband of 15 - 800 Hz. The wireless ECG signal is filtered at a passband of 0.5 – 100 Hz. The wired EMG signal is connected to an ADC module through a USB communication cable. The wireless EMG and ECG systems transfer the signal data via Bluetooth LE using two microcontrollers that serve as an ADC module and Bluetooth central and peripheral devices. Using MATLAB, the signal data is then evaluated and utilized for other applications.

Table of Contributions

Section Title	Primary Author(s)	Primary Editor(s)
Abstract	Khadijah Ibrahim	Alexandra Meraz
Executive Summary	Khadijah Ibrahim, Athina Katsoula, Alexandra Meraz	All
Introduction	Nghia Nguyen	All
Background	Nghia Nguyen	All
EMG	Alexandra Meraz	All
ECG	Khadijah Ibrahim	All
Measuring of ECG and EMG Systems	Athina Katsoula	All
Front End Analog Design		All
Differential and Instrumentation Amplifier	Nghia Nguyen	All
Band-Pass and Band-Reject Filters	Nghia Nguyen	All
Design Options	Athina Katsoula	All
System Requirements and Design Goals	Nghia Nguyen	All
Design Specifications	Khadijah Ibrahim	All
Wired System	Khadijah Ibrahim	All
Design Option 1	Khadijah Ibrahim	All
Design Option 2	Khadijah Ibrahim	All
Design Option 3	Khadijah Ibrahim	All

ADC	Khadijah Ibrahim	All
Wireless System	Athina Katsoula, Alexandra Meraz	
Final Design		
Wired	Khadijah Ibrahim	Nghia Nguyen
Wireless	Alexandra Meraz	Athina Katsoula
Design Implementation		
Wired Electromyogram System		
Filter Design	Nghia Nguyen	Khadijah Ibrahim
Selectable Gain	Nghia Nguyen	Khadijah Ibrahim
ADC Power Configurations	Khadijah Ibrahim	Nghia Nguyen
System PCB Implementation	Khadijah Ibrahim	Nghia Nguyen
Component Selection	Khadijah Ibrahim	Nghia Nguyen
PCB Layout and Fabrication	Nghia Nguyen	Khadijah Ibrahim
PCB Assembling and Testing	Nghia Nguyen	Khadijah Ibrahim
Wireless Electromyogram System	Alexandra Meraz	Athina Katsoula
Wireless Electrocardiogram System	Athina Katsoula	Alexandra Meraz
Discussion	Khadijah Ibrahim, Athina Katsoula, Alexandra Meraz	All
Conclusion	Alexandra Meraz	All
Appendix A	All	All

Appendix B	All	All
Appendix C	All	All
Appendix D	Khadijah Ibrahim	All
Appendix E	Athina Katsoula	All

Executive Summary

The study of biopotential signals produced by the human body is crucial for the development and progression of medicine in addition to technological advancement in healthcare. Electromyography (EMG) and electrocardiography (ECG) are diagnostic procedures widely used to assess the health of skeletal muscles and the heart, respectively. In our advancing world, these assessments can provide information for countless conditions which can later be investigated further or treated. In addition, the study of these signals contributes to the development of technical and mechanical artificial devices that can provide patients with support and an enhanced experience. Specifically, an EMG signal is a valuable resource for controlling a prosthetic device which can allow an amputee to move their artificial parts according to remnant muscle contractions. When it comes to an ECG signal, the use and significance of its study is universally known, especially for older adults who are more prone to suffer from cardiovascular diseases. The prevention and control of such problems can be easier if the patient has access to physiological monitoring devices that are easy to use and able to measure and process these signals offering some information in accordance with the measurements.

Due to the benefits of these biopotential signals, the focus of our MQP project was the design and implementation of three wired and wireless devices that measure ECG and EMG signals. The analog circuit design of the front end of the systems that acquire these data, is similar for both EMG and ECG. The frequency range that the ECG signal can be recorded is 0.05 Hz to 150 Hz and 15 Hz to 800 Hz is the range for acquiring EMG signals. The acquisition systems for these biopotential signals typically use three electrodes attached to the patient's body to minimize noise. However, a much simpler implementation using two electrodes is possible for certain less complex and non-medical devices. For this project, one wired EMG device was designed using a three-electrode input, and two wireless devices for EMG and ECG were also implemented.

The wired system had three different design options that were all centered around different ADC modules that could be used. The three options consisted of using an ADC for each channel, one PC-based ADC for all channels, or based on an IC system-on-a-chip (ADS1291). Design options one and two used electronic components the group was familiar with compared to the IC ADS1291 chip, which would involve learning its custom programming language and transmitting

data to a microcontroller. Cost for the PC-based USB ADC modules were more expensive than the IC ADS1291 chip, but easier to function.

For the wireless systems, the main design option faced was microcontroller selection. The two options were the TI CC26X2R1 and the Nordic nRF52832. The substantial difference between those two options was the existing knowledge and framework provided by supporting faculty to this project. Other than that, the two MCUs are comparable in price and function.

The final design for our four-channel wired EMG system consisted of completing the front-end of the system. A set of encased electrode-amplifiers that had instrumentation amplifiers enclosed were provided for testing. The front end began with fourth order Butterworth high-pass and low-pass filters with cut off frequencies of 15 Hz and 800 Hz, respectively. A non-inverting amplifier was placed between the passband filters to construct selectable gain. The selectable gain values are 2, 4, 8, 16, and 32. The output was received at the low-pass filter and connected to an ADC module to digitize the signal. The design was simulated using NI Multisim, tested using a protoboard, and then implemented as a PCB. The PCB design used EAGLE Autodesk. The system is fully powered using an XP Power ECP40UT01 medically isolated power supply. The final test for the wired EMG system resulted in successfully commanding movements of a hand-wrist prosthesis.
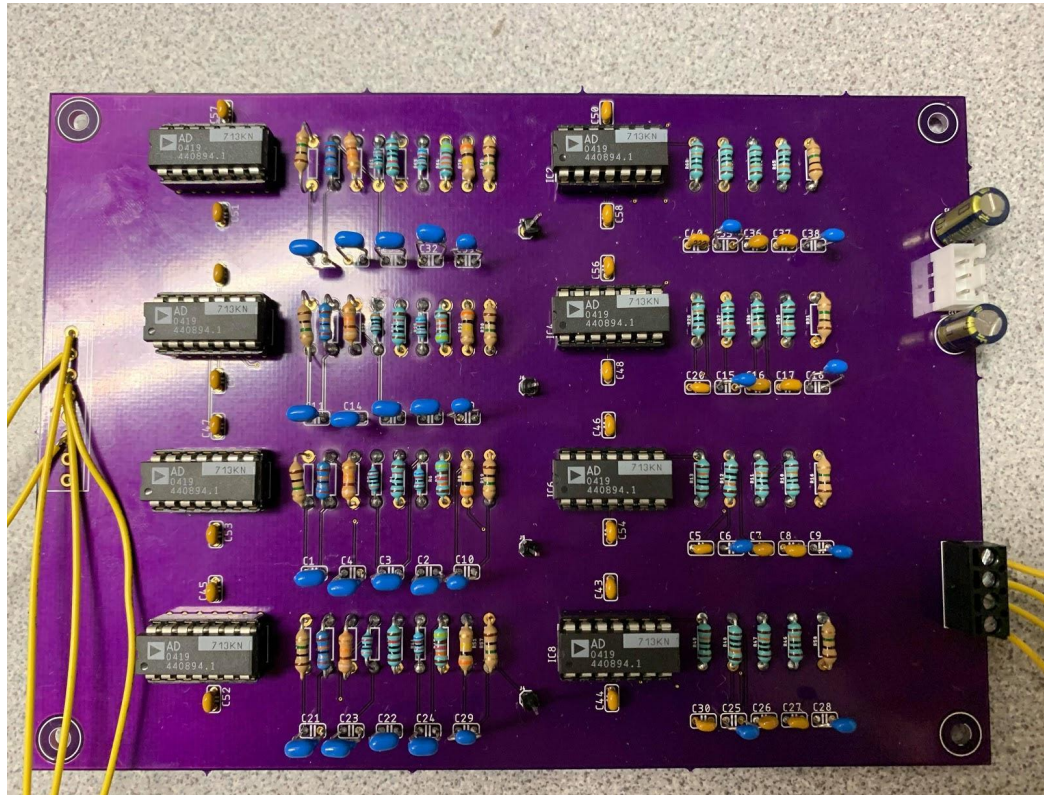
Final PCB design of 4-channel wired EMG system
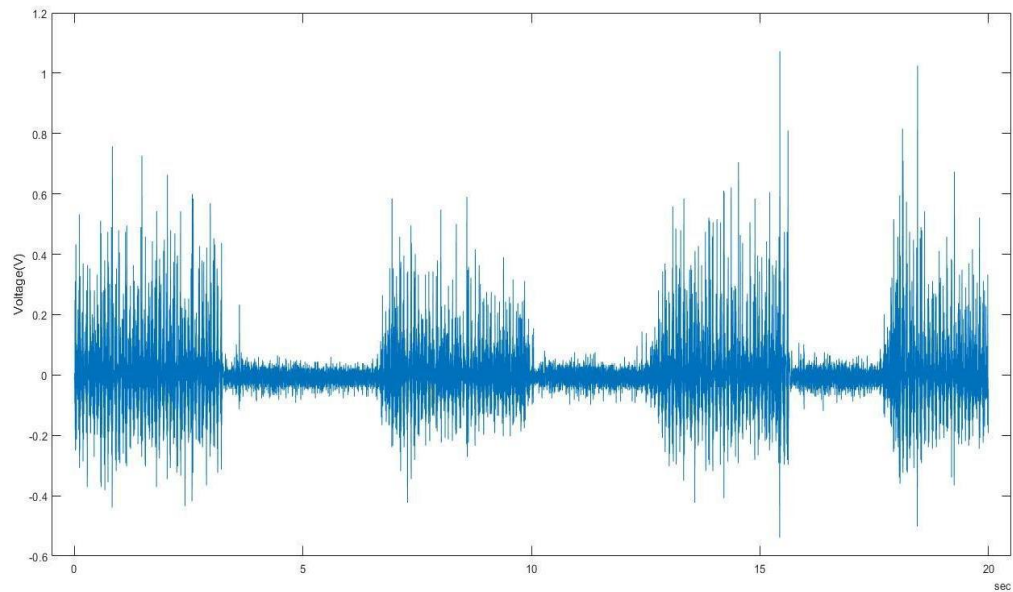
Raw Data collected by channel 1 of wired EMG with a set gain of 8.

The front end of the wireless EMG system consists of the cascade of an instrumentation amplifier, a high pass filter, a selectable gain, a low pass filter, a level shifter, and a microcontroller (MCU, Texas Instruments CCX2R1) with embedded ADC and Bluetooth wireless transmission. The filters are each second-order creating a passband of 15–800 Hz. This design was simulated in NI Multisim, then built on a protoboard once the filters were confirmed to have the necessary passband. A signal was then captured from the protoboard using surface boards attached over the biceps muscles. These acquired data were then sent to a central node via Bluetooth. The central node communicated with a PC via the serial port and those data were displayed in real time in a MATLAB application. The data could be notch filtered in MATLAB, to attenuate power-line noise (60 Hz). When comparing the magnitudes of the signal at varying levels of force, the magnitude was correlated with the strength of the force and confirmed to be an EMG signal.
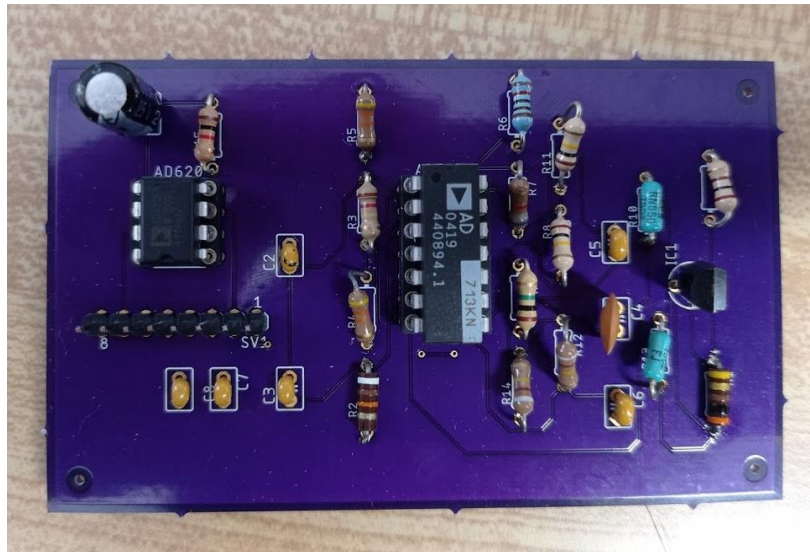
PCB design of wireless EMG system
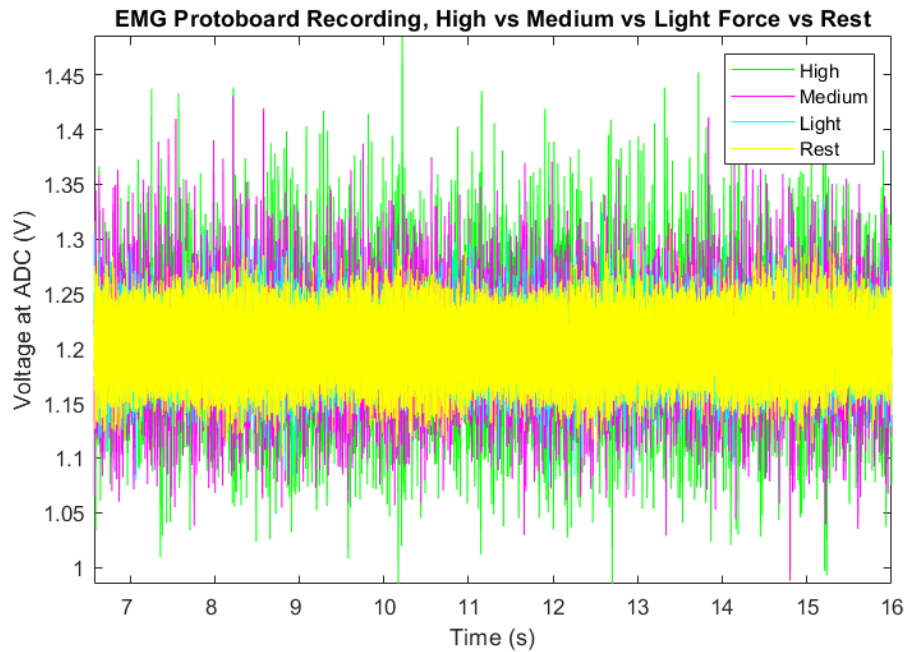
High, Medium, Light, Rest EMG recordings (after notch filtering)

The implementation of the wireless ECG circuit includes the same front end stages as the wireless EMG system mentioned above, with the only difference being the bandwidth of the filters were designed to be from 0.5 Hz to 100 Hz. This system was simulated using Multisim and then built on a breadboard circuit. Testing was performed and data were acquired using the two-electrode design from Lead I placed across a person's chest. Next, once the system's function was verified, we designed, fabricated, assembled and tested a PCB version. Lead I ECG data were agained acquired by attaching two electrodes on the upper right and left side of the chest. The data were wirelessly sent from a peripheral TI CC26X2R1 to a central one and displayed on a PC using our graphical user interface. Later, signal processing was required for filtering the power line noise to clearly graph the ECG signal collected.
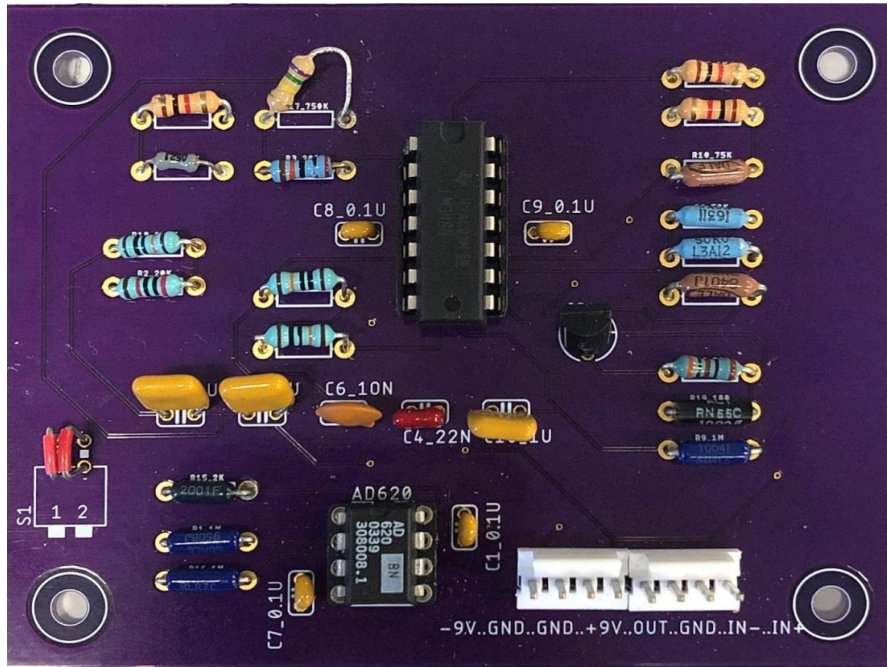
The finished PCB for the ECG Wireless Circuit
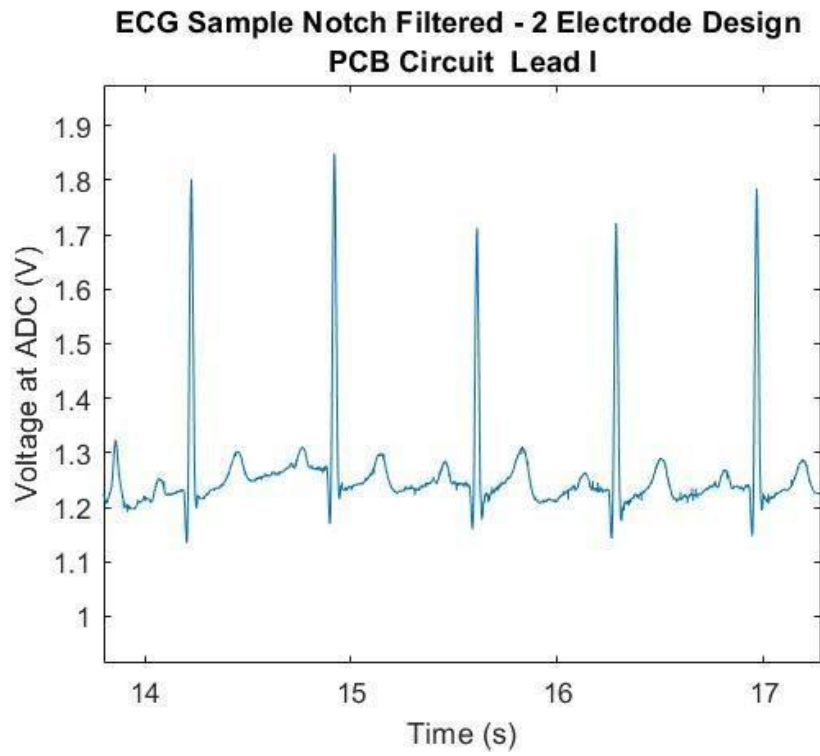
Wireless ECG Sample Notch Filtered- 2 Electrode Design PCB Circuit Lead I

Ultimately, the goals of this report for both the wired and wireless portions were accomplished. This project was able to deliver the design and prototype for a wired EMG system, a wireless EMG system, and wireless ECG systems. In addition, successful PCBs were designed and printed for the wired EMG and wireless ECG systems. Moreover, a successful transmission of data between a peripheral and central node was implemented for each wireless system. This data transmission can be displayed in real time using MATLAB. These deliverables were made possible through research and design based on design specifications laid out early in the project.

Contents

List of Figures

17

19

List of Tables

1 Introduction

The human body is composed of many complex systems, and some systems produce electrical activity that can be measured and used to diagnose diseases. Electromyography (EMG) and electrocardiography (ECG) are procedures that are widely used to measure the electrical activity of a person's skeletal muscles and heart, respectively. A clinical EMG test is conducted by attaching electrodes over or onto the subject's muscles. Then, the electrical activity of the muscles is monitored during muscle contraction and muscle rest. EMG is also used by rehabilitation and assistive devices and in research studies. The main difference between the ECG and EMG systems is the placement of the electrodes, with the electrodes placed near the heart for accurate ECG measurements. From the recording, the subject's heart rate is measured, and abnormal activity of the heart can also be identified. The goal of this project was to design ECG and EMG signal acquisition systems that are compact and precise.

2 Background

This chapter focuses on background information gathered through existing literature in order to understand how the signals being measured are produced by the body, measured by a system, and conditioned as a signal to be useful.

2.1 EMG

Electromyography (EMG) is a tool that detects, analyzes, and utilizes electrical signals from skeletal muscles, also known as myoelectric signals. EMG boasts many applications such as assessing and diagnosing movement and controlling prostheses. The muscles associated with movement are called skeletal muscles because they attach to the skeleton with tendons and pull on bones as they contract. For movement to occur, a signal is sent by the central nervous system to the group of muscles required for the specific movement. Each muscle fiber contracts as the action potential causes the resting potential to change from around -85 mV to about 30 mV. As the muscle fibers contract, the muscle itself contracts and pulls on the bone it is attached to, creating tension and movement. The EMG measures the electrical excitation of the muscle fibers. (Weiss et al. 2015)

Myoelectric signals can be detected by electrodes placed on the skin (surface electrodes) or inserted into muscle tissue (needle or wire electrodes). If used for prosthesis control, user comfort becomes a major factor in development. Therefore, surface electrodes are often used for this application because they are noninvasive and easy to use. Moreover, ASET — The Neurodiagnostic Society — suggests that needle electrodes are better suited to clinical and surgical settings. An EMG using needle electrodes meets the definition of an invasive procedure, where proper training and diligence with regard to electrical safety and infection control are recommended. (ASET - The Neurodiagnostic Society, 1997)

When measuring the signal, greater force generated by muscles is correlated with a higher EMG signal, because more motor units are activated. Motor units are bundles of myofibrils which contain muscle fibers and are interconnected with a shared motor nerve "input." The electrode should be placed between the innervation zone (or motor point) and the tendinous insertion (or belly of the muscle). This achieves an improved superimposed signal (Jamal, 2012). The motor

unit action potentials (MUAP) that are detectable under the electrode site are electrically superimposed. MUAP signals are observed as bipolar with a symmetric distribution of positive and negative amplitudes. These signals combine to form the interference pattern. Moreover, the firing frequency and recruitment of MUAPS are two important mechanisms that influence the magnitude and density of the observed EMG signal. Figure 2.1 below shows how individual motor units superimpose into the surface signal (Konrad, 2005). Each pulse in the first four signals in Figure 2.1 indicates the activation of the corresponding motor unit (MU). The first four signals are then superimposed which is shown as the fifth signal in Figure 2.1. An active unit continues firing at a random time interval. This final signal is the surface EMG or "interference pattern" which measures the sum of many MUs near the electrode pair.
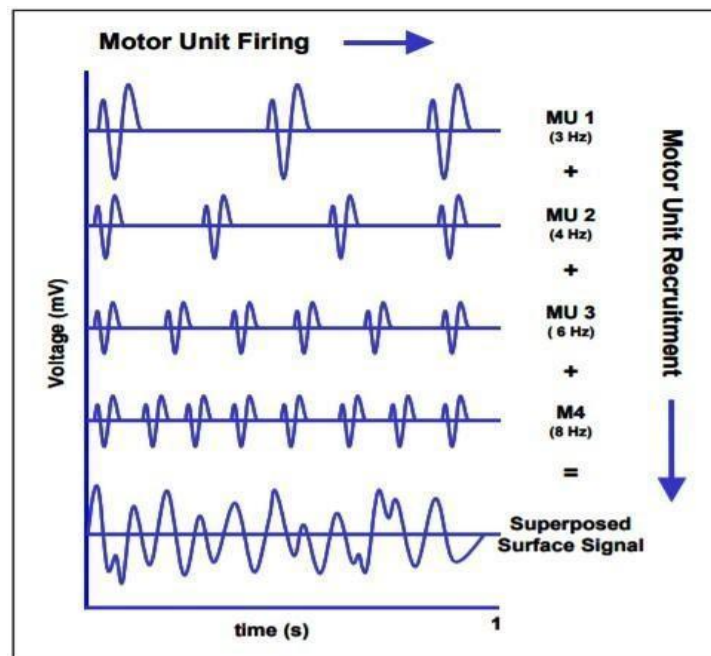
Figure 2.1: Demonstration of superimposed signal from various motor units (Konrad 2005)

An example of a raw EMG recording is shown below. The signal is mostly unfiltered, with the exception that it has been put through an amplifier bandpass. The recording shows three static contractions of the biceps brachii muscle (Konrad, 2005).
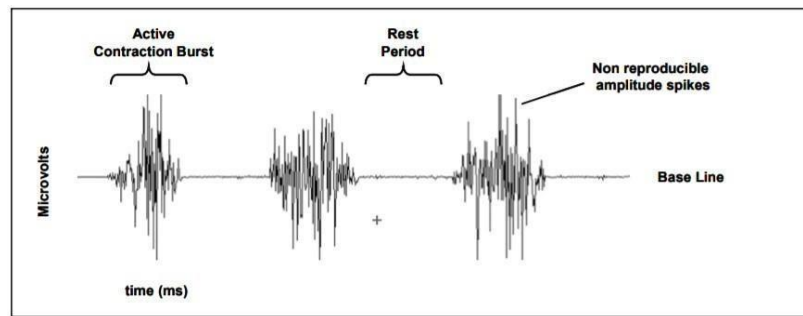
Figure 2.2: Raw ECG Recording (Konrad 2005)

2.1.1 EMG Signal Characteristics

To successfully utilize the signal achieved at the surface, also known as surface EMG or sEMG, the following are a few useful properties to know. An EMG signal amplitude is between 1-10 mV peak. Most of the EMG signal power occurs between 0-500 Hz, with the most dominant information located in between 50-150 Hz. There can be useful information located in frequencies over 1000 Hz. Moreover, the signal is highly influenced by noise. Most notable is the 50-60 Hz noise from electromagnetic radiation and 0-20 Hz of noise coming from the instability of the electrode skin interface and motion artifact. (Jamal, 2012)

Tissue characteristics of the human body vary from subject to subject, within the same subject, tissue type, thickness, and due to physiological changes. Physiological crosstalk can come from neighboring muscles. Crosstalk is a disturbance in an EMG, recorded over one muscle channel caused by the electric or magnetic fields of an adjacent muscle. The "crosstalk" does not typically exceed 10-15% of the overall signal contents or is not available at all. Certain muscle measurements are more susceptible to crosstalk. There are changes in the geometry between muscle belly and electrode site that come from dynamic movement. External noise can come from many electrical environments, but power hum (often produced by incorrect grounding of other external devices) is the most demanding direct interference. Electrodes and internal amplifier noise may add signal contents to the EMG baseline. Though some of the interference can be minimized during the preparation and execution of the EMG procedure, the signal will have to be conditioned which is explained in section 2.4. (Konrad, 2005)

2.2 ECG

An electrocardiogram, or ECG, is the measurement of electrical impulses throughout the heart as it contracts and relaxes. The electrical signals can be measured internally or with electrodes placed on the skin. Placement of these electrodes determines the specific view of the electrical impulses produced. An ECG allows us to analyze heart rate, rhythm, myocardial infarction and abnormalities of the heart.

The center of the cardiovascular system is the heart. Blood flows in a continuous cycle at the right atrium and goes across the tricuspid valve to the right ventricle. The blood is then pumped across the pulmonary valve and into the pulmonary arteries. The pulmonary arteries distribute the blood to the lungs to reduce the carbon dioxide and increase the oxygen. Once oxygenated, the blood goes into the pulmonary veins which conducts blood to the left atrium and pumps blood into the left ventricle. The left ventricle pumps the blood across and through the aortic valve into the aorta where it is pumped throughout the entire body. The gross anatomy of the heart is depicted in Figure 2.3 (Reisner, 2007).
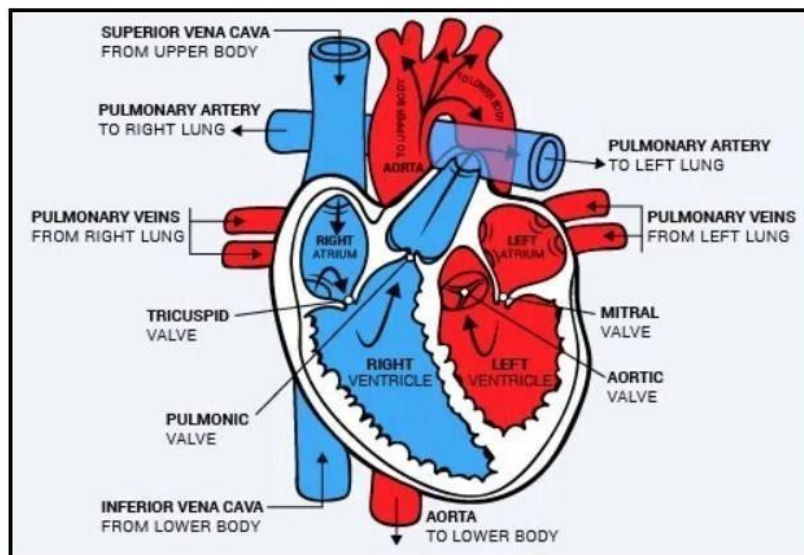
Figure 2.3: The gross anatomy of the heart (Davis, 2020).

In addition to pumping blood throughout the body, the heart also conducts electrical signals. The sinoatrial, or SA node, is the dominant pacemaker of the heart starting the process of producing a beat by causing the atrial muscle to excite electrically and then contract. The electrical

excitation travels to the atrioventricular node (AV). The AV node slows the electrical conduction to create a slight delay before electrical impulses are carried to the ventricles.

The Bundle of His fibers extend from the AV node to transmit impulses to the bundle branches divided into left and right branches. The left bundle branch conducts electrical impulse to the left ventricle. The right bundle branch conducts electrical impulses to the right ventricle. The Purkinje system spreads electrical impulses rapidly throughout the ventricle walls, causing the ventricle to contract. The electrical signal produced can then be seen with leads that can display the resulting signal of an ECG. (Jones, 2009).

- ### 2.2.1 ECG Signal Characteristics

An ECG allows you to record the heart's electrical activity from a specific view called a lead. For one lead, two electrodes are needed to monitor voltage changes between different areas on the body. Unipolar leads use one positive electrode and one reference point. Bipolar leads use two electrodes of opposite polarity.

Leads I, II, III, AVL, AVF and AVR are referred to as the limbs leads. Leads V1, V2, V3, V4, V5, V6 are referred to as the precordial or chest leads. The placement of the limbs and chest leads are shown in Figure 2.4 and 2.5.

Leads I, II, and III each require a bipolar lead. Leads V1, V2, V3, V4, V5, V6 require unipolar leads (Jones, 2009). The precordial leads show the activity in the horizontal plane and in practice they are placed around the torso. The limb leads are derived from four electrodes placed on each of the extremities of the patient. The central terminal is the average potential of these limb leads. The potential difference between the chest electrode and the central terminal are the basis for precordial leads. Lead I is the potential difference between the left arm (LA) and the right arm (RA). Lead II is the potential difference between the left leg (LL) and the RA. Lead III is the potential difference between the LL and the LA. The AVF lead is the difference between the LL and an average of the LA and RA leads. AVR is the difference between the RA and the average of the LL and LA. The AVL is the difference between the LA and the average of the RA and LL (Reisner, 2007). The augmented leads vector right (aVR), vector left (aVL) and vector (aVF) in combination with the bipolar limbs provide information on the frontal plane of the heart's electrical

axis (Sornmo & Laguna, 2005). The calculation of the augmented limb lead and bipolar limb leads are shown below (Novosel et al., 1999).

$$aVR = V_{RA} - 0.5\,(V_{LA} + V_{LL}) \qquad\qquad I = V_{LA} - V_{RA}$$

$$aVL = V_{LA} - 0.5\,(V_{RA} + V_{LL}) \qquad\qquad II = V_{LL} - V_{RA}$$

$$aVF = V_{LL} - 0.5\,(V_{LA} + V_{RA}) \qquad\qquad III = V_{LL} - V_{LA}$$
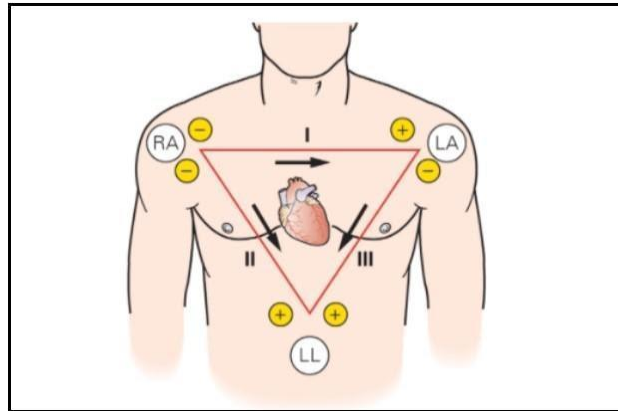
Figure 2.4: Einthoven's Triangle of the Bipolar Limb Leads based on the RA, LA and LL electrodes (Jones, 2009)
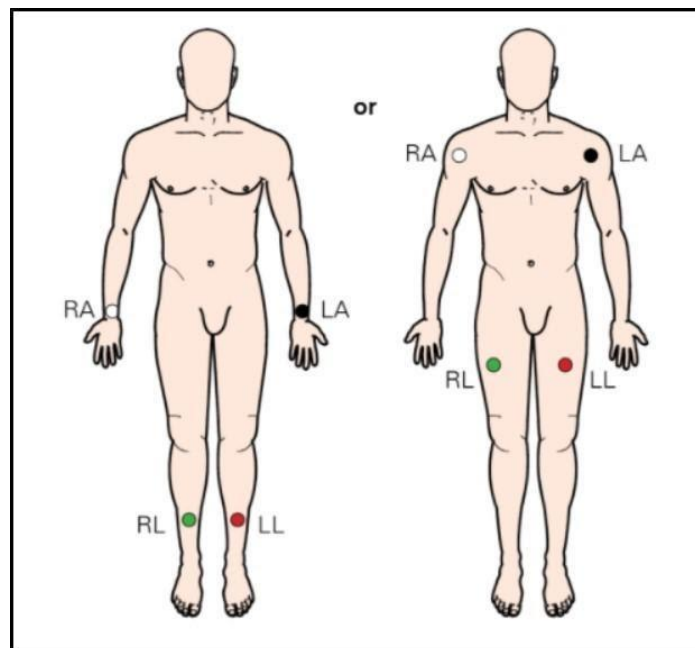
Figure 2.5: Placement of standard limb lead electrodes (Jones, 2009)

An ECG complex is used to represent the heartbeat. An ECG complex is composed of five waveforms, the P, Q, R, S, and T waves as shown in Figure 2.6. These waves can be broken into different segments. The P wave is the first upward movement that represents the start and depolarization of the atrial muscle. This depends on the lead that is being viewed. The PR interval is the time for the signal to travel from the SA node to the ventricles. The QRS interval is the spreading of the electrical impulse through the ventricles producing a vertical deflection. The ST interval is between the ventricular depolarization and ventricular repolarization. The T wave is the return and repolarization of the ventricles muscle to its resting state (Jones, 2009). The bandwidth of an ECG signal with a 12 lead historically has been 0.05 - 150 Hz, but with recent standards and the specific patient population being viewed, the values may range. The peak amplitude of the signal ranges from 0.01 mV to 5 mV (Tompkins, 2006).
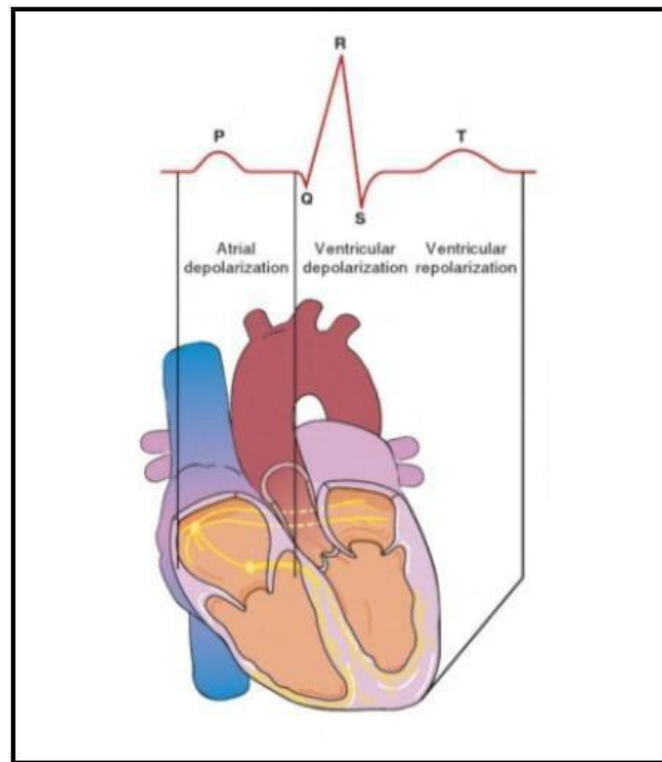
Figure 2.6: How a heartbeat is represented as a signal (Jones,2009)

2.3 Measuring for ECG and EMG Systems

The measurement of biopotential signals such as ECG and EMG provide vital information on the physiological health of an individual (Pu et al., 2012). Both biopotential signals are defined by low frequency and amplitude as well as strong background noise (Yamamoto et al., 2000). During an ECG, the electrical activity of the heart muscle is recorded as the heart depolarizes, sending electrical waves to the body surface (Bai et al., 2005). The amplitude of the ECG signal is low as mentioned in the previous section, yet measurements are achievable using ECG electrode attached to the skin.

▪ 2.3.1 Standard Twelve-Lead ECG

The most common ECG recording technique used in clinical routine is the 12-lead ECG system, requiring ten electrodes positioned in a specific configuration on the body. Nine electrodes are active plus one used as reference supporting different leads. The system is based on a combination of six bipolar limb leads and six unipolar precordial leads to acquire the signal.

There are six electrodes located on the front and left side of the chest shown in Figure 2.7 providing information on the horizontal axis of the heart. The precordial leads V1 and V2 measure the electrical activity of the right ventricle while V3 and V4 reveal the activity of the left ventricle and front of the heart. Leads V5 and V6 cover the side of the chest. The configuration of the unipolar leads is thought to generate signals of higher amplitude and less noise due to their proximity to the heart compared to the six limb leads, however, often the signal to noise ratio of the bipolar leads is less than the precordial (Sornmo & Laguna, 2005).
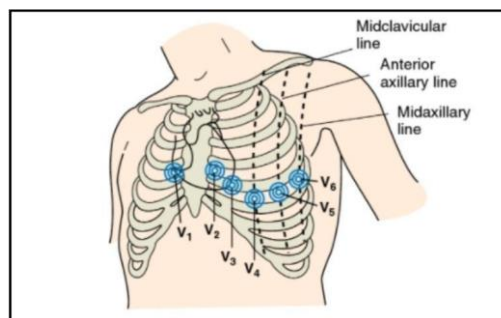
Figure 2.7: Placement of electrodes V1, V2, V3, V4, V5, and V6 for the Unipolar Precordial Leads (Jones, 2009)

The remaining three active electrodes and one reference electrode which complete the 12-lead ECG shown in Figure 2.8 include the aforementioned bipolar leads. The figure below shows the placement of the bipolar leads' electrodes noted as R for the right arm, L for left arm, N for right leg and F for left leg. The unipolar leads mentioned above are noted as C1,C2,C3,C4,C5 and C6 in the figure.
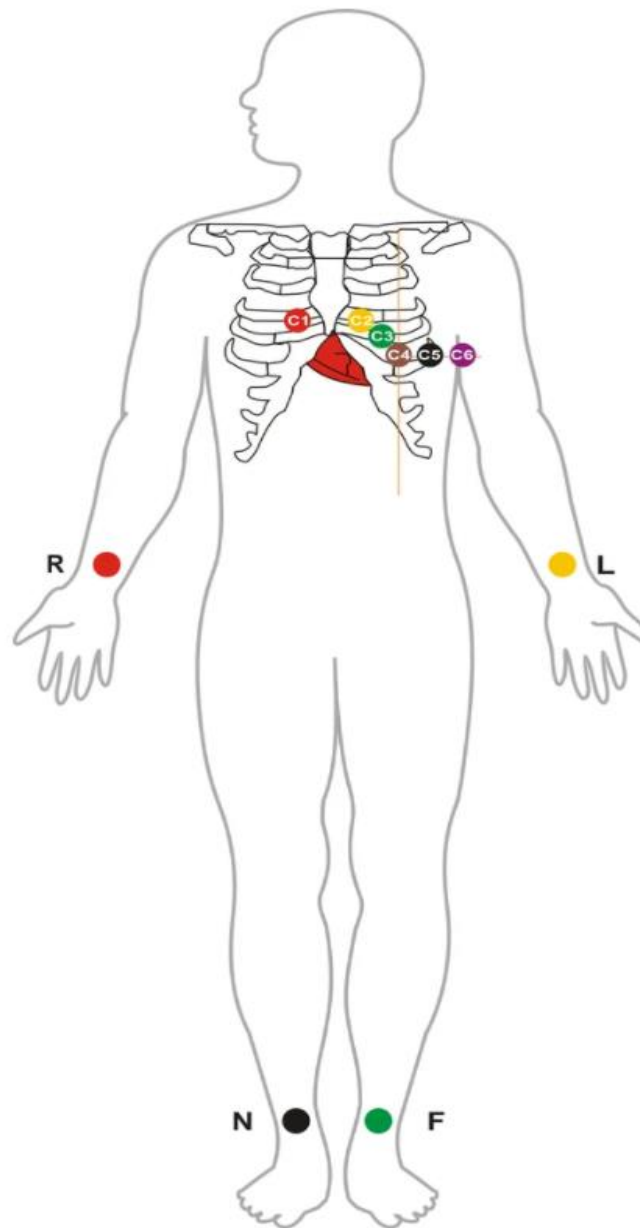
Figure 2.8: ECG 12 Lead - Ten Electrodes Placement (Kumar, 2020)

2.3.2 Three-Electrode Design

The three-electrode EMG design is implemented by two active electrodes recording the voltage difference across the desired muscle placed on the body surface and one common reference electrode placed at a distance to the two active electrodes as shown in Figure 2.9. This simple configuration is usually applied to any skeletal muscle but the biceps or forearm muscles are some of the most common applications. The two active electrodes should be positioned between the half length of the muscle and the end of the target muscle in the direction of the muscle fiber with a separation limited to around 1 to 2 centimeters edge to edge. The optimal placement for the reference electrode in this case would be the wrist (Mangukiya et al., 2017).

Reference Electrode
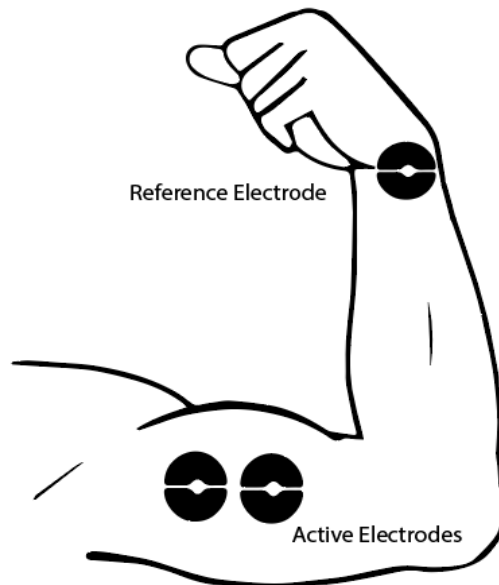
Active Electrodes

Figure 2.9: Three-electrode EMG system placement

Similarly, the three-electrode ECG system can measure all the three bipolar limb leads as it uses three electrodes, two of which are active monitoring and one acting as a reference point. The monitoring can be applied to each side of the Einthoven's triangle shown in Fig. 2.4 at a time according to the positions of the two active electrodes on the subject's torso. A recommended placement of the two active electrodes is shown in Figure 2.10 where the RA electrode is placed under the right clavicle near the right shoulder within the rib cage frame, the LA electrode is placed under the left clavicle near the left shoulder within the rib cage frame and the LL reference electrode is placed on the left side below the pectoral muscles lower edge of the left rib cage. The

reference electrode's position is not strictly defined as it can be placed in a convenient position isolated from the two active electrodes (Francis, 2016).
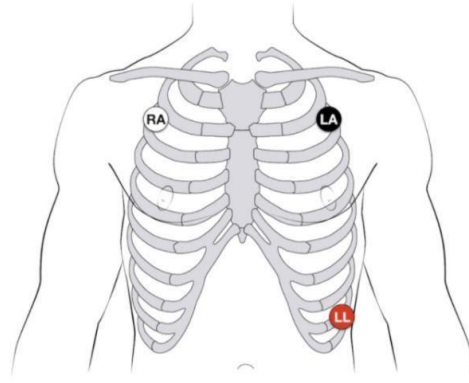
Figure 2.10: Three lead electrode placement (Cadogan, 2019)

2.3.3 Two Electrode Design

The two-electrode ECG system removes the electrode acting as reference and utilizes only the active two electrodes. The elimination of the reference electrode can benefit the ECG design as it reduces the number of required points of contact, minimizes danger of leaking current to the patient and can be applied to wireless and portable ECG systems (Pocock, 1972). The two-electrode design based on the bipolar limb lead, is deprived of the reference electrode that connected the two measuring electrodes and was used to level the reference potential between the device and body (Hsieh et al., 2019). A configuration of a two electrodes ECG system for Lead I proposed by Hsieh et al. successfully recorded the ECG signal. Yet, the recordings for Leads II and III did not accurately appear due to higher noise in the signal. Portable and wireless ECG has been implemented by two electrodes design on various exercise machines which utilizes metal bar electrodes to achieve contact with the hands. The main issue regarding this implementation is the high input noise of the documented signal due to the different potential reference between the body and the ECG device.

2.4 Front End Analog Design

To analyze human's electrical signals and accurately extract information, circuits that can manipulate, amplify, and filter signals are required. This section will discuss the reason behind choosing circuitry and analysis methods and explain how they work.

2.4.1 Differential and Instrumentation amplifier

Since the EMG and ECG signal can be obtained by comparing the voltages between two nodes on the electrodes, a circuit that can measure and output the difference between two input voltages is required, and because the EMG/ECG signal amplitudes are around 0-10 mV, the circuit also must be able to amplify the input signal. A differential amplifier, which is a simple circuit configuration that can measure the difference between the two input voltages and amplify the results, can be considered for this requirement.
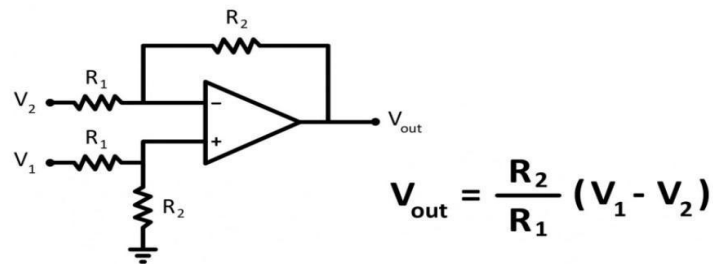
Figure 2.11: Differential amplifier circuit diagram

This circuit is a combination of an inverting amplifier and a non-inverting amplifier. If V1 is set to 0 V then it is an inverting amplifier. The output of the inverting amplifier is :

$$V_{out} = -\frac{R_2}{R_1} V_2$$

If V2 is set to 0 V then the circuit becomes a non-inverting amplifier with the output voltage value of :

$$V_{out} = (\frac{R_2}{R_1+R_2})V_1(\frac{R_1+R_2}{R_1}) = \frac{R_2}{R_1}V_1$$

By combining the equations above (superposition principle), the equation to calculate the output voltage of the differential amplifier is obtained (Sedra & Smith, 2020).

$$V_{out} = (V_1 - V_2)\frac{R_2}{R_1}$$

There are limitations with implementing this circuit as the front end of EMG/ECG acquisition systems. Although theoretically, an infinite gain can be obtained from this configuration, the gain is limited by the gain bandwidth product of the operational amplifier (op-amp). Another problem that we might encounter is the impedance of the input source. Because the value of R1 is in the denominator of the gain equation, a small value of R1 is desired compared to the value of R2. This configuration would work well if the input impedance is high, but if the input impedance is close to the resistance of R1, then the measurement would not be correct anymore. So to fix those problems, a circuit that can amplify the input signal and have a high input impedance is desired. We can achieve it by adding non-inverting amplifiers to the input of the differential amplifier, and this configuration is commonly known as an instrumentation amplifier.
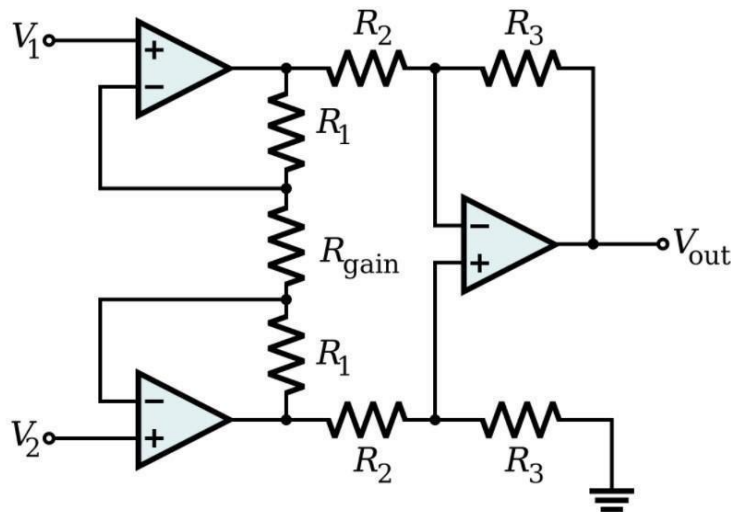
Figure 2.12: Instrumentation amplifier circuit diagram

An instrumentation amplifier is modeled as two non-inverting amplifiers at the input of the differential amplifier.
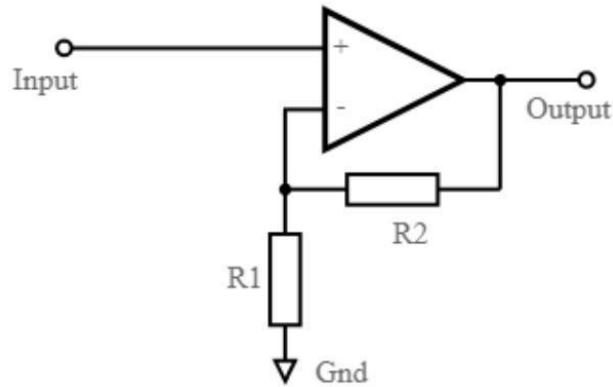
Figure 2.13: Non-inverting amplifier circuit diagram

The output of the non-inverting amplifier, which is the input of the differential amplifier, can be calculated using the following equation (Konar et al., 2019):

$$V_{1\,out} = (1 + \frac{2R_1}{R_{gain}})V_1$$

$$V_{2\,out} = (1 + \frac{2R_1}{R_{gain}})V_2$$

By combining the equations above with the differential amplifier output equation, the equation of the instrumentation amplifier can be obtained (Konar et al., 2019).

$$V_{out} = (V_2 - V_1)(1 + \frac{2R_1}{R_{gain}})(\frac{R_3}{R_2})$$

Furthermore, since the input impedance of the differential amplifier is connected to the output impedance of the non-inverting amplifier and not the input source, we can choose an impedance value that is low enough so that it would not interfere with the differential amplifier. The final result is a differential circuit that has a high input impedance and a low output impedance which also can amplify the results based on the selection of the resistor values and the parameters of the op-amps.

2.4.2 Band-pass and band-reject filters

Since the EMG and ECG signals usually have frequencies between 15-800 Hz and 0.05-100 Hz respectively and are highly influenced by noise, filtering techniques are used to eliminate the unwanted frequency band and noises. Some of the most common noises that can affect the

readings are 50-60 Hz noise from the frequency of the power lines, DC noise near   0 Hz and 0-20 Hz noise coming from the electrodes and motion artifact. Ideally, a band-pass filter is used to eliminate the noise outside of the frequency range, and a band-reject filter (or notch filter) to reject the 50-60 Hz noise from the power lines. Sallen-Key filter is one of the most common high-pass and low-pass circuit topologies.
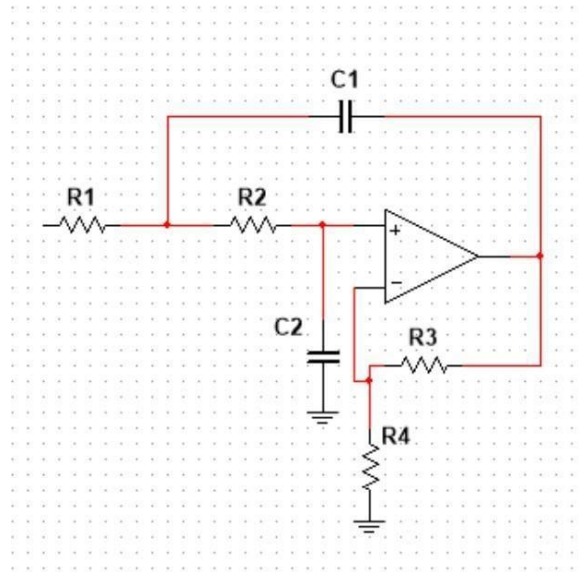
Figure 2.14: Second order Sallen-Key low-pass filter
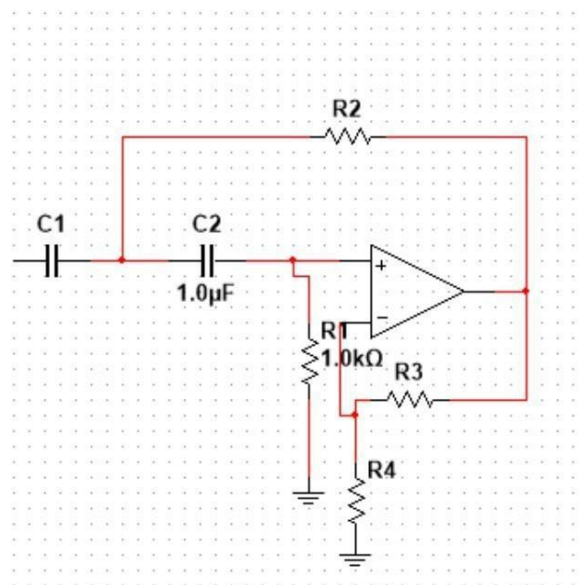
Figure 2.15: Second order Sallen-Key high-pass filter

The transfer function of the Sallen-Key second order high pass filter is (Clancy, 2020):

$$H(s) \ = \ \frac{\frac{R_3+R_4}{R_3}s^2 R_1 R_2 C_1 C_2}{s^2(R_1 R_2 C_1 C_2) + s(R_2(C_1+C_2) + R_1 C_2(1 - \frac{R_3+R_4}{R_3}))+1}$$

and the transfer function of the Sallen-Key second order low pass filter is (Clancy, 2020):

$$H(s) \ = \ \frac{\frac{R_3+R_4}{R_3}}{s^2(R_1 R_2 C_1 C_2)+s((R_1+R_2)C_1+(1-\frac{R_3+R_4}{R_3})R_1 C_2)+1}$$

Since an accurate filtered signal is desired, a filter with a flat magnitude response in the passband should be chosen.

Figure 2.16: Frequency response for a Butterworth lowpass filter

A Butterworth filter prioritizes the flatness of the passband, which is also the main difference compared to other filter options such as Chebyshev and Elliptic. The point where the frequency response drops 3 dB from the passband is called the cut-off frequency of the filter. At this point, the signals that pass this frequency get rejected and attenuated.

The cut-off frequency of the high pass and low pass Sallen Key filter, which is when the output amplitude is attenuated -3 dB, can be calculated using the following formula:

$$f_{3dB} \ = \ \frac{1}{2\pi R_1 C_1}(R_1 \ = \ R_2 \ and \ C_1 = C_2)$$

To improve the quality of the measurement from the filter, higher order filters are more desired. Looking at Figure 2.16, by increasing the order of the filter, the steepness of the roll-off also increases. Each time the order is increased, the roll-off is steeper at the rate of 20 dB/decade. So a first-order filter has a -20 dB/decade roll-off, a second-order filter has a -40 dB/decade roll-off, etc. High order high pass or low pass Butterworth filters can be designed by cascading multiple Sallen-Key second order circuits. Finally, the band pass filter is constructed by passing the output signal from the instrumentation amplifier through an nth-order high pass filter, then through an nth-order low pass filter.

Table 2-1: Butterworth filter circuit configurations for different filter's order

Butterworth filter's order	Configurations
First order	High-pass/Low-pass active filter circuit
Second order	Second order Sallen-Key circuit
Third order	High-pass/Low-pass active filter circuit in series with a second order Sallen-Key circuit
Fourth order	Two second-order Sallen-Key circuits in series
Fifth order	High-pass/Low-pass active filter circuit in series with two second-order Sallen-Key circuits

2.4.3 Passive High Pass Filter

A passive first-order high pass filter is achieved using a first-order RC circuit. The circuit used is shown below in Figure 2.18, where x(t) is the input and y(t) are the output. The filtering characteristic depends on the resistance and capacitance values, which also specify the time constant of the circuit.
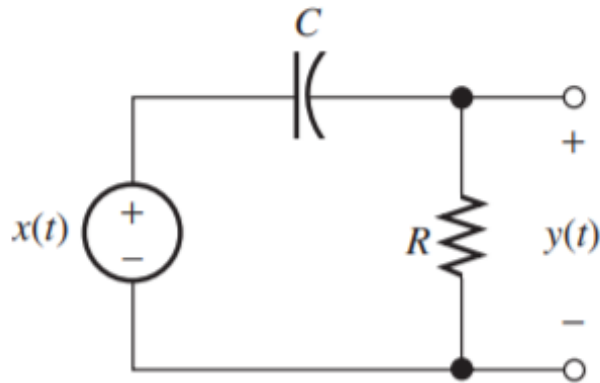
Figure 2.18: Passive high pass filter (Hambley, 2014)

Hambley (2014) defines the break frequency, f_b, as the point where the high frequency and low frequency magnitude response asymptotes meet, and where the phase equals 45 degrees. It is also known as the 3 dB frequency, cutoff frequency, and corner frequency. The 3dB breakpoint can be found using the equation below (Hambley, 2014):

$$f_b = \frac{1}{2\pi RC}$$

The transfer function is written as :

$$H(f) = \frac{V_{out}}{V_{in}} = \frac{j(\frac{f}{f_b})}{1 + j(\frac{f}{f_b})}$$

The magnitude of the transfer function is given by

$$|H(f)| = \frac{f/f_b}{\sqrt{1 + (\frac{f}{f_b})^2}}$$

Figure 2.19 shows the frequency response magnitude and phase. The figure shows how the magnitude is 0.707 (or -3 dB) at the break frequency. It also shows how the phase is 45 degrees at this point as well.
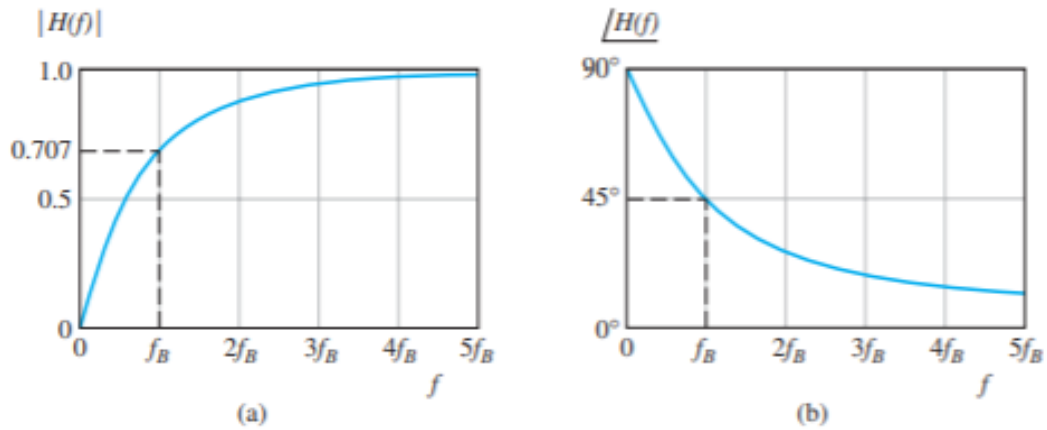
Figure 2.19: Magnitude (a) and Phase (b) response of the passive high pass filter (Hambley, 2014)

The passive low pass filter works similarly in that f_b is calculated the same way. Figure 2.20 shows how the circuit switches the positions of the resistor and capacitor in order to achieve a passive lowpass filter.
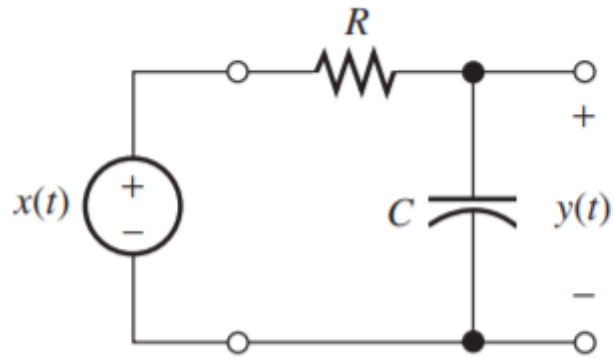
Figure 2.20: Passive low pass filter (Hambley, 2014)

3 Design Options

This MQP consists of two main parts: the wired and wireless devices. The wired circuit measures the EMG signal and the two wireless devices measure EMG and ECG signals. The circuits are similar in implementation of the front end components, however, there are differences in acquiring the signals and processing them depending on the characteristics of each signal.

Previous wired EMG systems have been developed by Professor Clancy (WPI project Advisor) and multiple other MQP teams and we were asked to provide a compact design. The wired device consists of 4 independent channels, each including one bipolar electrode-amplifier that obtains the differential signal between the two points of the muscle on the human body. There is a third electrode that is common to all of the channels serving as the reference electrode. The 4 channels provide the ability to estimate the action of multiple muscles or obtain more measurements on one muscle. We were asked to maintain the system as wired, since it is used exclusively in an on-campus laboratory and all 4 channels do not make it convenient for being a wireless device. The required analog signal conditioning for the wired system consists of the instrumentation amplifier, high pass filtering, gain selection, low pass filtering, analog to digital conversion and electrical isolation.

The wireless devices differ in terms of the measuring application. Namely, the EMG signals and the ECG signals utilize two types of electrode placements, respectively. The two system designs applicable to these devices consists of the three electrodes implemented in the wired EMG acquisition system and the two-electrode design that provides the opportunity of less attachments to the patient for a wireless implementation.

Single-channel ECG circuitry has been designed to work with the two-electrode system. For example, the two-electrode ECG system is typically used in exercise machines, providing elementary information on the heart function during activity. The two-electrode design requires a different circuit configuration due to the fact that the reference electrode is removed. This third electrode, typically placed on the subject's body at a distance from the active components, is a reference point to the active part of the circuit which includes the instrumentation amplifier. The elimination of the reference electrode in the circuit demands a different approach in the two-electrode design. The circuitry of the two-electrode system requires using high valued resistors

connecting the electrodes to a "center tap" of the power supply that is used as a reference point. The role of these input resistors of the two-electrode system includes DC offsetting, input range limitation and high frequency noise rejection configurations. A significant consideration for the design is to ensure safety by limiting the input current flow and upgrading the quality of the signal by rejecting high frequency noise. Electrical isolation for the wireless systems is inherent since the systems are powered by batteries and have no wired connection to the receiver.

Two-electrode circuitry has not been a common approach for EMG signal acquisition due to the higher level of interference and noise generated during measurements, combined with the ready availability of a reference electrode site. The mobility and comfort provided by eliminating one of the electrodes can be convenient for the patients during the acquisition; however, the quality and accuracy of the signal is often considered more vital.

3.1 System Requirements and Design Goals

To complete the wired EMG system, three design options have been developed and evaluated for consideration. To design the wireless EMG and ECG systems, one design approach has been derived. Along with explaining the design approaches, this section will discuss their advantages and disadvantages.

Due to the similarity between the ECG and EMG signals, ECG signals have a frequency range of 0.05 Hz to 150 Hz and EMG signals have a frequency range of 15 Hz to 800 Hz, the filtering and amplifying circuitry of both the wired and wireless system are similar except for distinct passive component values.
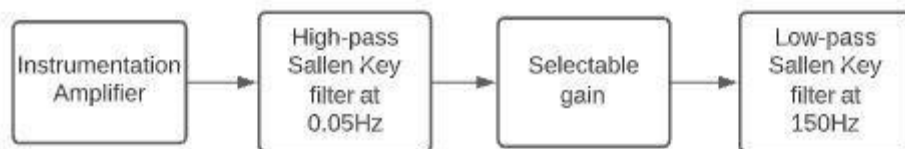
Figure 3.1: The principal functions needed for an EMG or ECG system
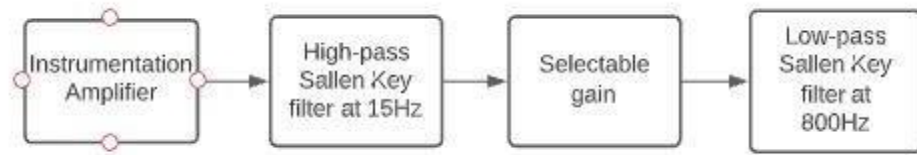
Figure 3.2: The principal functions needed for an EMG system.

To acquire the ECG and EMG signals, the voltage difference of the two electrodes connected to the subject must be measured. An instrumentation amplifier is used to measure the voltage difference between the electrodes and amplify it with the gain selected through a resistor. Because the DC offset of the ECG and EMG signals is specified as a maximum of 300 mV, if the signal is not filtered, the DC offset will be amplified during the amplifying stage, which would interfere with the desired signals. Therefore, a fourth-order Sallen-Key high-pass filter at 15 Hz for the EMG system and 0.05 Hz for the wired ECG system is used to eliminate the DC offset (or signal at 0 Hz). This filter is a fourth-order Butterworth filter that has the attenuation of 80 dB/decade, and is ideal for this application. After that, the signal will be processed through an amplifying stage, which would be a non-inverting amplifier with selectable gain to increase the precision of the system by amplifying the signal to use the full range of the ADC. This can be achieved by implementing a set of resistors that can be selected using a switch. Because the maximum frequency ranges of the ECG signal are less than 150 Hz and 800 Hz for EMG signal, a 4th order low-pass Sallen-Key filter at 15 Hz or 800 Hz will be used, respectively. Finally, if the system is powered by a power outlet, a notch filter at 60 Hz is used to eliminate the power line noise created by the alternating current from the power output. If the system is powered by batteries, then the notch filter is not needed.

3.2 Design Specifications

The following is a table of the design specifications that the design options attempted to meet. These values were derived from information gathered in the background such as signal characteristics.

Table 3-1: Design Specifications

System	Wired - EMG	Wireless - EMG/ECG
Input signal Amplitude	±15 mV	
Input signal Frequency	15-800 Hz	ECG: 0.05 - 150 Hz EMG 15-800 Hz
Selectable gain	1,2,4,8,16	1 (else, manually adjusted)
CMRR	≥ 80 dB at 60 Hz	
Noise	≤ 1 µV RMS RTI for full frequency band	
Size/Weight	Ideally small, something that can be contained within a small box.	
Power	5 V (Depends on ADC and use of USB Power)	5 V
ADC	16 - 24 bit resolution	12-24 bit resolution
Isolation	Medically isolated	Medically isolated
Current Consumption	≤ 350 mA @ 5 V (if possible)	Undetermined

3.3 Wired System

A 16-channel EMG system previously developed by Clancy, serves as the topology for the wired system. In addition to the 16 channels it includes instrumentation amplifiers with a gain of 50. Our project will focus on a 4-channel wired EMG system. Three design options were considered for the wired system and are described below.

3.3.1 Wired EMG: Design Option 1:

This option results in 4 signals that go into 4 ADCs, respectively. The signals from the ADCs are processed by a microprocessor into a PC. The first design option is shown in Figure 3.3 and is described below.
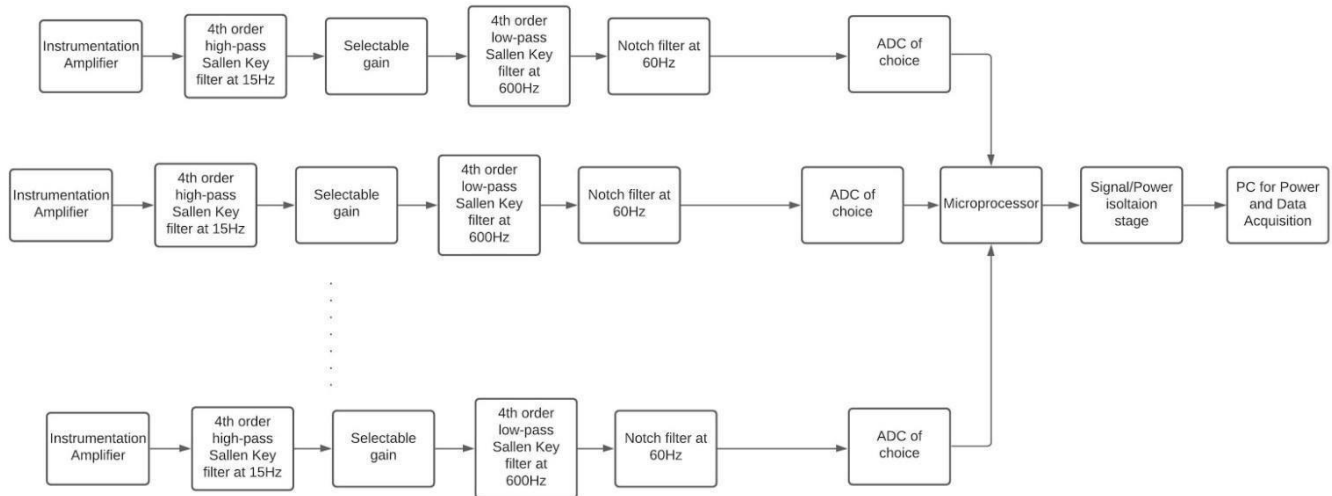
Figure 3.3: Block diagram for design option one

This design option involves having the signals from the bipolar electrode-amplifiers go through a fourth-order high pass filter followed by a selectable gain, thus eliminating saturation caused by movement and noise. Following the selectable gain is a fourth-order lowpass filter and an ADC. This iteration would be implemented within each channel. Recommended frequency cutoff values for the high pass filter is 15 Hz and at least 600 Hz for the low pass. The EMG signals from the channel are processed using an embedded microcontroller. The embedded microcontroller will multiplex the data efficiently into a PC. This design option will include an ADC connected at the end of each channel, giving us a total of 4 ADC's. Before the information can be given to the PC via the USB port, an isolation box will electrically isolate the EMG signal and the power supply from earth ground. The power would be supplied from a wall outlet.

Advantages of this design option include the fact that substantial information is known about each of the components and different implementations have already been attempted previously. The software used for the EMG will also be similar for the wireless systems and eliminates the processes of producing completely new software. A disadvantage of this design choice is that we currently do not know the design specifications of the system or specific types of components as

we are still early in our design process. Our power source will have a big impact on how the system operates. Using a wall outlet requires that the signal be isolated. Another approach is using a medically isolated power supply.

3.3.2 Wired EMG: Design Option 2:

This option uses the same filtering steps as before, but the 4 signals all go into one 4 channel ADC. The signal that comes from the ADC is processed by a microprocessor and sent to a PC through the USB port. The second design option is shown in Figure 3.4 and is described below.
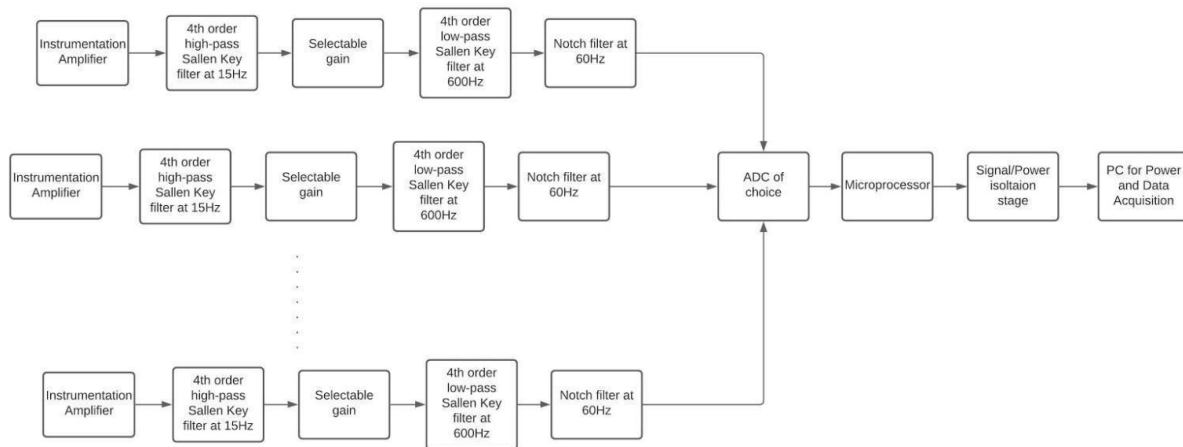
Figure 3.4: Block diagram for design option two

The second design option consists of one PC based USB connected ADC processing all the information from the 4 channels instead of the 4 ADCs used in the first option. The single ADC carries over all of the gathered information to the microprocessor. Once the information is processed, an isolation box will be necessary to ensure electrical isolation before the EMG signal is sent to the PC.

Advantages of this design include the fact that less materials (number of ADCs) are required which can make the EMG system more space efficient. Moreover, this design gives way to more options for selecting an ADC. A disadvantage of this design selection is that the ADC requires specifications to handle 4 inputs efficiently. In addition, the specification for power that the ADC needs will alter the power needed for the entire system. Therefore, this system is highly dependent on the chosen ADC.

3.3.3 Wired EMG: Design Option 3:

This option consists of an ADS 1291 chip that can execute several of the signal conditioning steps in one component. These 4 signals are sent to a microcontroller which sends a single signal to a PC. The third design option is shown in Figure 3.5 and is described below.
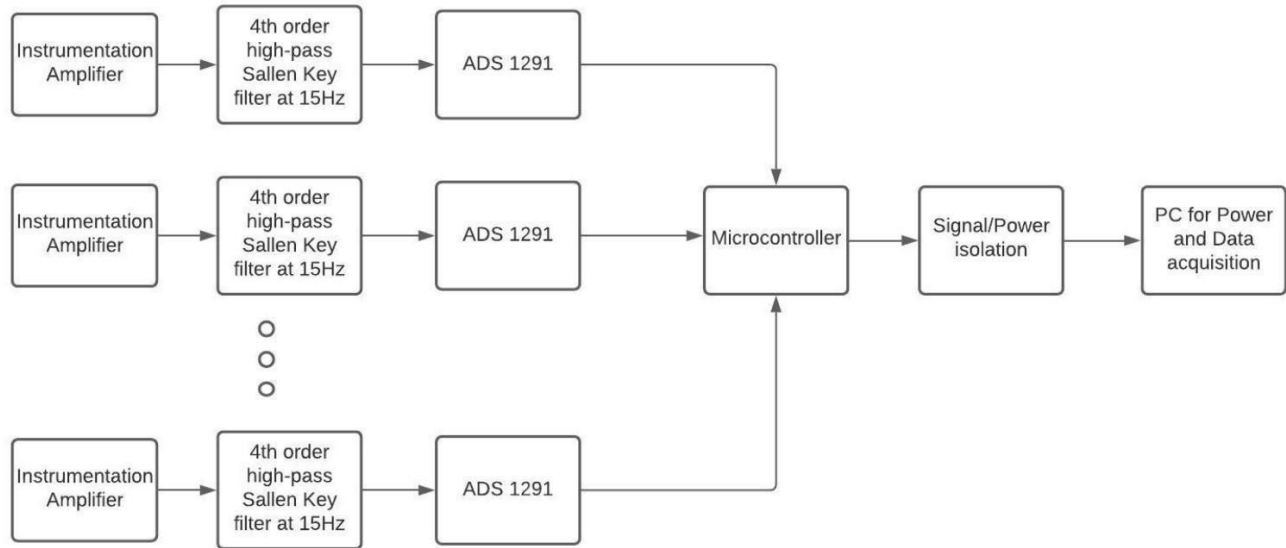
Figure 3.5: Block diagram for design option three

Design option three uses the Texas Instrument (TI) ADS1291 ADC. The ADS1291 is a delta-sigma ADC, a low power device with one input channel. It is equipped with low noise programmable gain amplifiers (PGA's) and two high resolution amplifiers. The programmable gain values are 1,2,3,4,6,8, and 12. The ADS1291 also has a 24 bit resolution ADC and a built-in oscillator. The ADS1291 has RC circuits that function as anti-aliasing filters for the PGA differential amplifier. The signal is then sent through the ADC and ADC modulator for digital filtering. The ADS1291 can replace the selectable gain, low pass filter, and ADC shown in design option one. An instrumentation amplifier and high pass filter will need to be placed before the ADS1291. The delta sigma ADC equipped in the ADS1291 will output the EMG signals into a microprocessor which will then go into an isolation box and be processed by the PC.

An advantage of using the ADS1291 is that it will require less space and components, making the EMG system smaller in size and more adjustable. Additionally, the ADS1291 is designed for EMG and ECG systems and is embedded with many parameters and specifications needed for the signals. Disadvantages include that the ADS1291 is a new product for us and will

involve substantial software. We do not have freedom to change any of the specifications of the ADS1291 and must use what is provided.

3.3.4 ADC

With all of our design choices, the ADC is the component where there is the most flexibility. ADC's that can be utilized are the integrated circuit ADS1291 from Texas Instruments (TI), sigma delta ADC from TI or one of the USB-1608G series ADC modules from Measurement Computing (MC). The ADS1291 is a delta-sigma ADC, a low power device with one input channel with low noise programmable gain amplifiers (PGA's), two high resolution amplifiers, and a built-in oscillator. A sigma delta ADC uses a sigma modulator and digital filtering. Filtering the signal involves oversampling, noise shaping, digital filtering and decimation. The ADC modules that are a part of the USB-1608G series have a 16 analog input device that can efficiently connect to a PC through a USB port and has 16 bit resolution. The difference between the USB-1608G series is the measurement rate. The USB-1608G has a measurement rate of up to 250 kS/S. The USB-1608GX has a measurement rate of up to 500 kS/S.

There is a significant difference in the price associated with these ADC's. The ADS1291 is around $7 USD per unit which is very cost efficient for a project that will use multiple ADC's. The ADS1291 will require more software installation and configuration to the microcontroller and the PC. The USB 1608G ADC's range between $400 - $800 USD. The USB 1608 GX cost around $200 more than the USB-1608 G. Both USB-1608G ADC's have the same parameters for power measurement range, 16 channel analog inputs, and software. The PC based devices are more expensive compared to our other options. But, are being considered because we will not need multiple USB-1608G ADC's. The noise and gain parameters for the ADC will have an impact on the entire wired system. The ADC plays a role in how much power the system will need and how to properly isolate the power supply. The use of a PC based USB connection can make this a challenging task. The table below summarizes the different options for ADCs.

Table 3-2: Pros and Cons between ADCs

Design options	Pros	Cons	Cost
Standard components with PC and ADC card	- Have a better idea of what to do/ have more resources and info - Are able to test different methods	- Building and testing in a lab may be more difficult. - Have to determine specific hardware to use.	$25 for 8-10 lead ADC
Sigma-delta ADC Pi-16 ADC -Alchemy Power Inc	- Within a reasonable price range - Have differential amplifier and integrator - Programmable gain amplifier - Uses noise shaping - Precise measurements - Compatible to a Raspberry Pi	- Input power is 5 V sourced from the Raspberry Pi - Uses Python code for ADC use (would prefer MATLAB) - Must route data to PC in real-time	$ 35-40
ADS1291- Texas Instruments	- Cheap - Designed for ECG, sports, and fitness applications - Programmable gain amplifier (PGA) - Sigma delta ADC - Low power 1 channel at 24 bits - USB powered	- Requires software installation - Requires coding (sample code is provided on Texas instruments) - Installation of USB drivers - Will require more time to learn how to properly implement - Must route data to PC in real-time	$7.29
USB - 1608G - Measurement Computing	16-bit resolution 500 kS/s sampling rate - Input range is software-selectable. 8 digital I/O channels - PC - USB	- Requires more power - ranges are +- 10 V, 5 V, 2 V and 1 V. - More expensive - Will require MATLAB code	$440 - $880 USD.(USB Peripheral)

	• Supported on Windows, Android, and Linux • Has MATLAB support driver		

3.4   Wireless System

The following chart describes the topology of the wireless ECG and EMG system. The front end of both systems consists of the same series of signal conditioning steps for both the ECG and EMG systems, but with different values in the components according to the signal characteristics.

These steps consist of an instrumentation amplifier, a 2nd order Sallen-Key high pass filter, selectable gain, 2nd order Sallen-Key low-pass filter, ADC, Bluetooth transceiver and a Bluetooth Receiver. The high pass filter was set to 0.5 Hz for ECG and 15 Hz for EMG. The low pass filter was set to 150 Hz for ECG and 800 Hz for EMG. Together, these steps form the front end (boxed in green in Figure 3.6) which conditions the signal appropriately for our use. This signal can then be sent through an ADC on the microcontroller unit (MCU). The digital signal is then sent via a Bluetooth transceiver on the unit to a Bluetooth receiver located on a separate base unit. This base unit will consist of either a 2nd MCU that can be connected to a PC via USB or it will consist of a phone. The first MCU contains the ADC and Bluetooth transceiver combination and is highlighted in red in Figure 3.6 while the second MCU and its Bluetooth receiver are highlighted in blue.
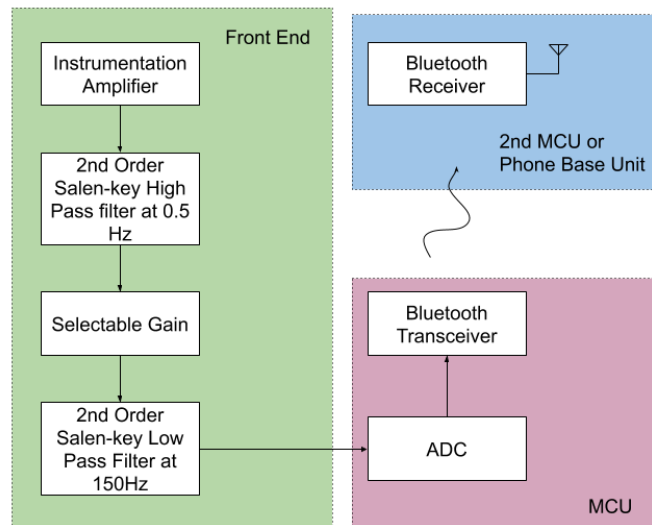
Figure 3.6: Block diagram for a wireless ECG system

Design options for the MCU have been narrowed down to the TI CC26X2R1 and the Nordic nRF52832. Both systems have similar specifications for the components we will be utilizing in the chosen design. The Bluetooth characteristics are similar with the TI MCU having a receiver sensitivity of -97 dBm and the Nordic MCU having a receiver sensitivity of -96 dBm. Moreover, both have a 12-bit ADC sampling at a maximum rate of 200 kS/s. While the Nordic MCU has a higher clock speed and more memory, both units have enough memory and speed required to carry out the necessary tasks. Therefore, these higher specs are not critical to our project. While the Nordic MCU is slightly more expensive, the difference is miniscule for the prototypes that are created. In addition, EMG systems (and to a lesser extent ECG systems) belong to a comparatively small-scale market where variation in component pricing isn't as impactful on profits. Therefore, cost was not a large factor in the decision making of this section.

The primary advantage for using the TI CC26X2R1 MCU is the existing knowledge and framework provided by supporting faculty to this project. Working with the TI unit would save time that would have been spent learning to use the Nordic unit. The time saved can be used to improve the scope of the wireless system design. Outside of this major benefit, there is not a substantial difference between the two MCUs for our application and the few relevant differences that exist were not critical factors. Table 3-3 below shows the pros and cons generated when

comparing the TI CC26X2R1 and Nordic nRF52832 MCUs. Next, Table 3-4 shows selected specifications that pertain to the overall performance, price, and the tasks which utilize the MCU.

Table 3-3: Pros and Cons between TI and Nordic MCU

Design Options	Pros	Cons
MCU		
TI CC26X2R1	- Low power - Operation on coin cell batteries - ideal for autonomously collecting analog or digital data while rest of sleep mode - designed for various applications including vitals monitoring - Bluetooth - Less expensive (half price for just the MCU)	Lower Flash memory and RAM
Nordic nRF52832	- Low power - designed for various applications including connected health products - Bluetooth	- less "in-house" experience with this family of devices - More expensive

Table 3-4: MCU features comparison

	TI CC26X2R1	Nordic nRF52832
Price	$1-2 MCU alone Observed development kits ranging from $30-35	$3-6 MCU alone Observed development kits ranging from $32-48
Microcontroller	ARM® Cortex® -M3	ARM® Cortex-M4F
Clock Speed	48 MHz	64 MHz
Memory	128 KB Flash + 20 KB SRAM + 8 KB Flash	512/256 KB Flash + 64/32 KB RAM

ADC	12-bit, 200 kS/s	12-bit 200 kS/s
Receiver Sensitivity	-97 dBm	-96 dBm

4 Final Design Selection

Wired EMG:

After comparing our three design options for the wired EMG, the final design choice is design option 2. This design will contain an instrumentation amplifier stage(already available as a standalone component available to our system), 4th order highpass filter followed by selectable gain, 4th order low pass filter, and a 16 channel PC-based USB-connected ADC. This design choice was the most flexible because more testing could be done and time can be utilized towards the ADC performance. The power of the system will vary depending on the ADC. The ADC of choice is between the USB 1608 G and the Pi-16ADC sigma delta. The USB- 1608G is more expensive compared to the Pi-16ADC but since we will only have one system, the use of a high end ADC can make the system more efficient in the future. The Pi-16ADC has the advantage of not only being cheaper but being compatible with a Raspberry Pi and sample code is provided for the Pi-16 ADC. The USB-1608G has the advantage of direct software support on the PC within MATLAB and National Instruments LabVIEW. Design option 2 uses a small amount of components while meeting the design specifications.

Design option 1 was eliminated due to the excess use of ADC's. Design option 1 involved having one ADC per channel. Using 4 ADC's would make the system more cluttered and require more equipment which does not meet the design specification of the desired system size. Design option 3 was eliminated because of the time that it will take to properly learn how to utilize the ADS1291 ADC. The ADS1291 is a well-developed product that meets the design specifications but there would be a large amount of software that would be required. The lack of experience with the ADS1291 could require more tools and resources since it can replace the selectable gain, low pass filter, and ADC.

Wireless EMG/ECG:

Our implementations of an ECG circuit focused on a two-electrode system, encouraging the mobility granted by the elimination of the third reference electrode. For the EMG circuit, our choice was narrowed down by the limited use of the two–electrode design in existing products, thus we chose the three-electrode system. We were interested in the most accurate results for EMG

due to the higher noise of the signal and did not focus on less attachments to the patient in this case. Overall, this selection gave us the opportunity to design and evaluate both a two-electrode and a three-electrode system.

Once the electrode system was determined for each device, the main choice faced by the wireless system was the microcontroller unit (MCU). The TI CC26X2R1 became the preferred option. As previously mentioned, the primary advantage of this MCU was the support existing for this device through faculty who have experience with this device. This existing framework of knowledge was judged to outweigh the miniscule benefits of using the nRF52832. The specifications of the TI CC26X2R1 met all the needs of this project.

5   Design Implementation

5.1. Wired Electromyogram System

5.1.1. Wired EMG Filter design:

For the EMG signal, the desired frequency of the output signal ranges from 15 Hz to   800 Hz. To implement this passband, fourth-order Butterworth high-pass and low pass filters with cut off frequencies of 15 Hz and 800 Hz , respectively, were cascaded using the Sallen-Key topology discussed previously in section 2.4.2. The values of the resistors and capacitors in the filters were found using the MATLAB function "butter_hi_design" and "butter_lo_design" (available within our research laboratory). These functions show the magnitude response of the filters, and can be used to construct the theoretical frequency response of the filters.

The circuit diagram is presented in Figure 5.1 with a gain of 4 for the high-pass filter and a gain of 1 for the low-pass filter. These gain values were chosen to ensure that the output signal from the ADC achieves the maximum resolution. Two 0.1 µF capacitors were also used for each op-amp integrated circuit as bypass capacitors, which are connected to the power supply rails and the ground. These bypass capacitors are used to eliminate any AC noise that is present on the voltage supply. A pull-down resistor with a value of 1 MΩ was also added in parallel with the input of each channel of the filter. The pull-down resistor is used to make sure that the voltage at the beginning of the filters stays at 0 V when an input signal is not present. A selectable gain stage was constructed to adjust the amplitude of the output signal to achieve the desired resolution. To obtain the simulated magnitude response of the circuit, the system was modeled in NI Multisim 14.2 and simulated using the "Interactive simulation" function and the "Bode plotter" equipment. Figure 5.4 shows the simulated magnitude response of the filter. From the simulated magnitude response plot, the high-pass and low-pass cutoff frequencies were measured to be around 14.8 Hz and 803 Hz respectively, which is similar to the theoretical cut-off frequencies of 15 Hz and 800 Hz.
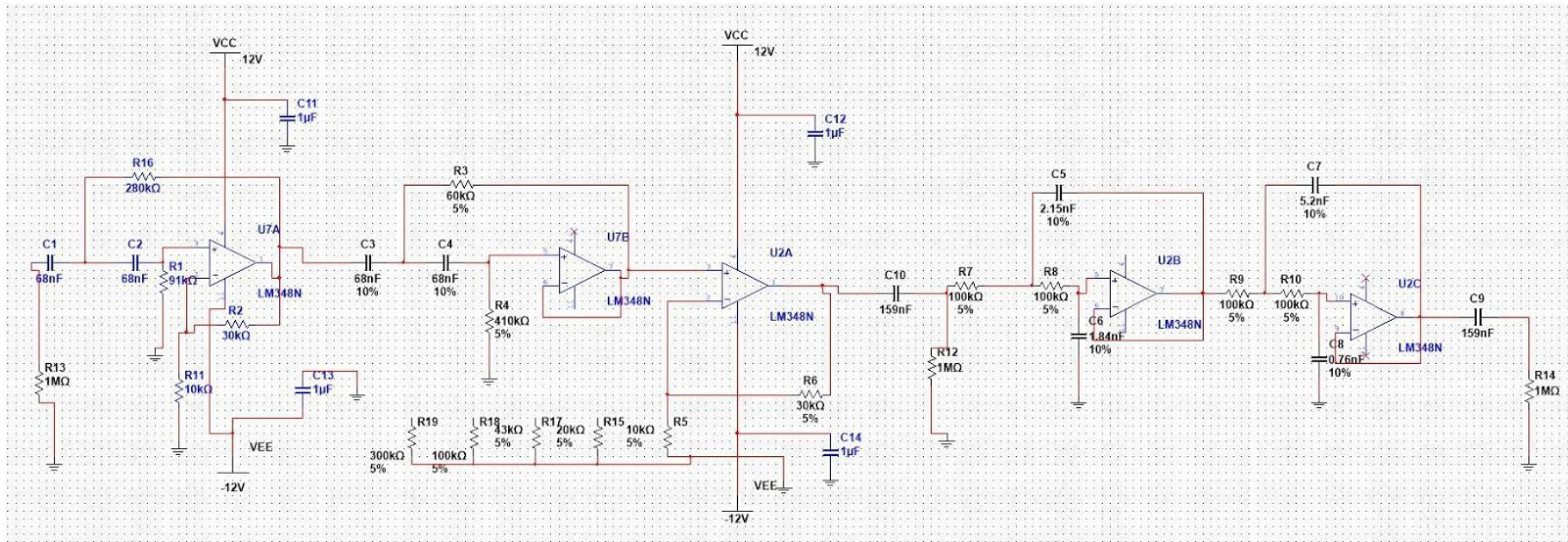
Figure 5.1: The circuit diagram of the filters and selectable gain.
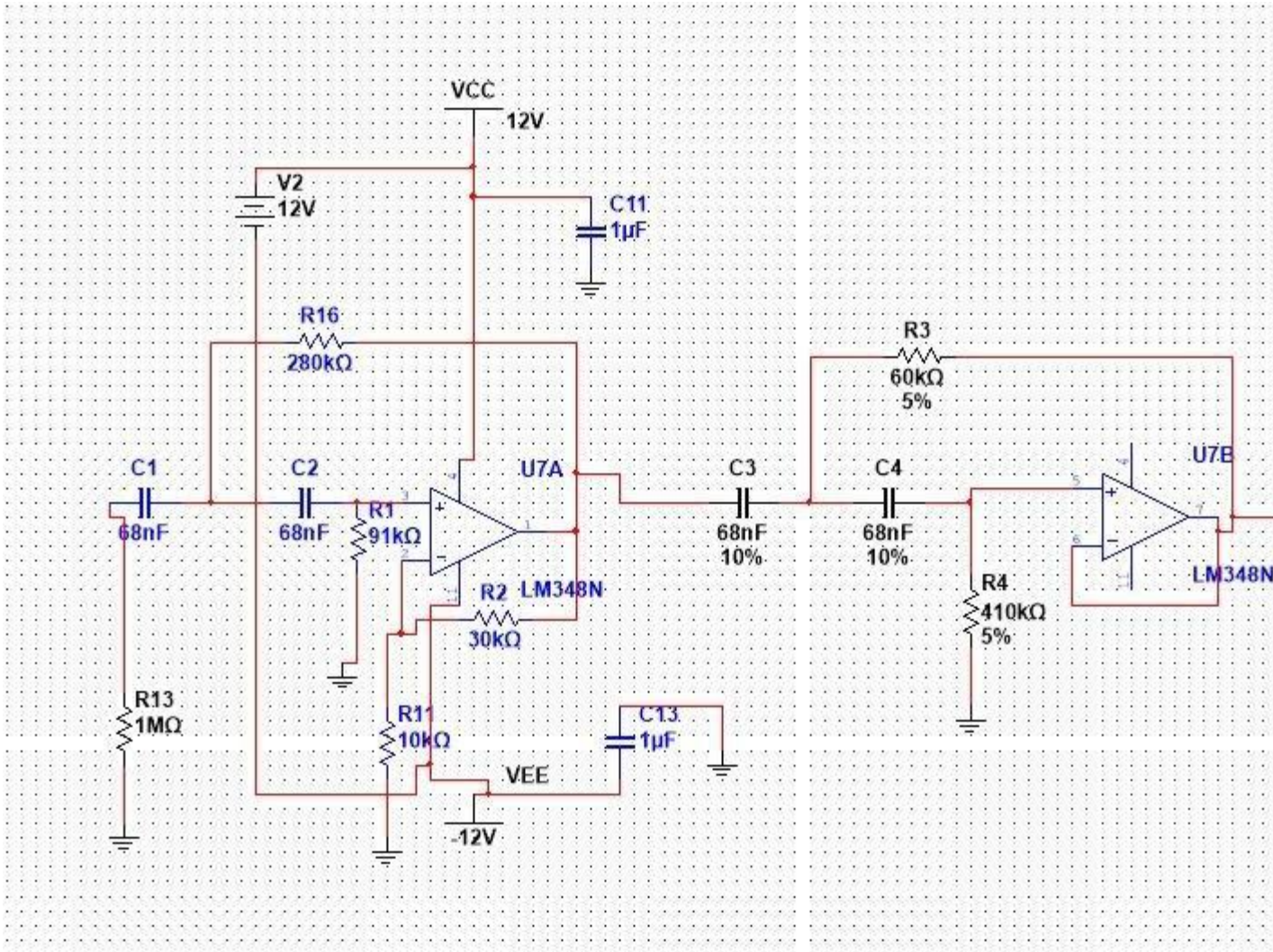
Figure 5.2: High-pass filter circuit diagram
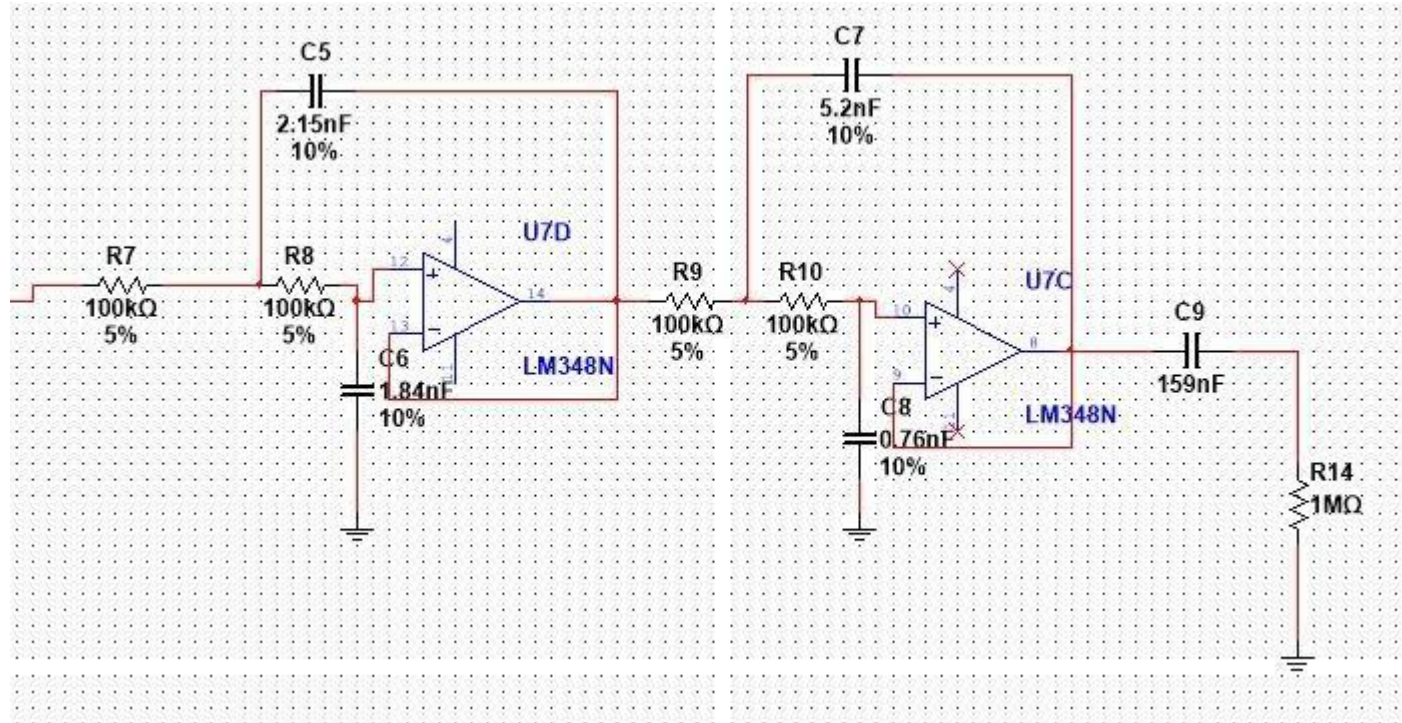
Figure 5.3: Low-pass filter circuit diagram
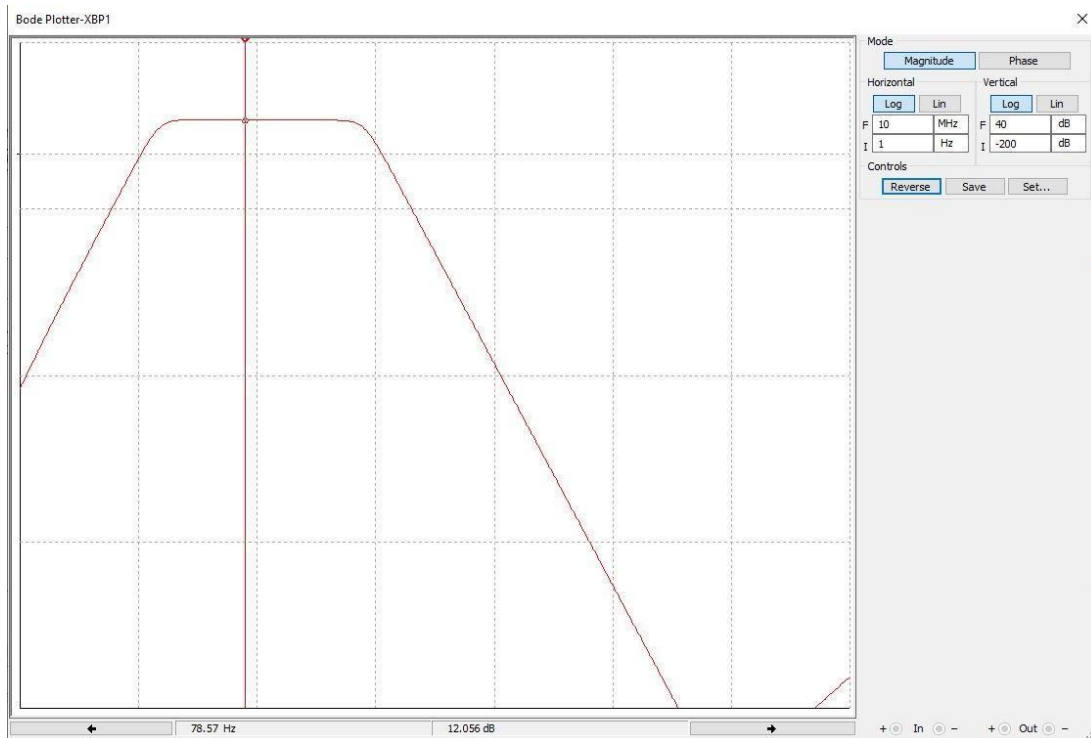
Figure 5.4: Simulated magnitude response. The horizontal axis is the frequency from 1 Hz to 10 MHz. The vertical axis is the magnitude of the output signal from -200 dB to 40 dB. Both axes are on a logarithmic scale.

Next, the circuit was built on a breadboard and tested using the GW INSTEK GPS-3303 power supply, the GW INSTEK GFG-8219A function generator and the Tektronix TDS2004B oscilloscope. The evaluation was conducted by connecting the function generator as an input of the filter, and the output of the filter was recorded using the oscilloscope. Then, the function generator was adjusted to produce a sine wave input with a frequency range from 1 Hz to around 10 kHz and the output signal would not be saturated. The magnitude response was measured and calculated by measuring the amplitude of the input and output signal of the system at each selected frequency. The input signal that we used for our test was a sine wave with an amplitude of 500 mV and an offset of 0 V. The output signal when the total gain of the filter is 4 is around 2 V with an offset of 0 V. Finally, the frequency response in decibels was calculated using the following equation:

$$Magnitude\ response\ (dB) = 20\ log\ (\frac{V_{out}}{V_{in}})$$
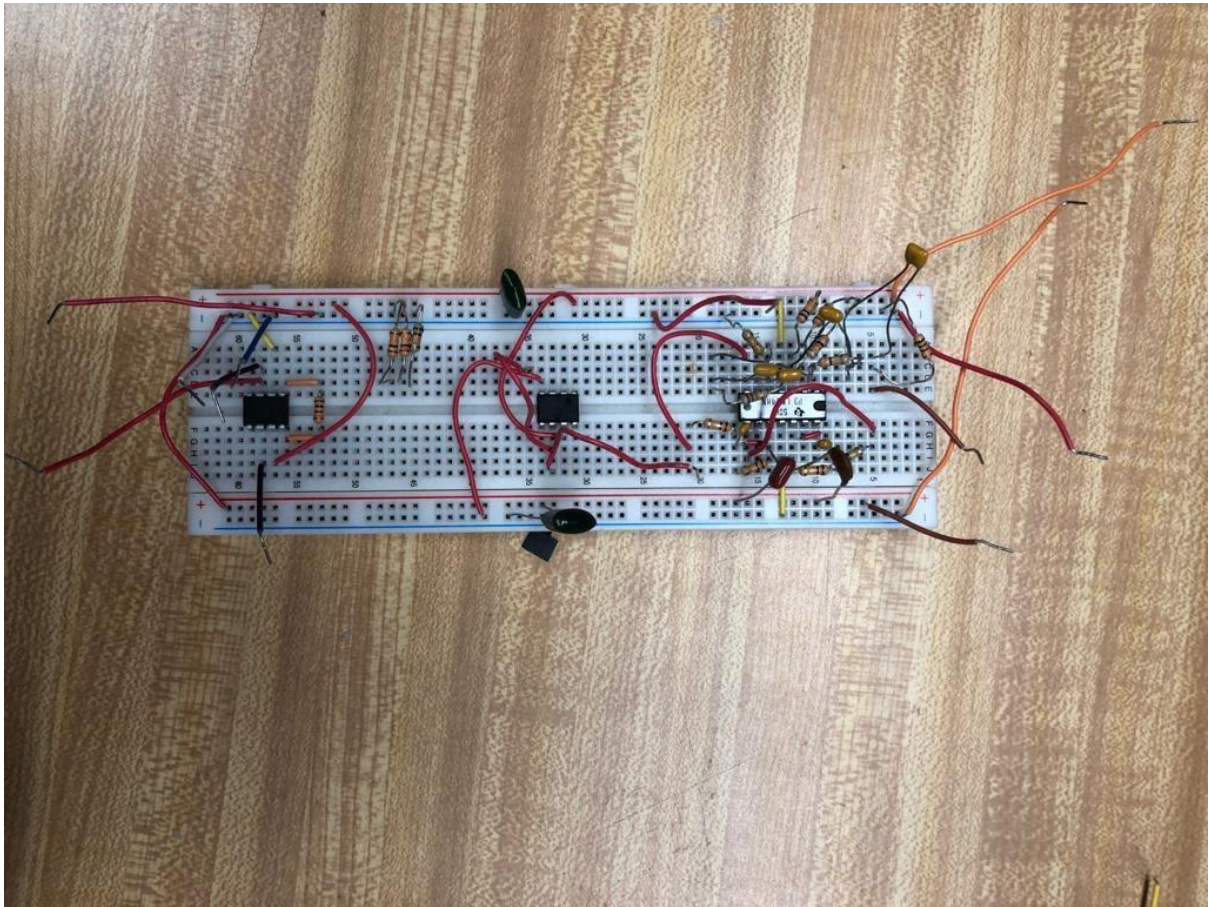
Figure 5.5: Prototype of the filter.

After measuring the experimental magnitude response of the system, all of the magnitude response graphs were plotted using the custom function "theoretical" in MATLAB. Figure 5.6 shows the theoretical, simulated and experimental frequency responses of the system.
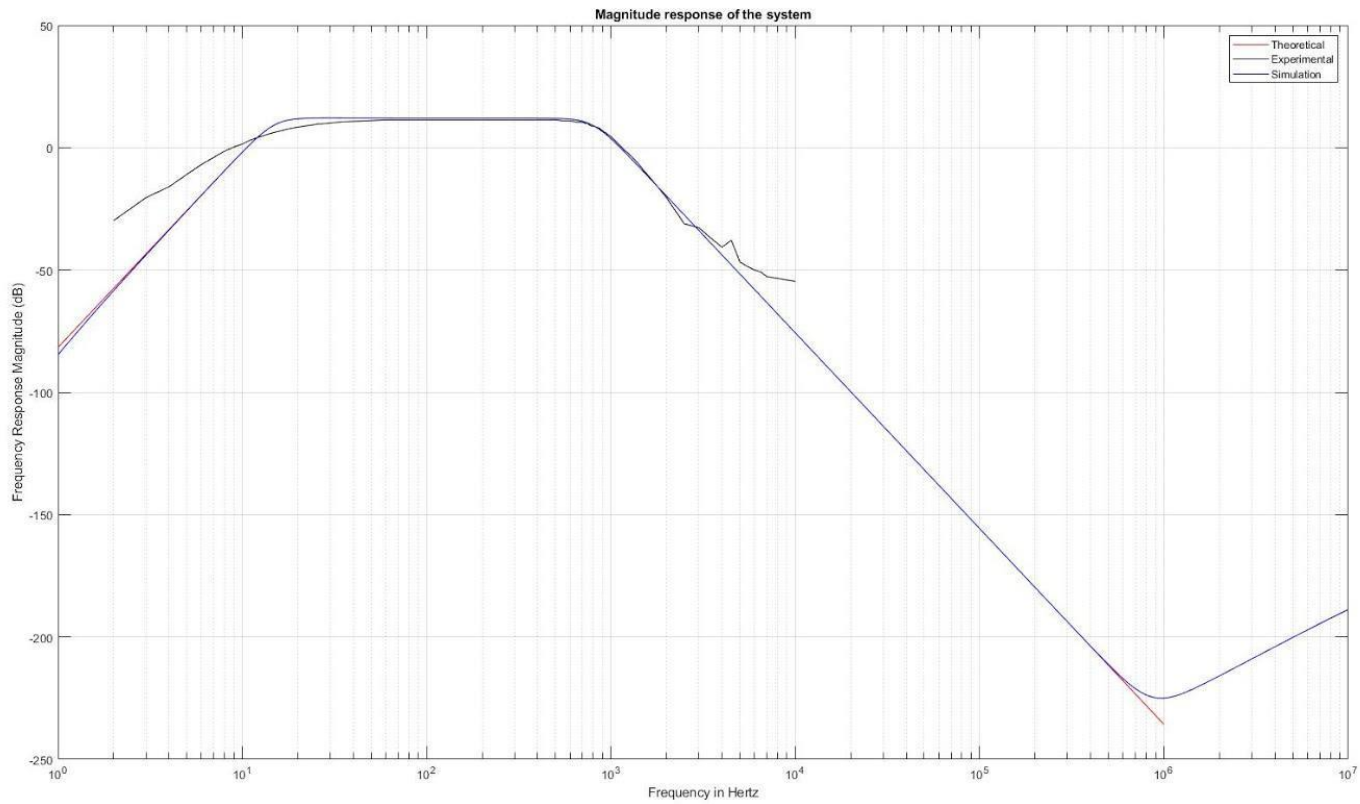
Figure 5.6: Magnitude response of the system. The red line is the theoretical frequency response, the blue line is the simulated frequency response, and the black line is the experimental response.

As shown by Figure 5.6, the theoretical and simulated responses overlap while the experimental response diverges from the theoretical and simulated responses. This is because the experimental circuit has non-ideal components, so adding up the tolerance of the components would significantly change the result of the experiment. Furthermore, at extremely low and high frequencies, the output signal was so miniscule that the oscilloscope display became noisy, which reduced the accuracy of the measurements. Overall, the filters work as expected.

5.1.2 Wired EMG Selectable gain:
The selectable gain was constructed using a non-inverting amplifier. From Chapter 2 we know that the gain of the amplifier is calculated using the equation below:

$$V_{out} = \left(1 + \frac{R_2}{R_1}\right) V_{in}$$

Thus, the selectable gain was built using an array of resistors as R_1 and a 300 kΩ resistor as R_2. R_1 was chosen to be 300 kΩ, 100 kΩ, 43 kΩ, 20 kΩ, and 10 kΩ to obtain gains of 2, 4, 8, 16 and 32, respectively. To get the gain of 1, R_2 is disconnected from the resistor array, which converts the non-inverting amplifier to a unity gain amplifier. Figure 5.7 shows the circuit diagram of the selectable gain stage.
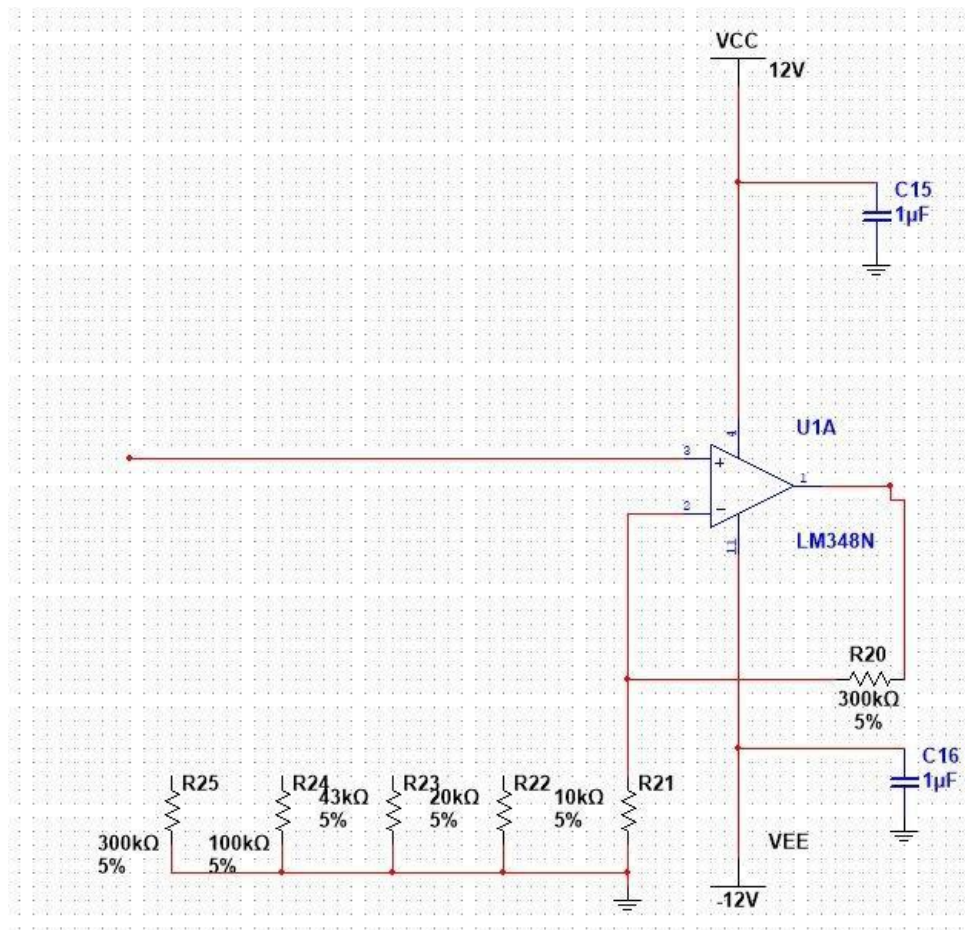
Figure 5.7: Circuit diagram of the selectable gain

The total gain of the output of the filter and gain system is 4, 8, 16, 32, 64, or 128 when the selectable gain is 1, 2, 4, 8, 16 or 32, respectively.

5.1.3 Wired EMG ADC Power Supply Configuration:

The wired EMG acquisition system requires a power source that can supply the required input voltages for the front end and the ADC module. The front end of the wired EMG system is designed to receive ± 12 V and the ADC module needs +5 V. One solution is using a medically isolated power supply. The ECP40UT01 manufactured by XP Power is the medically isolated power supply used to power the EMG wired system.

a) ECP40UT01 power supply (top view)

b) *Full picture of the ECP40UT01 (XP Power; 2020).*
Figure 5.8: a) the ECP40UT01 while being used for testing and b) without any wires attached.

The medical isolated power supply provides electrically isolated power. To provide signal isolation to the signal path, a USB ADC module was inserted in series at the USB connection.

The ADC used for the wired EMG system is the NI USB 6000 from National Instruments. This ADC was used because it was already available in our laboratory. A higher resolution can be substituted in the future if additional resolution is desired. The NI USB 6000 is a multifunction I/O device with 8 single-ended analog inputs and 12 bit resolution. The maximum input voltage range for the NI USB 6000 ADC module is listed as ± 10 V. The EMG system is designed to use +5 V for the ADC. The NI USB 6000 has software configuration in

MATLAB that reads data from the ADC. The code records data for a specified amount of time and returns the results. The code used to configure the ADC is outlined in Appendix A.
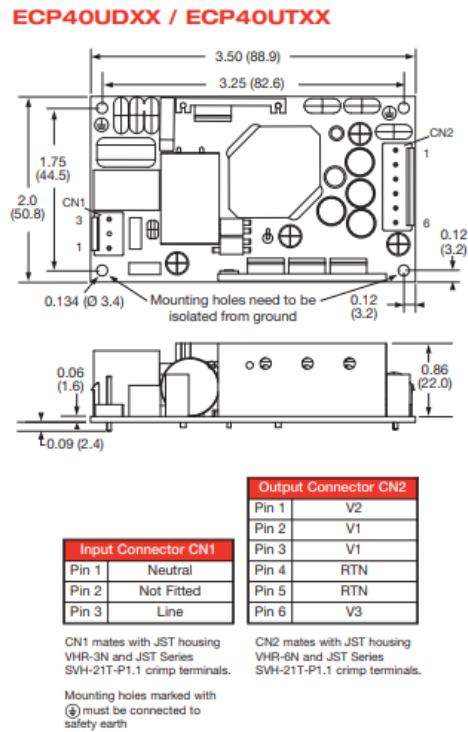
Figure 5.9: Location of the input and output pins on the ECP40UT01 (XP Power. (2020)).

Figure 5.10: National Instruments NI USB 6000 ADC (National Instruments, 2020)

The front end, ADC, and power supply for the wired EMG prototype were all tested individually. Once we were able to verify that each unit was working as desired, the entire

prototype was set up to use the isolated power supply and process data using the ADC module. This prototype is shown in Figure 5.12. For testing, the ADC was powered by the isolated power supply and received an input using BitScope BS10, a programmable PC based oscilloscope, shown in Figure 5.11. The function generator was set to 200 Hz input with a 500 mV amplitude and 10,000 Hz sample rate to display at least one period of a sine wave. Figure 5.13 displays the output sine wave recorded in MATLAB, from the ADC module. Overall, the system prototype is fully powered with the isolated power supply and the NI USB 6000 is properly sending data. These data are properly recorded on the PC using MATLAB software.
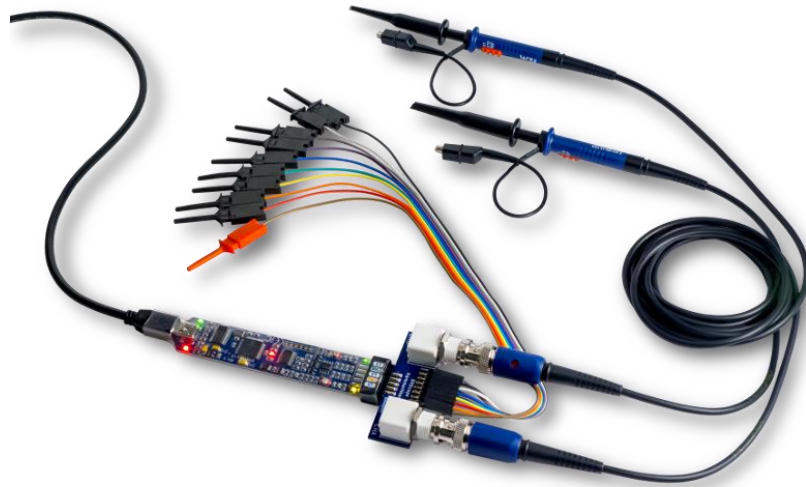
Figure 5.11: BitScope Micro PC Based Oscilloscope (Bitscope,2020).
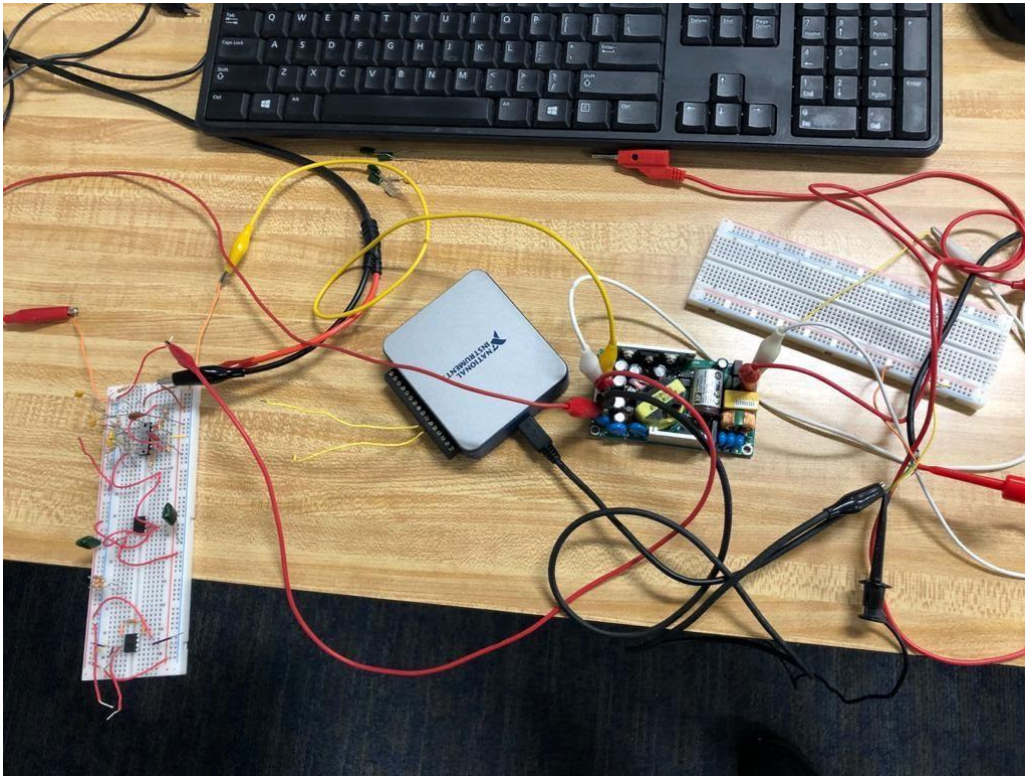
Figure 5.12: Wired EMG prototype.
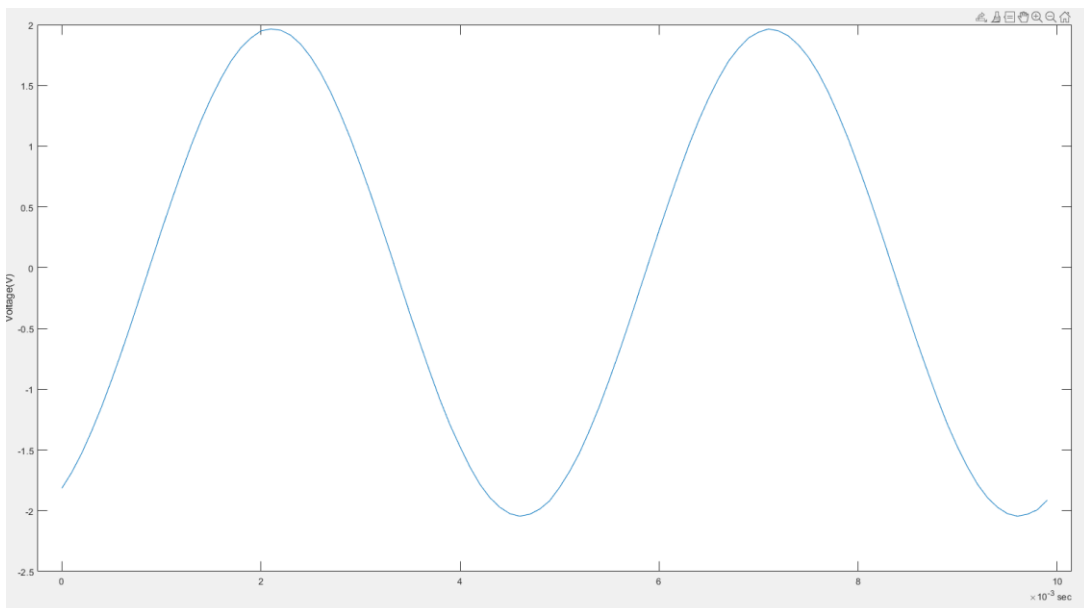
Figure 5.13: 200 Hz input, 500 mV amplitude and 10,000 Hz sample rate sine wave ADC result for the wired EMG prototype.

5.1.4 Wired EMG System PCB Implementation:

The final design for the wired application is a 4-channel system. The channels are processed using the ADC module and powered with the medically isolated power supply mentioned above. The selection of components for the printed circuit board (PCB) design are the same component values as the breadboard implementation listed in Figure 5.1.

The wired system was simulated using the software NI-Multisim 14.2. Hence, that schematic was transitioned over to EAGLE Auto-Desk software. EAGLE was used to convert the schematic into a PCB layout. The Multisim schematic is shown in Figure 5.1 and EAGLE PCB top layer is shown in Figure 5.14. The final selection of components used to supply the highpass and lowpass filters, ADC, and selectable gain are shown in Table 5-1.
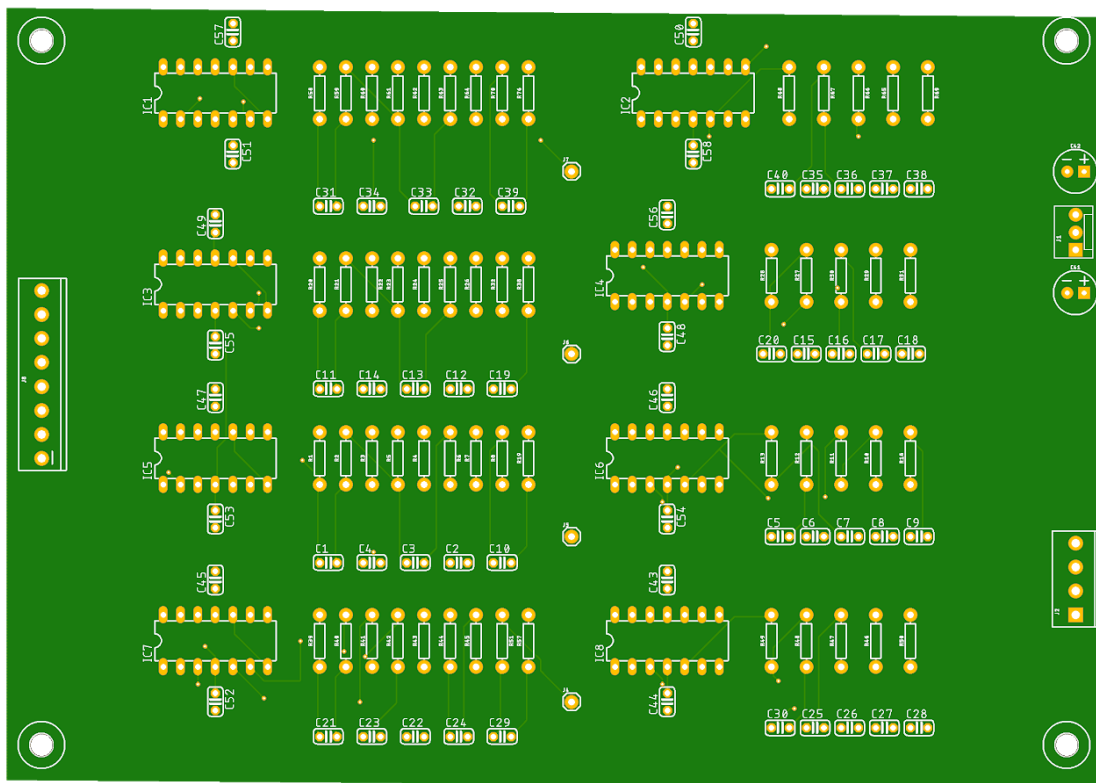
Figure 5.14: Top layer of the Wired EMG PCB Design (four channel system).

Table 5-1: Component specification for Wired EMG Implementation

Name	Component	Application	Image
AD713	Quad Operational Amplifier (14-pins)	Highpass/ lowpass filtering and selectable gain	
ECU40UT01	Medically isolated power supply	Powered the PCB and ADC	
NI-USB 6000	8 input 12 bits ADC	ADC	
DPS9111AK2	Push wheel switch	Selectable gain	

The AD713 is a quad operational amplifier that is used for applications of active filtering and has the desired CMRR of 80-100 dB at 60 Hz. Previous iterations of the EMG wired system were successful with the use of this IC, making it suitable for the PCB design. For each channel, two AD713 ICs are utilized. One IC is used for the high-pass filter and selectable gain. The other IC is used for the low-pass filtering. Any amplifiers not in current use were connected as a voltage follower with their inputs connected to ground/reference.

The DPS9111AK2 is a switch that allows you to adjust the gain selection for the wired system. The selectable gain values are, 1, 2, 4, 8 and 16. These values are achieved by switching

between various resistor values. The resistor values can be soldered directly to the switch housing, reducing wiring since the switch is mounted remotely from the circuit board. Each channel is allocated its own switch and it can display values from 0-9. The PCB also includes three connectors. An 8 pin connector is used to connect the electrodes provided to the 4 channel EMG system. A 3 pin connector is used for connecting the isolated power supply to the PCB board. The 4 pin connector is used to connect all 4 channels to the ADC module. The layout of the PCB, power supply, and ADC layout for the 4-channel system is shown in Figure 5.15.
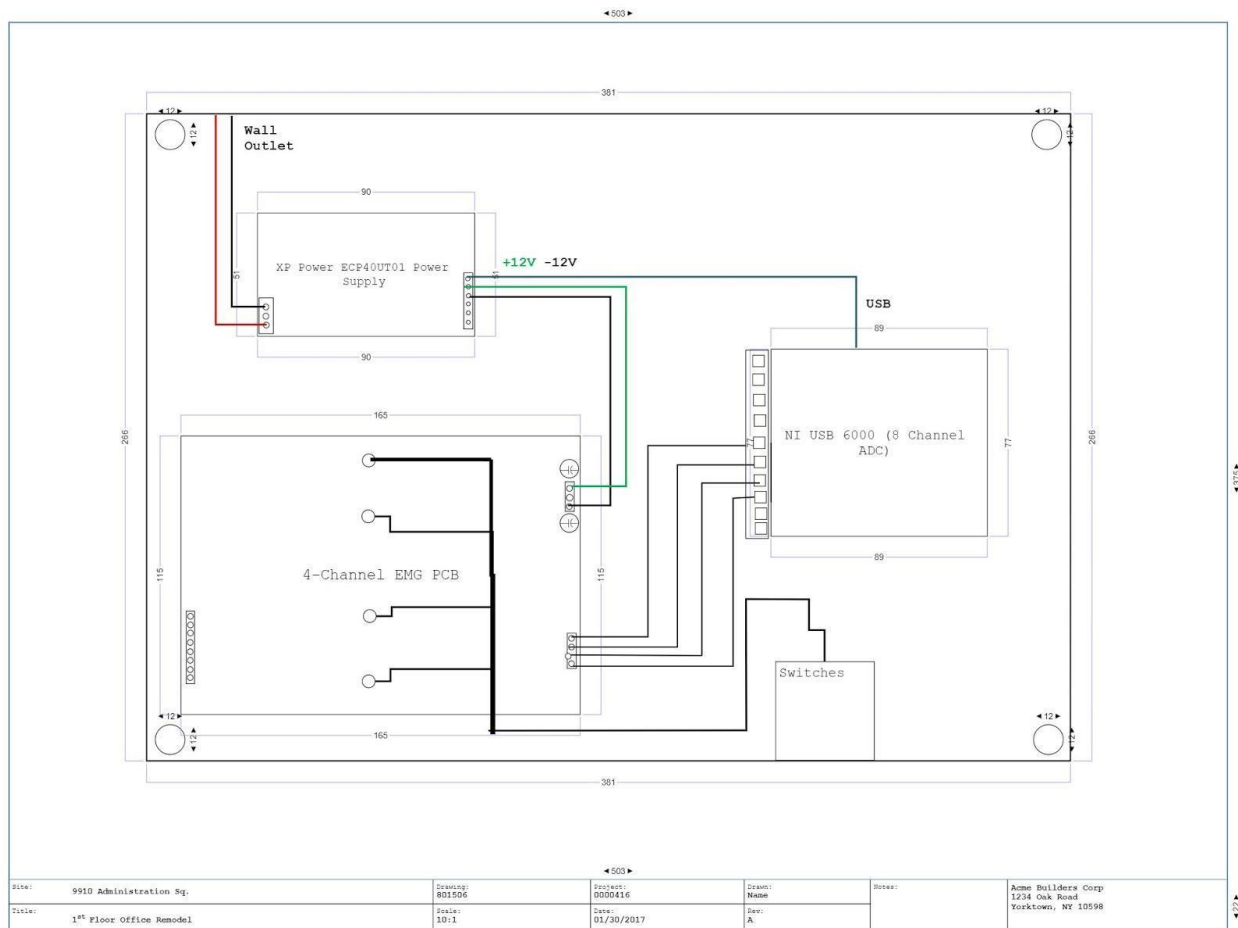
Figure 5.15: PCB, ADC Module, and Power Layout.

5.1.5 Wired EMG Component Selection:

EAGLE Auto-Desk provides several different footprint selections for each component. An additional library was added to EAGLE in order to use other packages. The SparkFun library contained the packages for the full-sized components needed for PCB development. The datasheets

for each component provide information on the size and specification for PCB layouts. The following figures show the selected packages for each component.

For the AD713 ICs, dip IC sockets are used to connect the ICs to the PCB. The dip sockets allow for easy testing and convenience to remove any ICs for debugging.
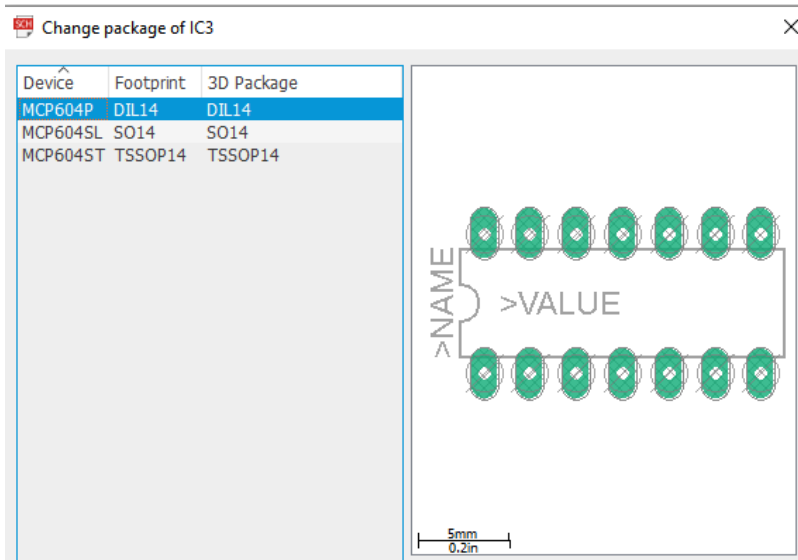
Figure 5.16: Package Specification for 14 Pin Dip Sockets In EAGLE.

The selectable gain is located on each channel. A 1 pin header is connected to the selectable gain IC in order to connect a wire to the switches and are found on the PCB layout in Figure 5.14.
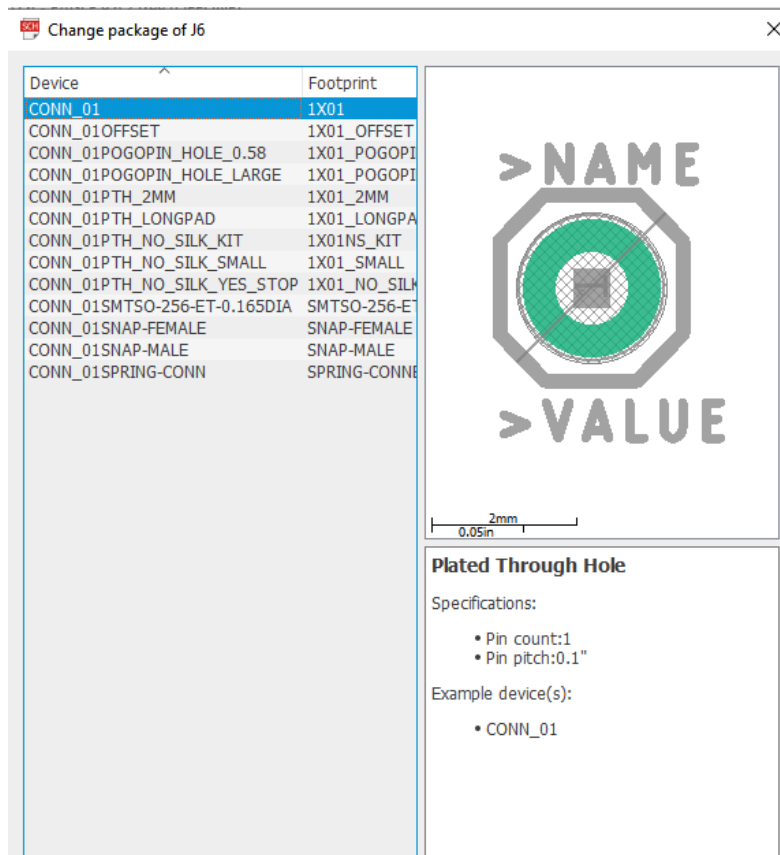
Figure 5.17: Package Specification for 1 Pin Header In EAGLE.

To connect all the components more efficiently, screw terminals and connectors are utilized in the overall PCB design to connect the power supply, ADC, and electrodes to the 4 EMG channels. Additionally, the PCB uses full size components so the accompanying packages for each component is outlined below. The resistors and capacitors used the same packages for all values.
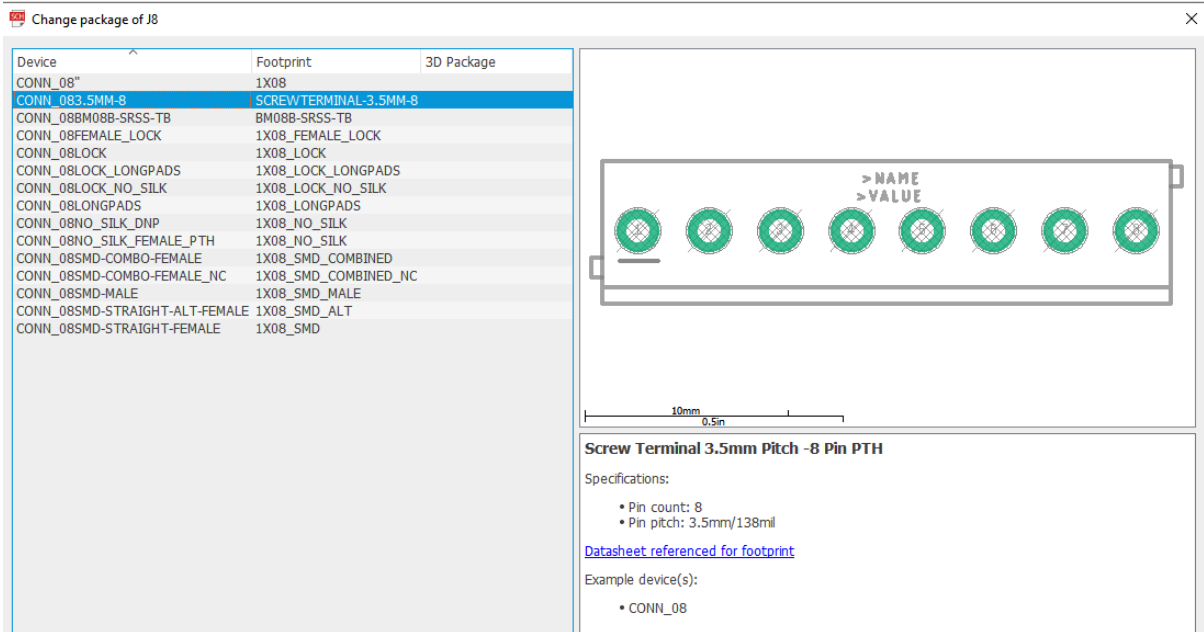
Figure 5.18: Package Specification for 8 Pin Header In EAGLE.
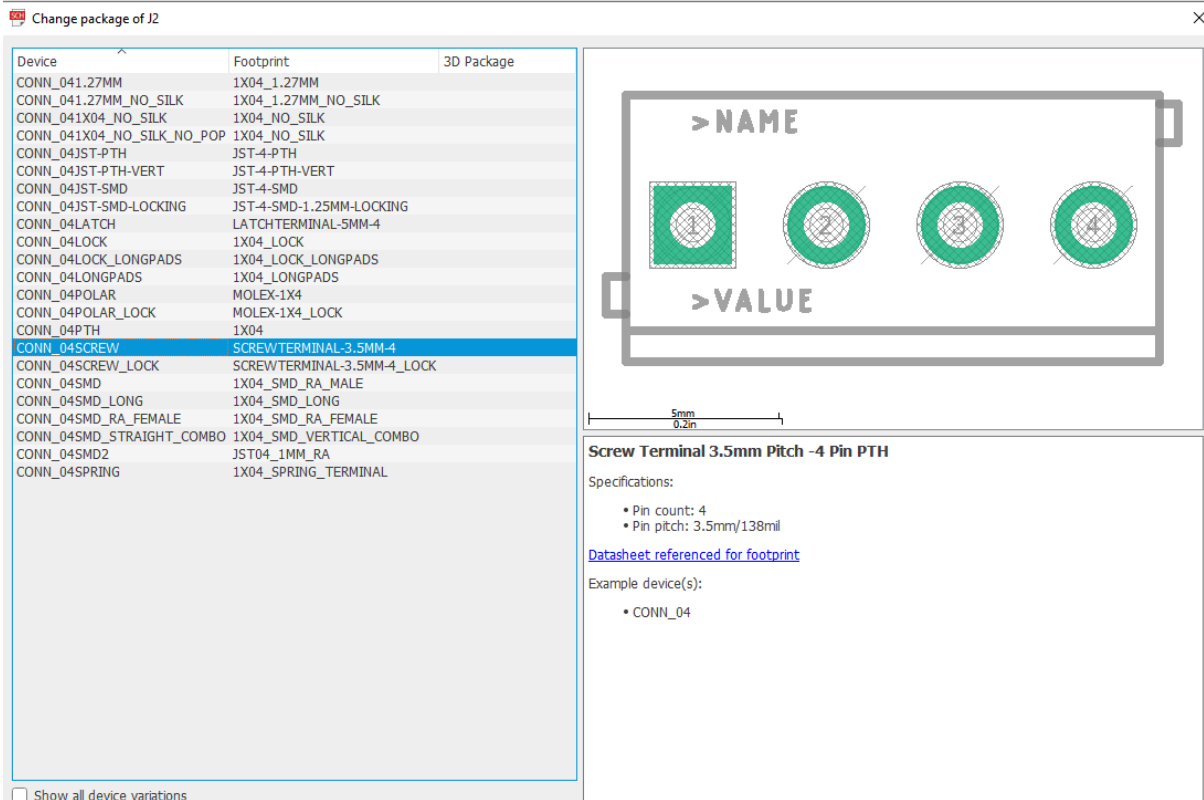
Figure 5.19: Package Specification for 4 Pin Header In EAGLE.
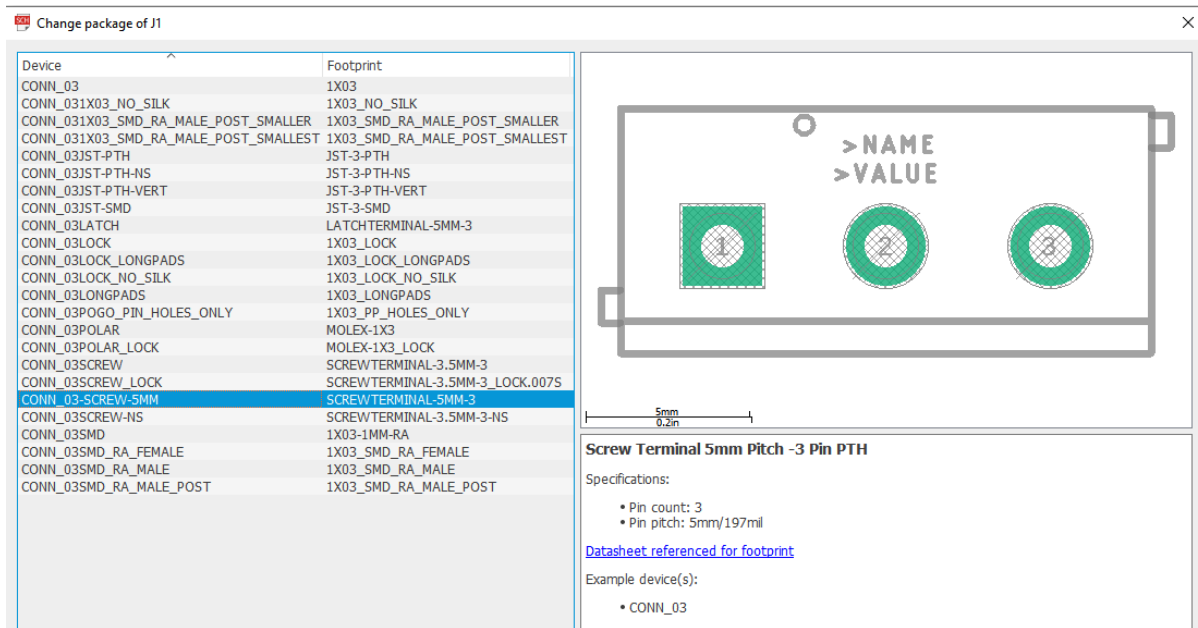
Figure 5.20: Package Specification for 3 Pin Header Used In EAGLE.
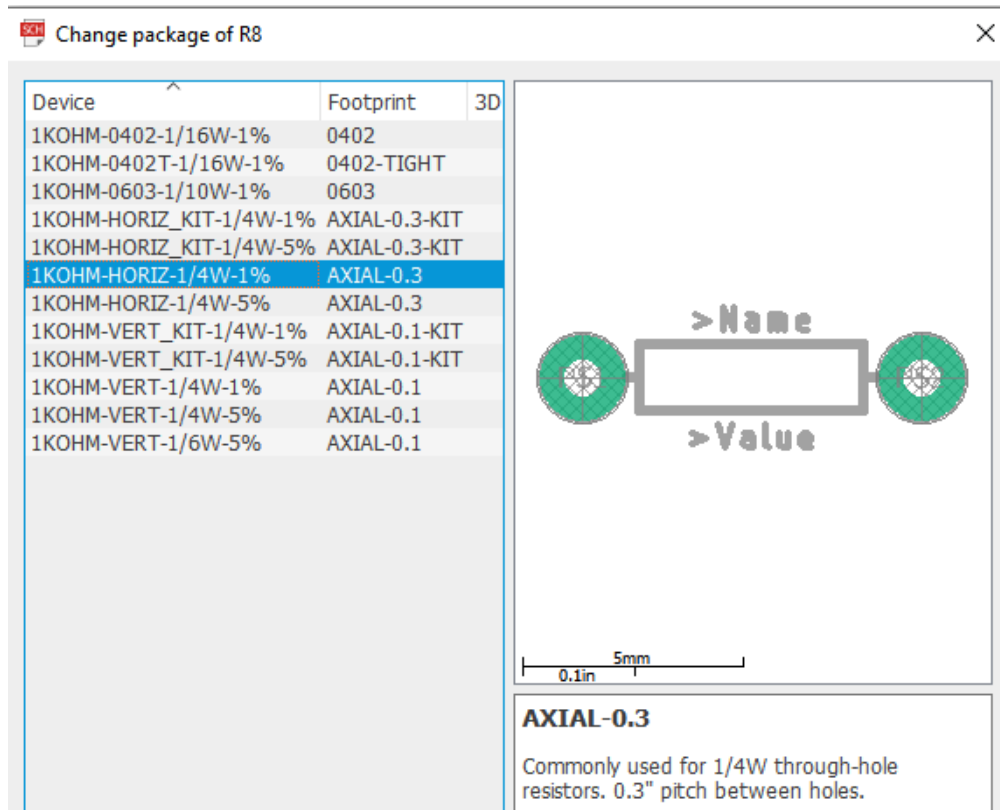
Figure 5.21: Package Specification For Resistors In EAGLE.
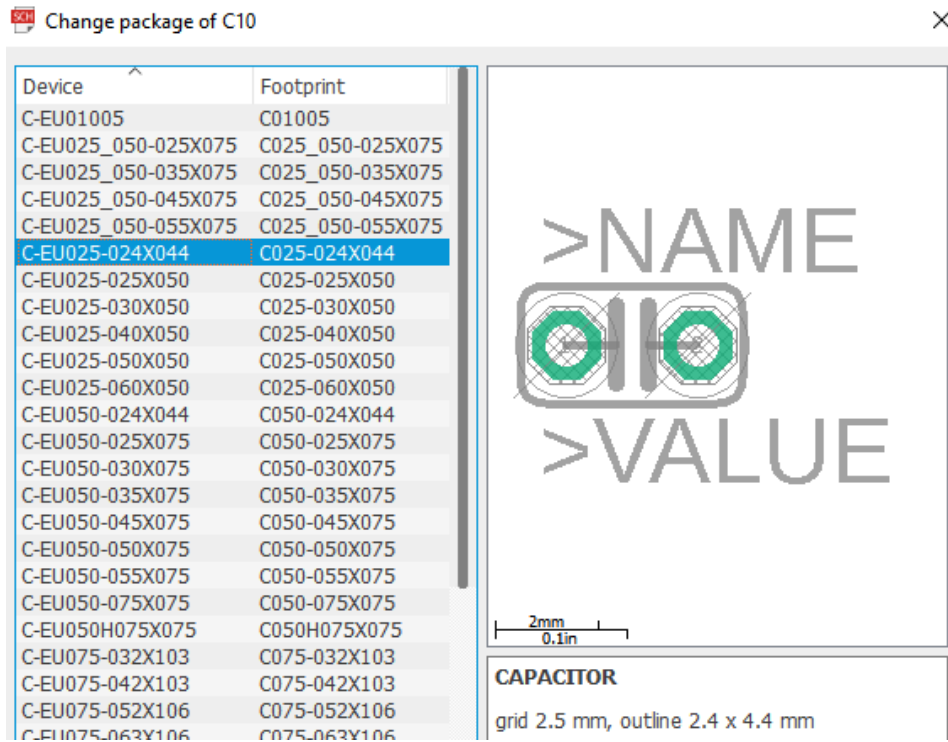
Figure 5.22: Package Specification For Capacitors In EAGLE.

Table 5-2: Component Packages

Component	Packages (Footprint)
1-pin Connector	1X01
3-pin Connector	SCREW TERMINAL-5MM-3
4-pin Connector	SCREW TERMINAL-3.5MM-4
8-pin Connector	SCREW TERMINAL-3.5MM-8
Resistors	Axial-0.3
Capacitors	C025-024X044
Dip IC Sockets	DIP14

5.1.6 PCB Layout and Fabrication:

The PCB schematic and physical layout were made using EAGLE Autodesk. The schematic on EAGLE is identical to Multisim's schematic. Connectors for the input and output

signals and for the power supply were added. The PCB is powered by a ± 12 V power supply, which is connected to the board through a 3-pin JST connector. A pair of 100 µF decoupling capacitors were connected to the power supply pins to attenuate noise from the power supply. By having a pair of large decoupling capacitors next to the power supply and a pair of small decoupling capacitors next to the power supply rail of each op-amp IC, the voltage that is used to supply the ICs will be more constant. The input signals from the electrodes are connected to an 8-pin screw terminal connector. The first four pins are connected to the input signals, the next three pins are connected to the ± 12 V power supply and ground, and one pin is not used. Finally, the output of the filters is connected to a 4-pin screw terminal so that they could be wired to the ADC. Four mounting holes are added to keep the PCB stationary inside the enclosure.
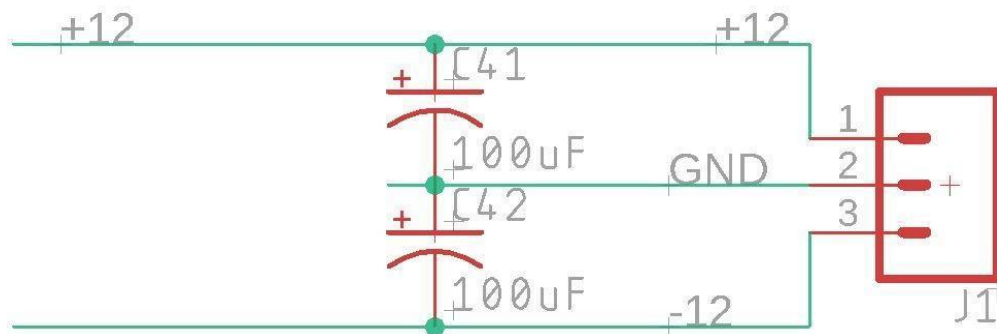
Figure 5.23: The schematic of the power supply connector
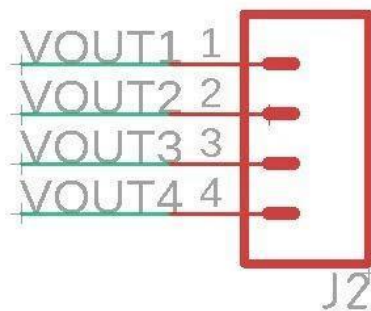
Figure 5.24: The schematic of the 4-pin connector
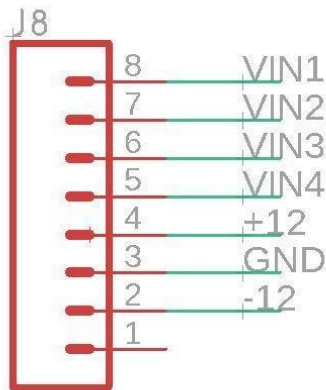
Figure 5.25: The schematic of the 8-pin connector.

Then, the schematic is converted into a physical layout using the "Schematic to Board" function in EAGLE. Due to the simplicity of the application and its technical requirements, the board consists of only two layers, which are top and bottom. The first consideration we had to make is the placement of the components' packages within the enclosure. We put the board in the lower left corner of the enclosure and the power supply and the ADC in the upper and lower right corner of the enclosure. Therefore, the input pins are placed on the left side of the board, and the output power supply pins on the right side of the board. The op-amp ICs, resistors, and capacitors are placed on the board in the same order as the schematic for ease of assembly. The decoupling capacitors are placed as close to the IC and the power supply pins as possible to optimize their purpose.

The next consideration that we had to make is the width and the clearance of the traces. According to the datasheet from Analog Devices, The AD713K IC has a maximum quiescent current of 12 mA, so for eight ICs the maximum current is 96 mA. Since that is not a large amount of current, the width of the copper traces is set to 6 mils. Furthermore, because the signals don't have high frequency, the traces can be close to each other without interfering with the signals. Therefore, the clearance of the copper traces is set to 10 mils. These parameters can be adjusted in EAGLE in the "Net classes" menu. Even though different parameters can be set for different sets

of copper traces, we decided to set the same parameters for all of our copper traces since it matches the technical requirements that we want to achieve.
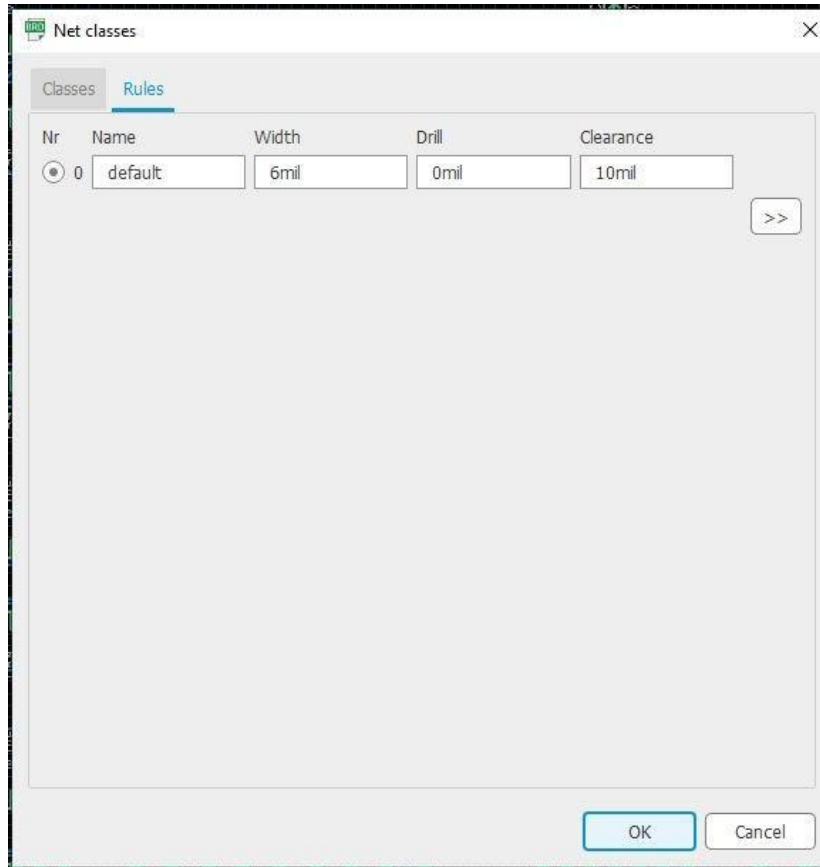
Figure 5.26: Net classes menu.

The last consideration that we had to make is the ground tracing. Because there is resistivity in copper traces, grounding components using traces could create inaccuracy in the readings because of the unwanted resistivity. According to the equation to calculate the resistance of a wire, we can see that by increasing the width of the wire, the resistance is decreased. Furthermore, by using copper traces to connect components to ground, ground loops might be introduced. A ground loop can happen when multiple components are connected to the same ground through different wires. These loops can pick up interference currents, which would alter the measurement. Furthermore, wires that have different lengths would have different resistance, so the components' reference point might be different. We decided to create a ground plane on the top layer of the

PCB to solve those problems. Because the ground plane is large, its resistance is minimized and all components can be connected directly to ground without using ground traces. The equation below describes the resistance of a wire based on the resistivity of the element that the wire is made out of, the length, width, and thickness of the wires.

$$R = \frac{Resistivity \times Length}{Width \times Thickness}$$

The components are automatically wired using the "Autorouter" tool in EAGLE. The wiring is customized so that all of the traces run vertically on the top layer and horizontally on the bottom layer for ease of adjustment. To connect the top traces with the bottom traces, vias are added to the PCB. There are 26 vias in total on this board. The final PCB layout is shown in the figures below.
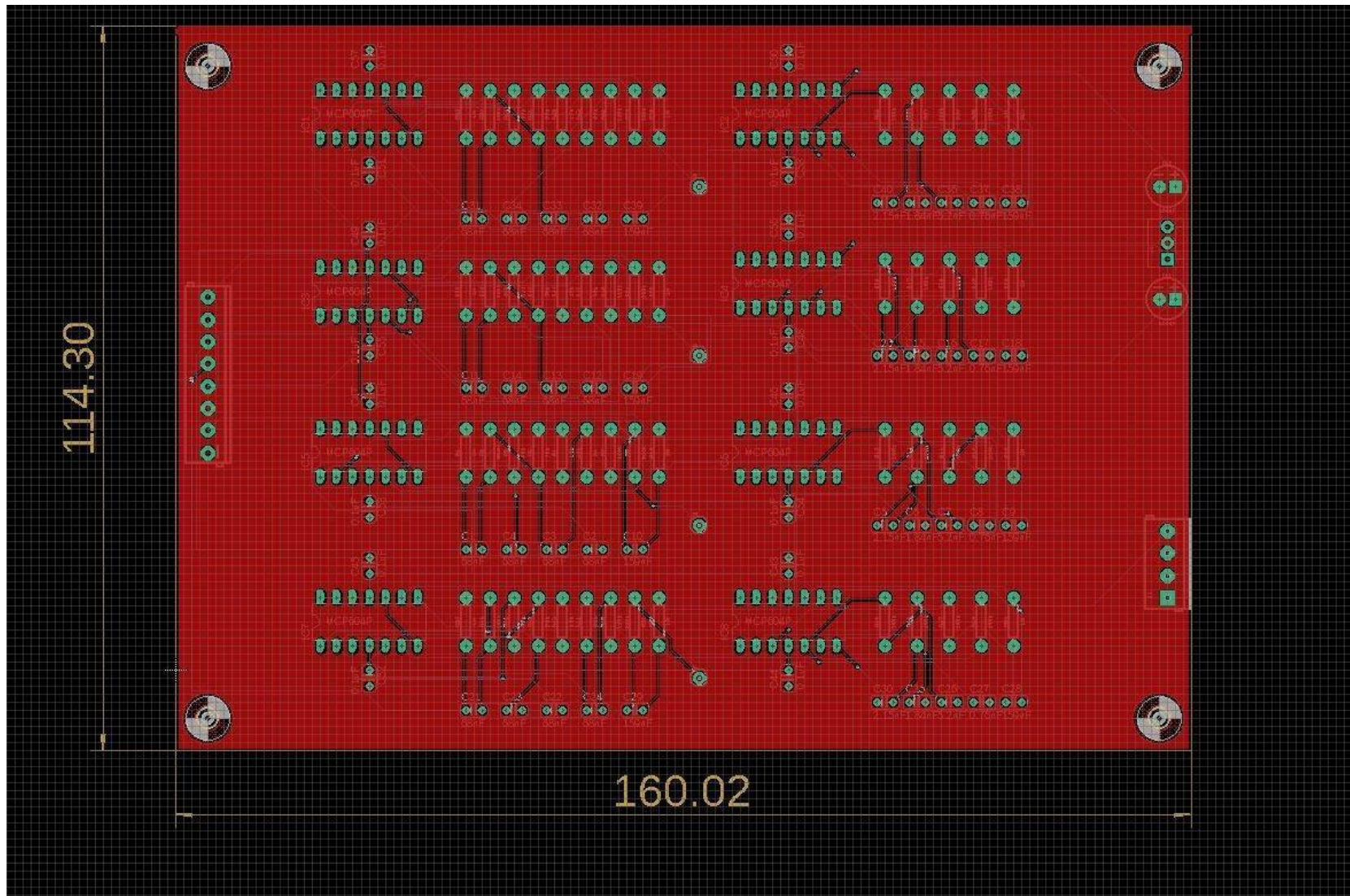
Figure 5.27: The top layer and the dimension of the PCB. The dimensions are measured in millimeters.
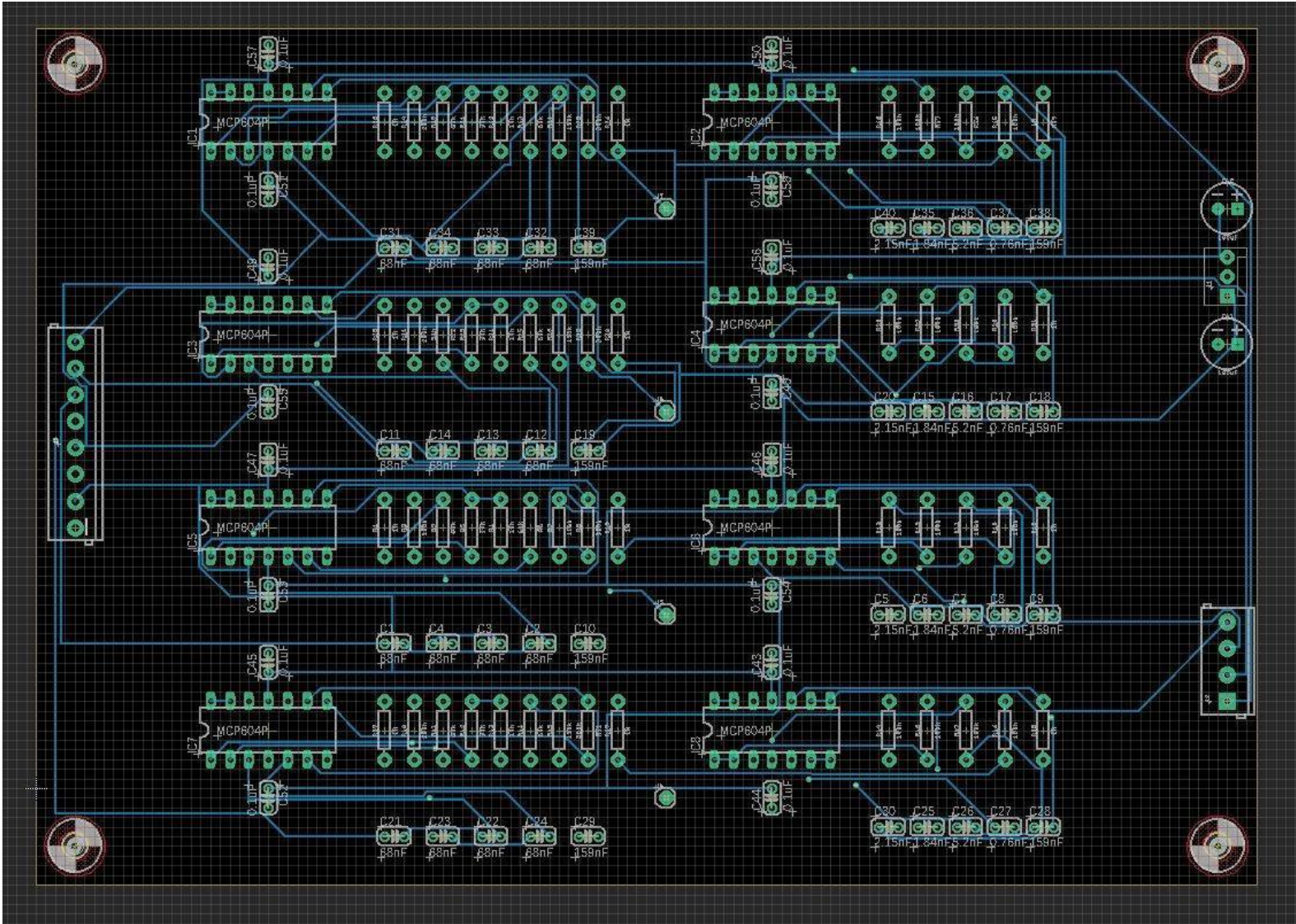
Figure 5.28: The bottom layer of the PCB.

We chose to use OSH Park to fabricate our PCB and they required a PCB mask to be put in Gerber format. Therefore, we downloaded the "OSH Park design check" to make sure that there are no critical errors on our PCB and converted the PCB mask to Gerber format. Once ordered, the fabrication process took 2 weeks to complete and we received 3 PCBs in one order. Below are the pictures of the PCB.
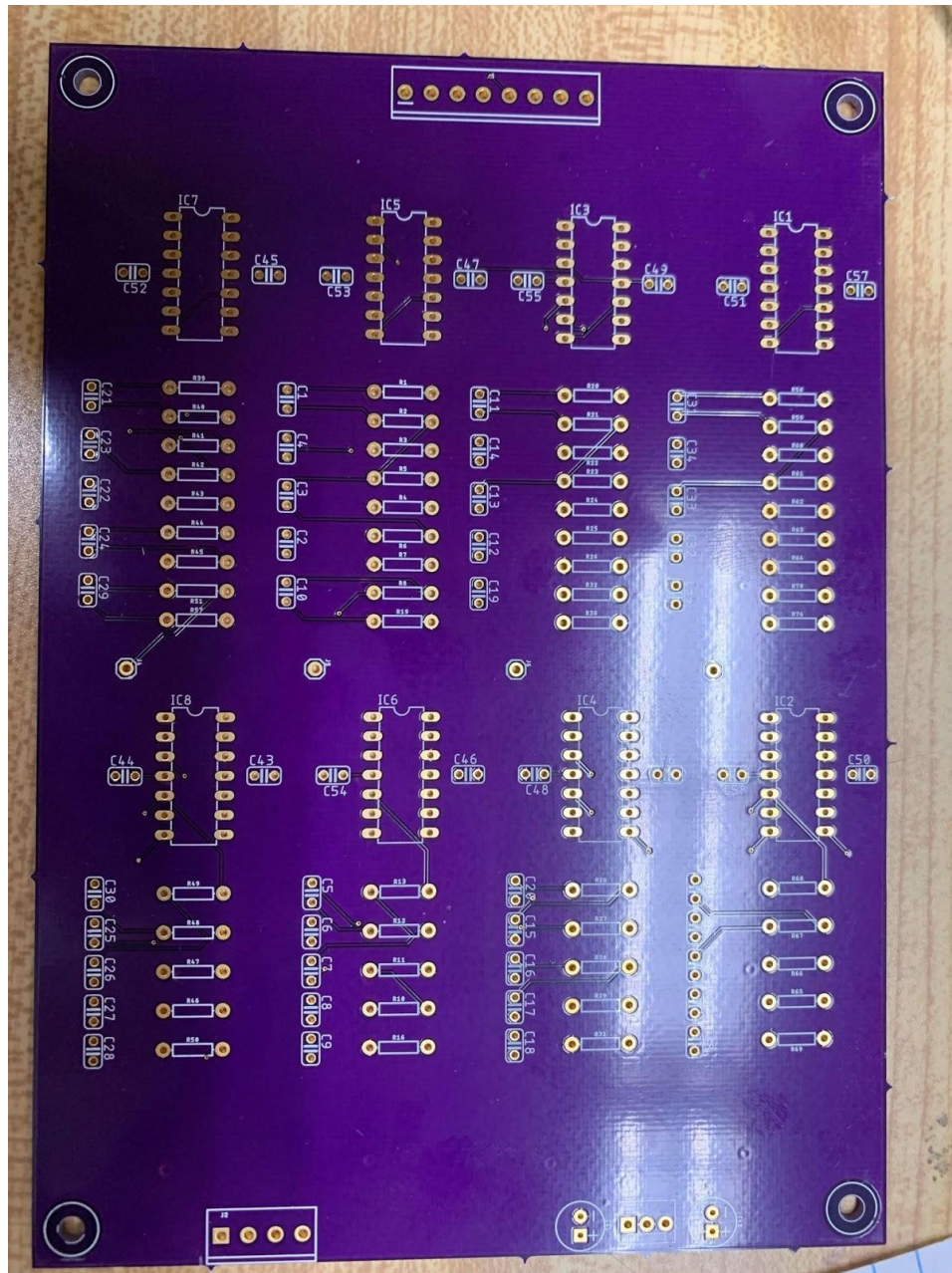
Figure 5.29: The top side of the PCB
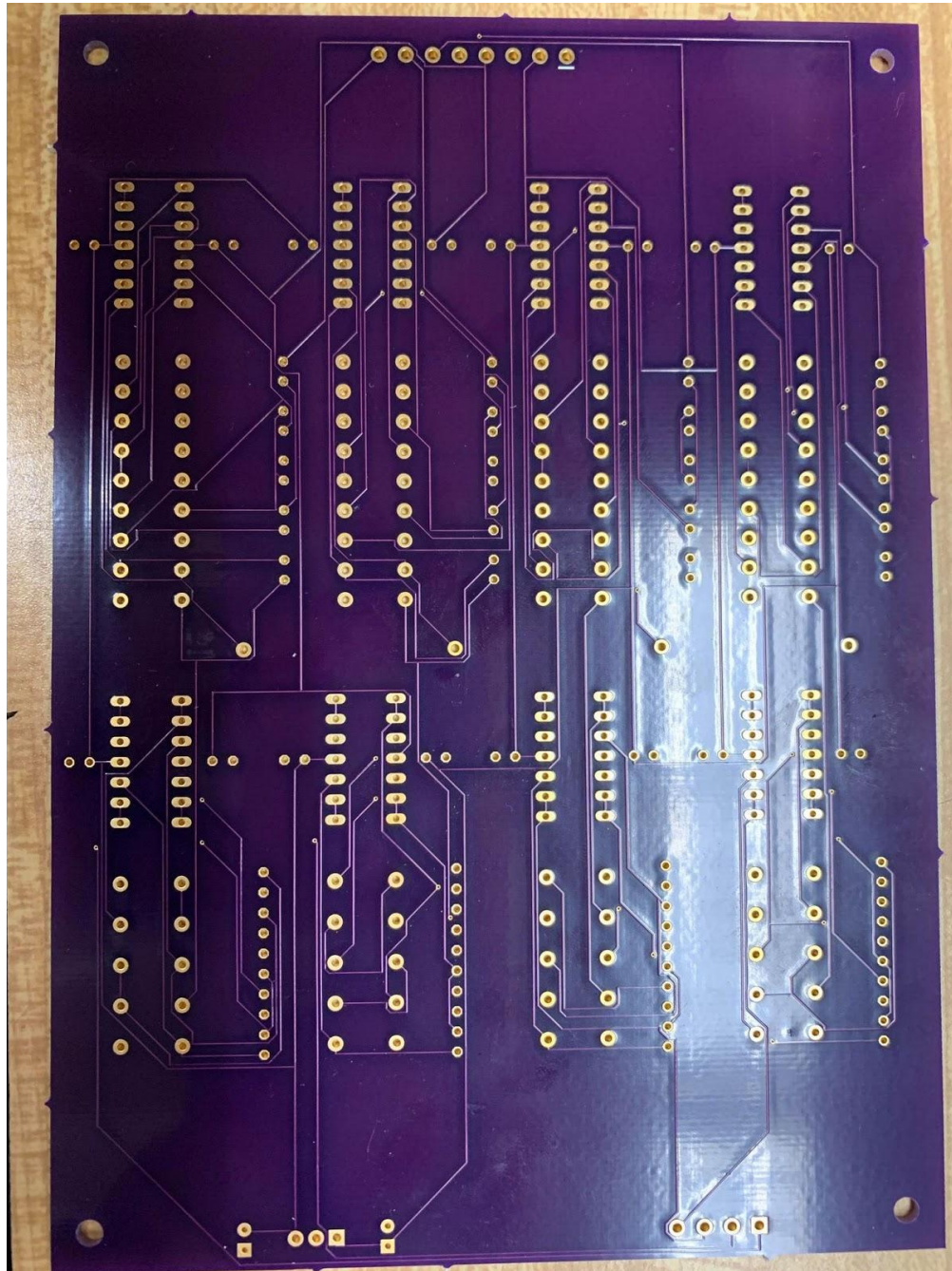
Figure 5.30: The bottom side of the PCB

5.1.5 Wired EMG PCB Assembly and Testing:

Below are pictures of the soldered PCB, the soldered selectable gain switch, and the connectors of the system. Since the components were placed on the PCB to maximize the ease of construction, the components are soldered from left to right.
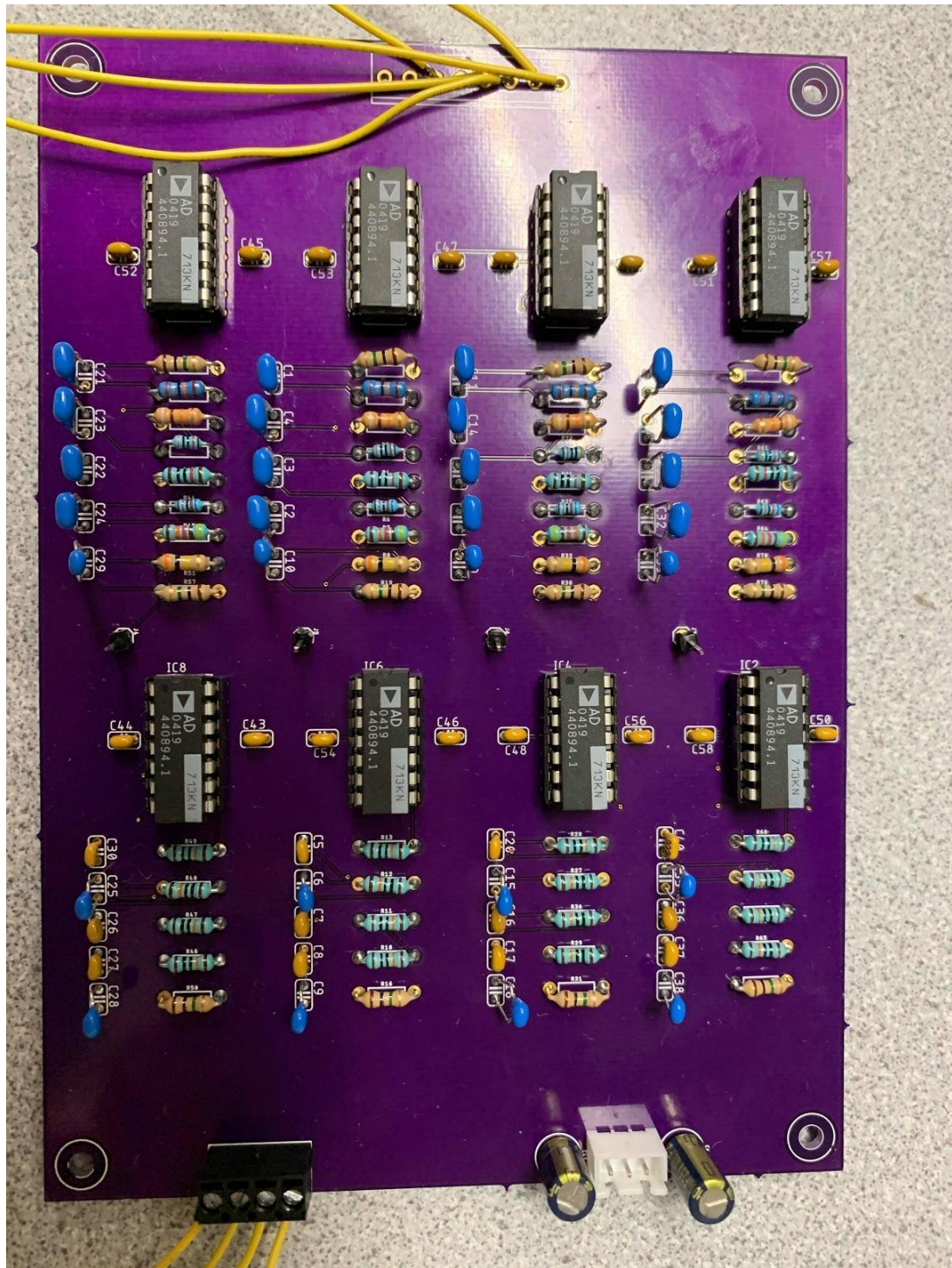
Figure 5.31: The finished PCB. One EMG channel per column
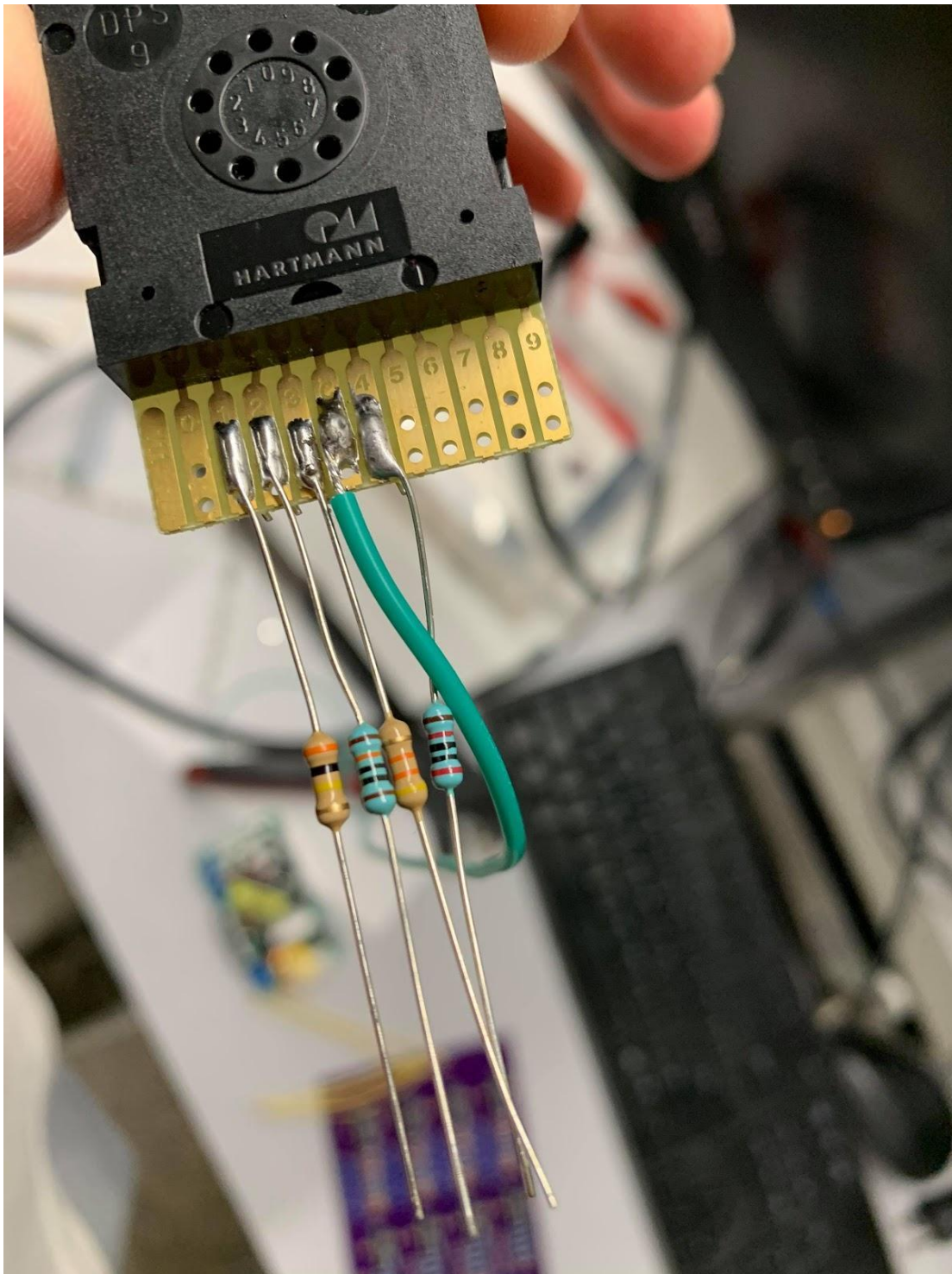
Figure 5.32: The resistors are soldered directly to the push wheel switch to create a switch that can select the gain of the channel.
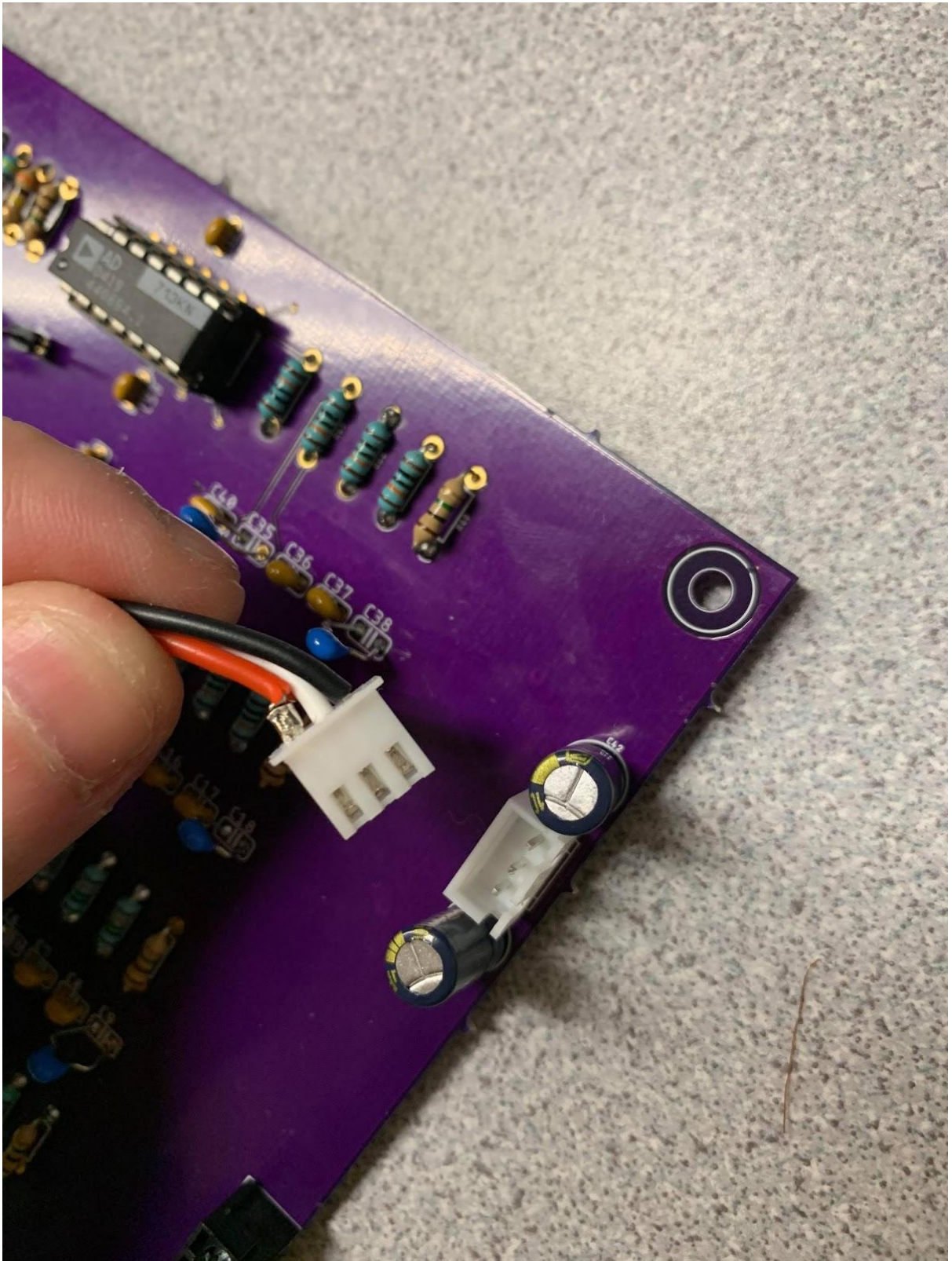
Figure 5.33: The JST-XH 3-pin connector used to connect the PCB to the power supply
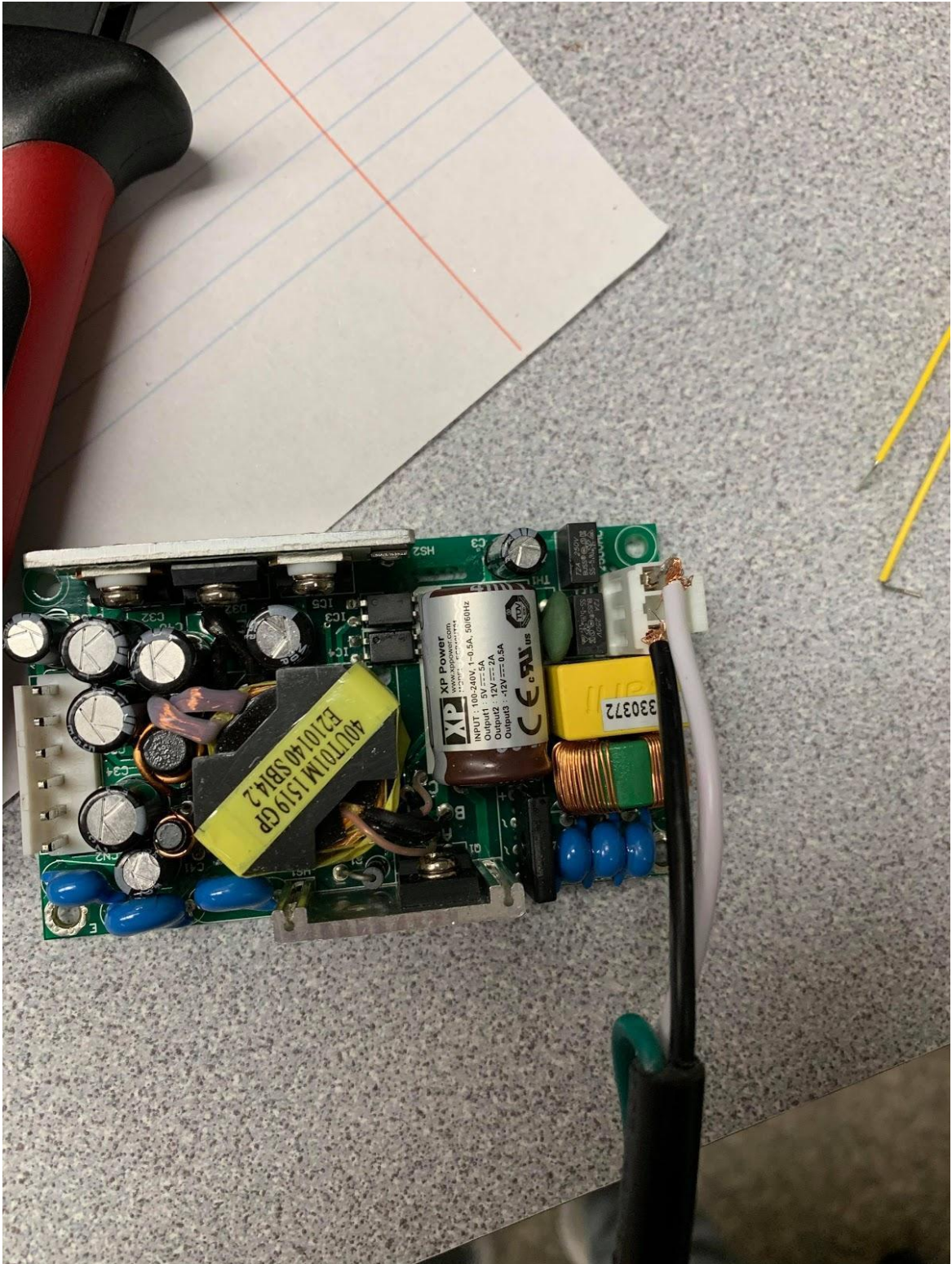
5.34a
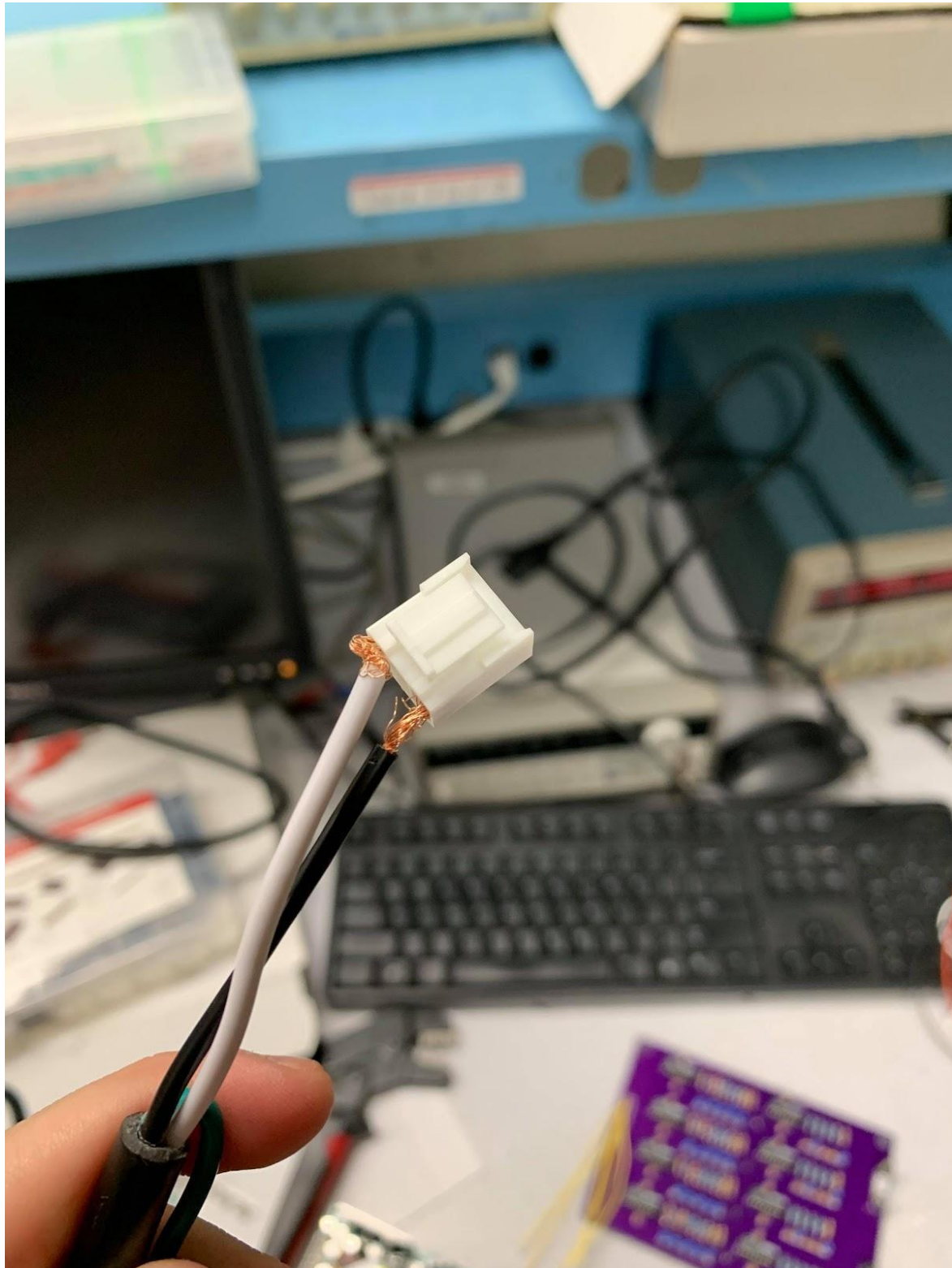
5.34b

5.34c
Figure 5.34a, b and c: The connectors used on the power supply are the JST VH 3-pin and 6-pin connectors.

When all components were soldered to the PCB, the PCB was tested to ensure the accuracy of the measurement. The magnitude response of all channels was recorded and plotted in MATLAB (PCB_Testing.m), which is shown in the figure below. The main difference between the theoretical and experimental magnitude response of all channels is due to the tolerance of the capacitors and resistors, and the thermal condition of the op-amp.
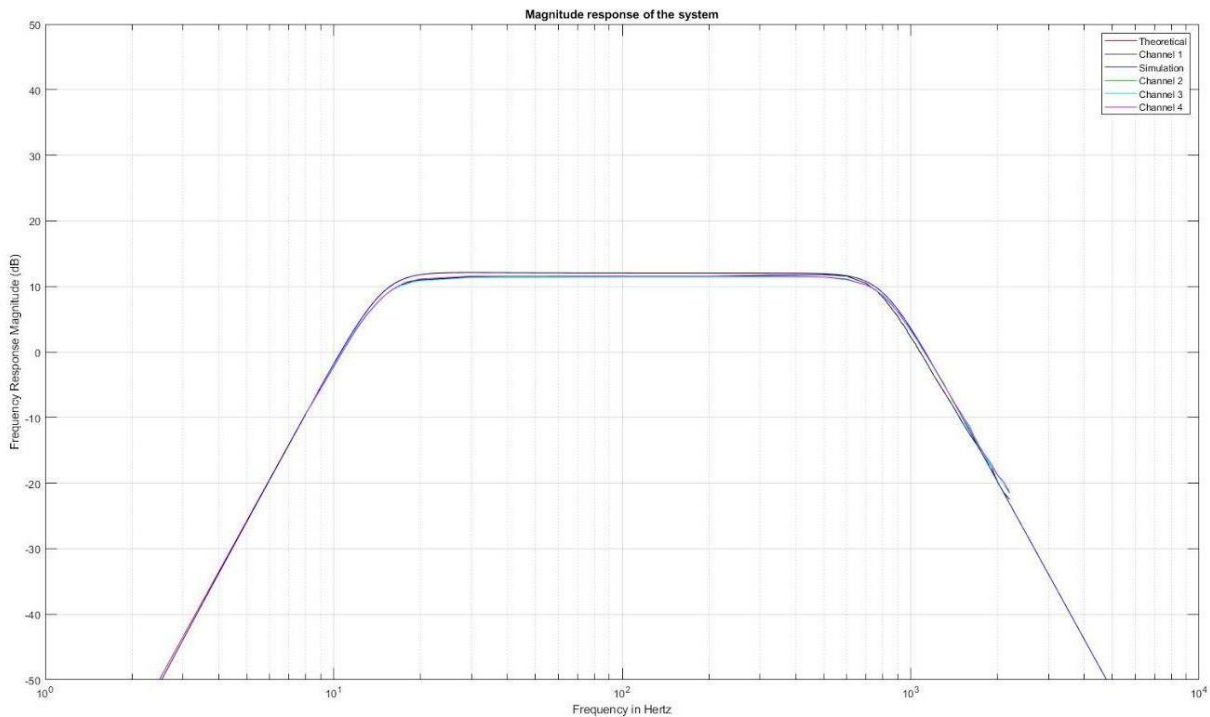
Figure 5.35: The magnitude response of all channels. The black, green, cyan and pink lines represent the frequency response of channel 1, channel 2, channel 3, and channel 4, respectively.

Furthermore, the selectable gain stage of the system was also tested. The test was conducted by amplifying an input sine wave with a frequency of 400 Hz and an amplitude of 0.232 V peak to peak. The result is shown in the table below. The error between the theoretical and experimental gain of the system exists because of the tolerance of the resistors and the non-ideal push wheel switch.

Table 5-3: Wired EMG experimental gain results

Theoretical gain (V/V)	The amplitude of the input signal (Vpk-pk)	The amplitude of the output signal (Vpk-pk)	Experimental gain (V/V)	Error percentage (%)
4	0.232	0.88	3.79	5.25
8	0.232	1.68	7.24	9.5
16	0.232	3.28	14.14	11.625
32	0.232	6.56	28.28	11.625
64	0.232	13	56.03	12.45

5.3.2

5.3.3   5.1.6: Wired EMG Signal Acquisition and Analysis

Finally, the system was tested using electrode-amplifiers to measure EMG signals. The electrode-amplifiers were connected to the input of the PCB. Then, they were attached to the forearm to measure the EMG signal at different points of the arm, which was recorded using the NI-USB 6000 ADC. To obtain a consistent reading, electrode gel was applied onto the forearm. The measurements were taken when the subject flexed their forearm for 5 seconds and rested for 5 seconds, then the action was repeated several times to ensure that we acquired enough data for the analysis. The raw data of the EMG measurement and the power spectral density (PSD) graph of the reading are presented in the figures below. In the figure, the EMG PSD was estimated using data while the arm was flexing and the noise PSD was estimated using data while the arm was resting.
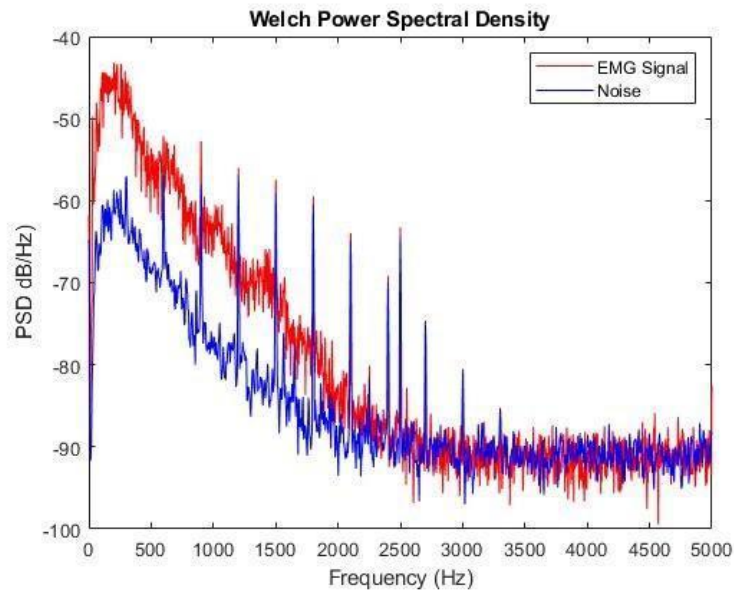
Figure 5.36: The Welch Power Spectral Density plot of the EMG signal and noise of the measurement.

As we can see from Figure 5.36, the power spectral density plot matches our expectations. At a significantly low frequency (i.e. <15 Hz), there is little power from the signal with a magnitude of around -80 dB. This is because, at low frequency, every signal is eliminated by the high-pass filter. Furthermore, we can see that the maximum PSD value for both measurements is at around 300 Hz, which is the frequency value that lies in the middle of the passband. However, starting from 600 Hz, there are signals that have a significant amount of power with a frequency increment of 300 Hz, which means that there is a 300 Hz noise inside our system. A possible solution to resolve this problem is to attach the electrodes 30 minutes before taking any measurement.

94
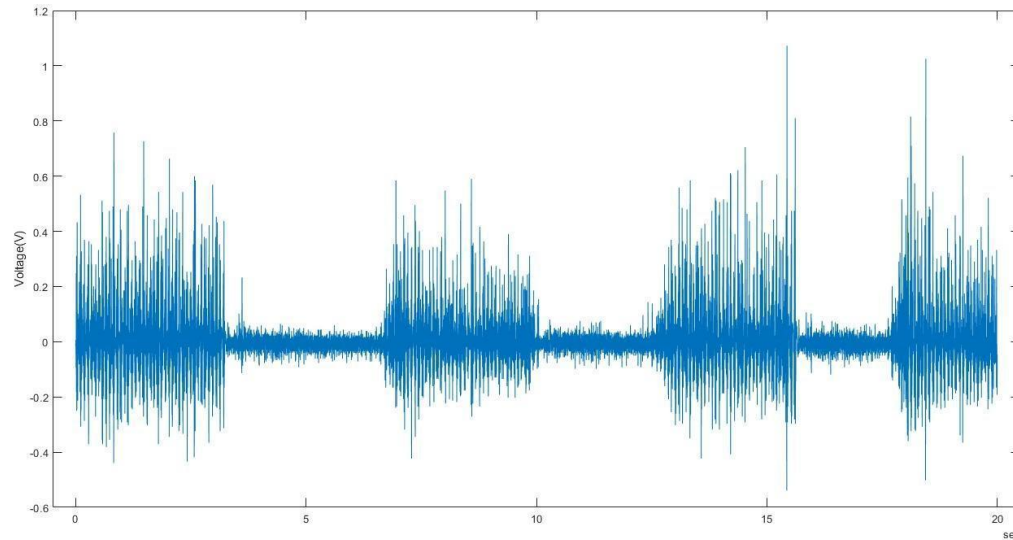
Figure 5.37: Raw data of the EMG signal from Channel 1 of the system with a gain of 8 from the selectable gain

5.1.7 Wired EMG-Further Testing of PCB :

With the system working as desired, the wired EMG system was tested using a prosthetic hand. Graduate students who work with Professor Clancy, were able to connect our front-end EMG system to the prosthetic hand-wrist system via a PC-based prosthesis controller. The wired EMG system was connected to the encased electrode-amplifiers and an ADC module that was provided by the graduate students. The ADC was USB-based and connected to the PC controller. The figures below display the set of the wired system and electrodes used to facilitate the testing. The link to video footage of the system working is here and can also be found in Appendix E. Our four-channel EMG system successfully controlled the prosthetic hand-wrist in both one degree of freedom and two degrees of freedom.
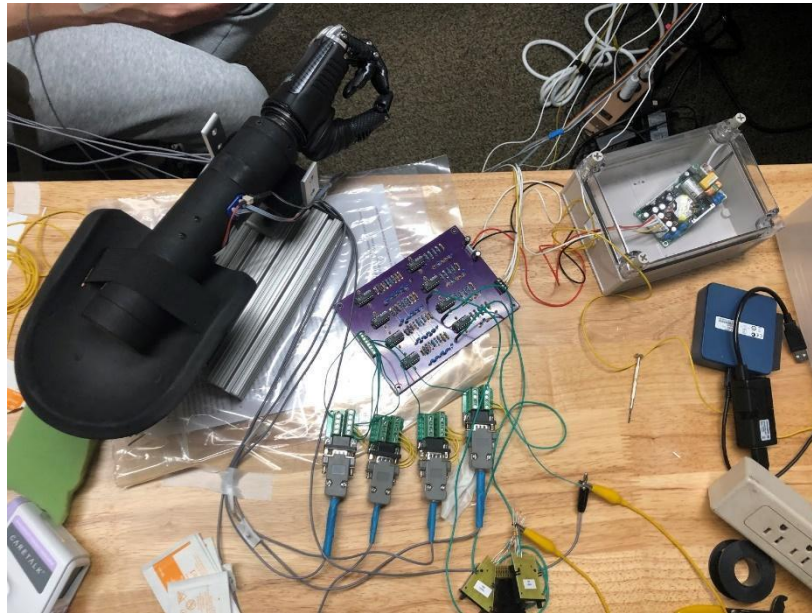
Figure 5.38: Wired EMG System Connected to Prosthetic Hand

Figure 5.39: Electrode Placement for Testing Wired EMG using Prosthetic Hand

5.2 Wireless EMG System Design Implementation

The wireless systems share many traits in their design implementations. Both systems consist of an instrumentation amplifier stage, a high pass filter, a selectable gain, a low pass filter, and a level shifter. Following the level shifter, the signal is fed into the ADC of a peripheral node microcontroller. This signal is then sent via Bluetooth to the central node—another microcontroller that connects via USB to a laptop and can show real time values in a MATLAB application.

5.2.1 Wireless EMG Instrumentation Amplifier

The first stage the signal goes through is the instrumentation amplifier. The instrumentation amplifier device used was an AD620 which has an internal resistor of 49.4 kΩ (in actuality, two internal resistors of 24.7 kΩ). The gain equation is as follows:

$$G = \frac{49.4 \, k \, \Omega}{R_G} + 1$$

The connection diagram of the AD620 shows the chip layout in Figure 5.40.

CONNECTION DIAGRAM
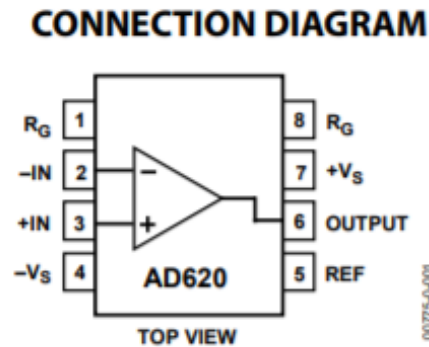
Figure 5.40: Connection Diagram of AD620 (www.analog.com)
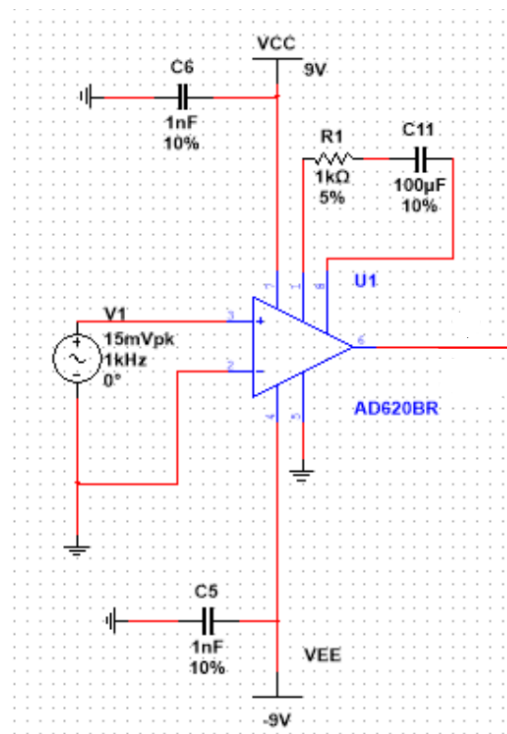
Figure 5.41: EMG Instrumentation Amplifier & Simulation Test Circuit

The configuration for the instrumentation amplifier is shown above in Figure 5.41. Connected to the instrumentation amplifier, is the 1 kΩ resistor , R1, for a gain of 50 and a 100 µF capacitor, C11, for the gain to be 1 at DC instead of 50. This creates an effect similar to that of a high pass filter where lower frequency signals are attenuated.

For simulation purposes, the input signal was set as a 15 mV peak sine wave to test the effect of the gains on a worst case scenario signal, one that could be too large and saturate the ADC. The value 15 mV was chosen for simulation because it is on the larger end of possible amplitudes in an EMG signal. The actual signal is expected to be much smaller. In order to gather an actual EMG signal from a person, three electrodes will be placed on that person. These electrodes provide the signals used to acquire an actual EMG signal and are the input signal to this system. The electrode configuration is further explained in the PCB subsection of this section.

For the experimental data, a 750 Ω resistor was used for a gain of 66. This resistor was replaced with a 1 kΩ resistor in the final system for a gain of 50. The experimental data show the

magnitude response plotted against an ideal response computed in MATLAB using the following function. The ideal response is based on the equation:

$$H(\omega) = 1 + \frac{2R_1}{R_G + \frac{1}{1j \times \omega \times C_G}}$$

where RG and CG are R1 and C11 from Figure 5.41, respectively. R1 is the internal resistor 24.7 kΩ. The frequency was plotted against a range of relevant frequencies to this project and experimental data were captured using the following method. Code is attached below in Appendix B. Using a Bitscope BS10, the input of the instrumentation amplifier was compared to the output and the gain was calculated by dividing the output peak to peak voltage by the input peak to peak voltage. These gains were calculated across the range of 0-200 Hz frequency for the input signal. Due to the high-pass like characteristic of the magnitude response, there was no need to go much further beyond 200 Hz frequency for testing as the gain levels out to a constant value. The data points were also limited (especially on the low end of frequencies) by the Bitscope BS10's capabilities; the function generator had limited frequency settings. The input signal was a 0.05 V sinusoidal wave produced by the Bitscope. The magnitude response of the instrumentation amplifier is shown in Figure 5.42 below. The recorded data correlates with the expected response.
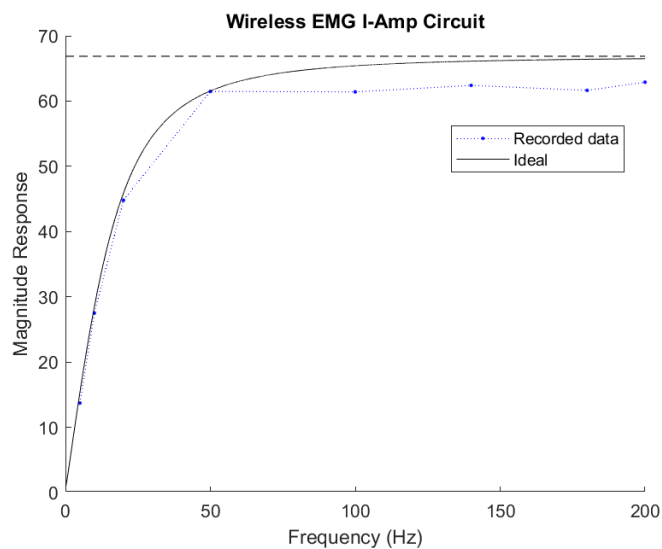
Figure 5.42: Magnitude Response of instrumentation amplifier in EMG circuit

5.2.2 Wireless EMG Filter Design

      This design cascades two second order Butterworth filters, one a high pass and the other a low pass. The filters were implemented with Sallen-Key topology described in background section 2.4.2 and their values were determined by MATLAB functions "butter_hi_design" and "butter_lo_design". The functions were designed to calculate the required resistors after pre-selecting convenient capacitors and the desired cutoff frequencies supplied.
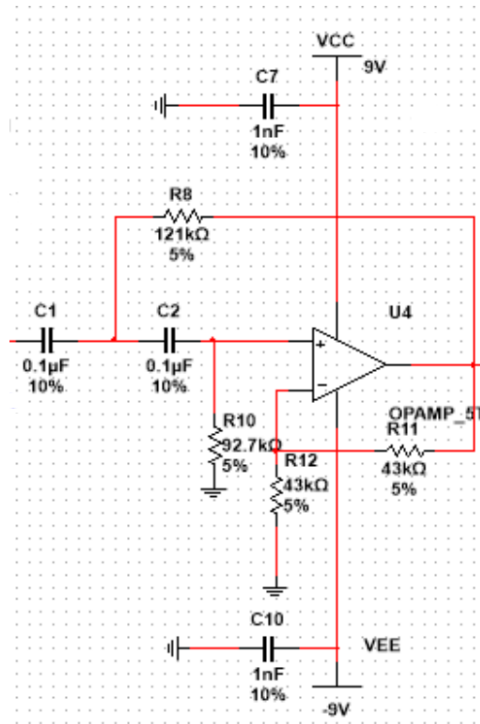
Figure 5.43: EMG high pass filter circuit diagram

      Figure 5.43 above shows the schematic for the high pass filter. The second order Sallen-Key high pass filter was designed to have a cut off frequency of 15 Hz and a gain of 2. Components C1, C2, R8, and R10 were selected as described previously, to achieve the necessary cut off frequency of 15 Hz. Meanwhile, the resistors R11, and R12 create the gain of 2 at the negative terminal of the op-amp. The two resistors had to be equal to each other.

      The value 43 kΩ was selected for both resistors because it was a convenient choice regarding inventory. In addition, higher resistances were preferred in order to keep current low.
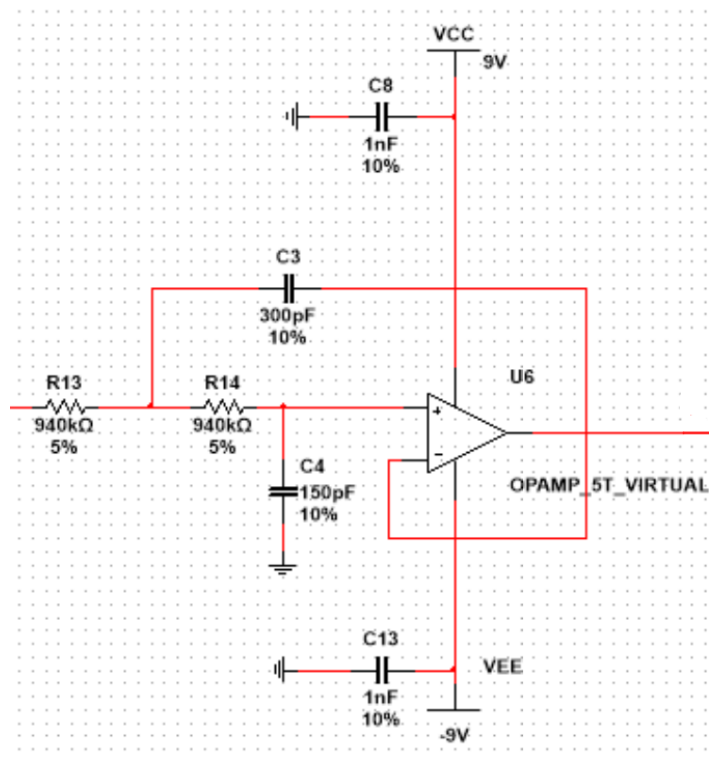
Figure 5.44: EMG low pass filter

The low pass filter, shown above in Figure 5.44 is designed for a cut off frequency of 800 Hz and a gain of 1. Components R13, R14, C3, and C4 determine the cutoff frequency. Because this stage does not add a gain to the system, no components were added to the negative feedback loop. Overall the frequency response of the cascaded system was meant to have a bandpass from 15-800 Hz.

The system was simulated using NI Multisim. The graph below shows the frequency magnitude response of the system which was captured using the bode plotter tool within Multisim. Once the simulation was approved as having the correct bandpass, the system was constructed on a breadboard. Then experimental data were gathered to verify the design. Figure 5.45 below shows the magnitude response achieved on the breadboard system. The 3-dB cutoff for the system is located as expected at around 15 Hz and 800 Hz.

| ← | 15.395 Hz | 3.242 dB | → | ← | 775.113 Hz | 3.257 dB | → |
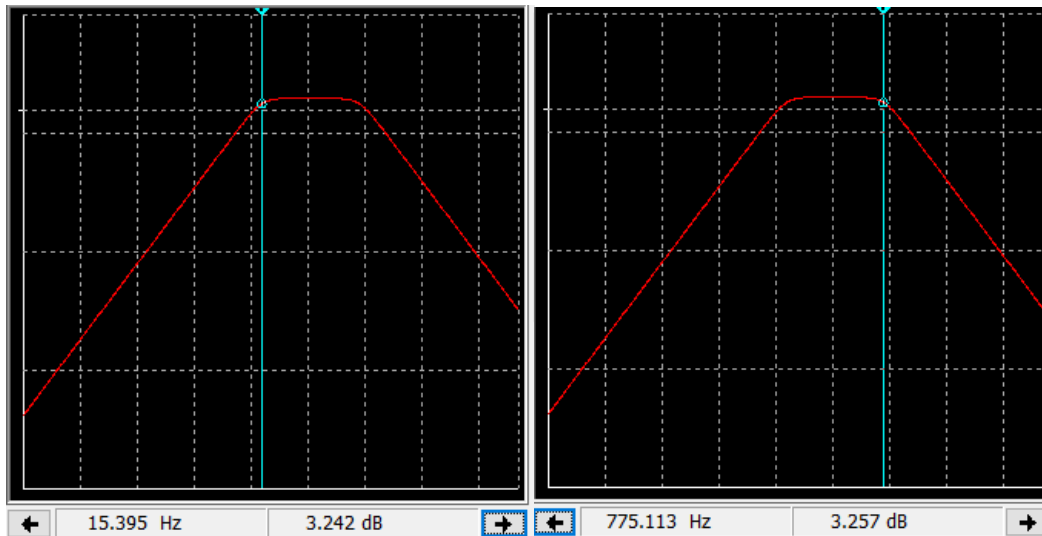
Figure 5.45: Bode plot of simulation for EMG low pass (left) and high pass (right) filters

The experimental data were collected by taking the peak to peak voltage of the input and comparing it to the peak to peak voltage of the output. The input was a 1 V peak to peak sine wave provided by a Tektronix CFG253 3 MHz Function Generator. The output of the filters was collected at different input wave frequencies using a Tektronix TDS 210 Two Channel Digital Real-Time Oscilloscope. The gain was calculated by dividing the output peak to peak voltage by the input peak to peak voltage. Figure 5.46 below shows the plotted ideal response, against the simulated response, and the experimental data captured in testing. The simulated response from Multisim and the MATLAB ideal response overlap completely, which is expected as both are meant to be ideal. In addition, the experimental data gathered aligns closely to the expected values. Differences in the experimental data and the ideal expected output can come from various sources, but one of the likely explanations is the component tolerances which can add to the margin of error significantly.
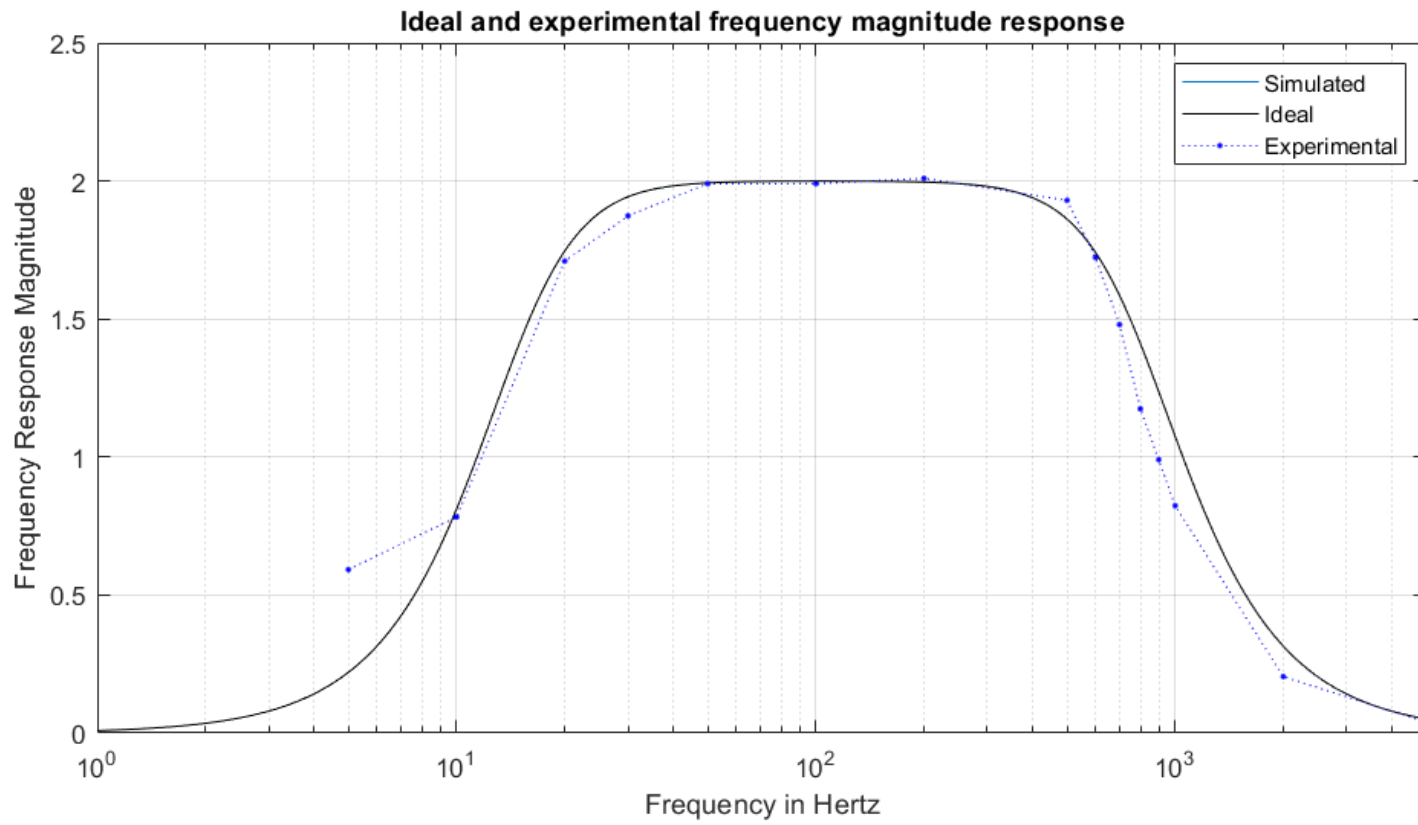
Figure 5.46: Experimental vs ideal vs simulated frequency magnitude response

5.2.3 Wireless EMG Selectable Gain

The selectable gain is a simple non-inverting operational amplifier. The gain was designed to keep the signal in the range of the ADC but can be modified depending on the resulting signal during testing. The configuration below is shown here in Figure 5.47.
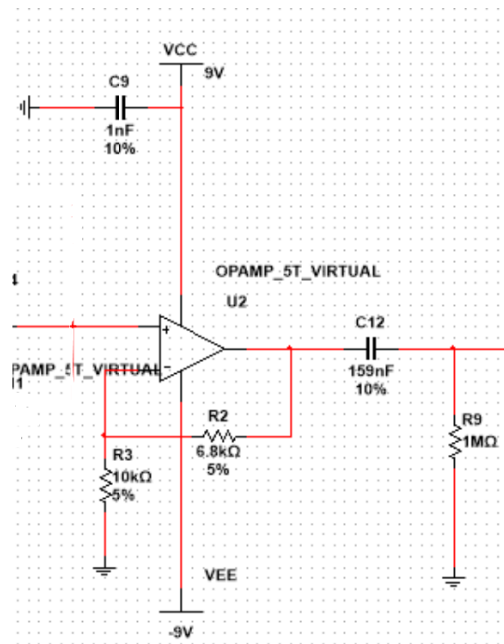
Figure 5.47: EMG selectable gain and passive RC filter

For the EMG system, the gain has been set to 1.68, which is suitable for making sure that a 15 mV signal (worst-case scenario) is in the range of the ADC which is about 3.3V. After passing through the instrumentation amplifier which has a gain of 50 and the high pass filter which has a gain of 2 the 15 mV peak to peak signal has been amplified into a 1.5 V peak to peak signal. With the addition of the selectable gain it becomes a 2.52 V peak to peak signal. The components R2 and R3 on the negative feedback loop determine the gain of this stage.

At the end of the selectable gain is an RC circuit, used as a filter, where the 159 nF capacitor, C12, and 1 MΩ resistor, R9, were chosen such that the frequency cutoff would be 1 Hz. The RC filter is described in background reference 2.4.3. This is placed here to eliminate offset acquired in the past two amplifying stages, without significantly altering the overall passband.

5.2.4 Wireless EMG Power Supply

The wireless systems are powered by two 9 V batteries, connected in series to produce a $\pm$ 9 V bipolar supply. The $\pm$ 9 V supply of the batteries provides us with capabilities and limitations in order to avoid saturation so that our systems work properly. Decoupling capacitors are added to keep the voltage stable. In addition, the reference lead (third electrode) of the EMG system will be connected to the intersection of the two batteries which also serves as a reference point for the rest of the circuit.

5.2.5 Wireless EMG Level Shifter

The final signal goes through a level shifter which consists of an adder circuit that adds a 1.6 V positive offset to the input signal of this stage. The signal requires this offset because it is a bipolar signal and the ADC is unipolar. The signal values range from negative to positive while the ADC can not read negative values. Centering the signal at 1.6 V (the middle of the range of the ADC) will allow the ADC to take in all values of the signal as long as it's peak to peak voltage amplitude is not larger than 3.3 V. The instrumentation amplifier gain, high pass gain, and selectable gain have all been chosen with this in mind. In the level shifter, the R4 and R5   75 kΩ resistors, shown in Figure 5.47, are equal in value to create a voltage divider where the 1.6 V and input signal are halved. Meanwhile the R7 and R6, 200 kΩ, resistors are equal in value for the gain to be 2. This reverses the effect of the input signals being halved. The calculations behind this circuit are explained in section 2.4.1. Figure 5.48 shows the level shifter configurations for the wireless systems.
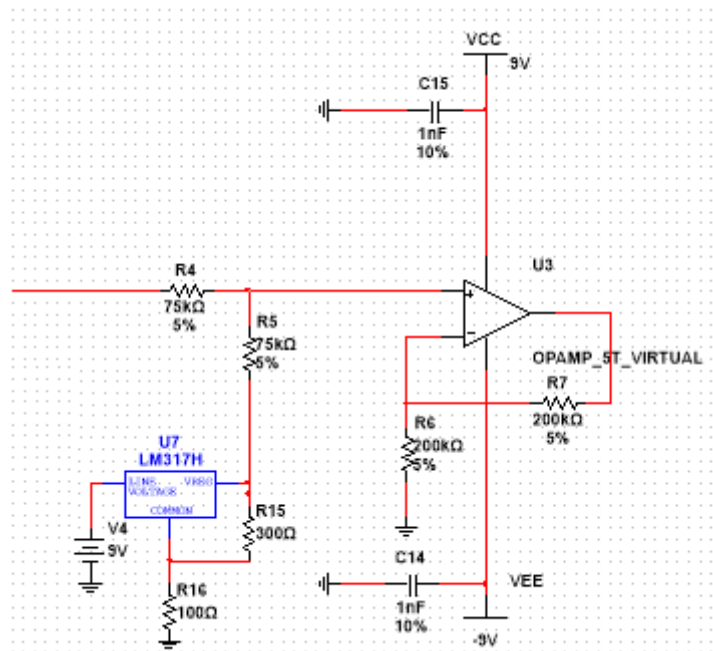
Figure 5.48: EMG/ECG level shifter circuit diagram

Voltage Reference Considerations

In order to achieve a positive offset that was necessary for ensuring that the acquired signal centered at 0V will be in the ADC's range on the TI microcontroller of 0-3.3V, the use of a voltage reference was required. In Figure 5.48, this reference voltage is the left output of U7 and is one of the inputs to the positive terminal of the op-amp. The amplitude of the offset was chosen to be around 1.6V, that is half of the allowed voltage range of the ADC, to establish a signal centered at 1.6V within the appropriate range.

The method of achieving 1.6 V consisted of using a voltage regulator. The LM317L voltage regulator has an adjustable voltage output ranging from 1.3 V to 37 V. Figure 5.49 shows the schematic diagram of this component.
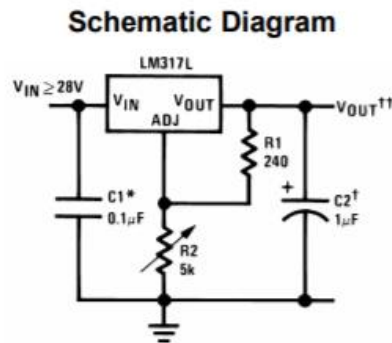
Figure 5.49: Schematic Diagram of LM317L Voltage Regulator

Via the component data sheet, the voltage output can be calculated as:

$$V_{OUT} = 1.25V \left(1 + \frac{R_2}{R_1}\right) + \frac{I_{ADJ}}{R_2}$$

To create an output of 1.6 V, R2 was selected as 200 Ω and R1 was selected as 750 Ω for the EMG circuit and as R2=100 Ω and R1=300 Ω for the ECG circuit for convenience. Ideally, this would create an output of 1.58 V, but it created an output of 1.6 in practice.

5.2.6 Testing Full Wireless EMG System

The completed schematics for the EMG circuit consists of five stages which were mentioned above providing the appropriate signal processing to obtain the desired biopotential signals in terms of the analog front end. Each of the stages that consists of an integrated circuit are connected to our power supply of a bipolar 9 V battery through coupling capacitors, with specific values determined according to each of the operational amplifier's data sheets when the specific models were chosen.

The front end of the wireless EMG system consists of an instrumentation amplifier, a high pass filter, selectable gain, RC circuit, low pass filter, and level shifter. The circuit diagram is shown below in Figure 5.50.
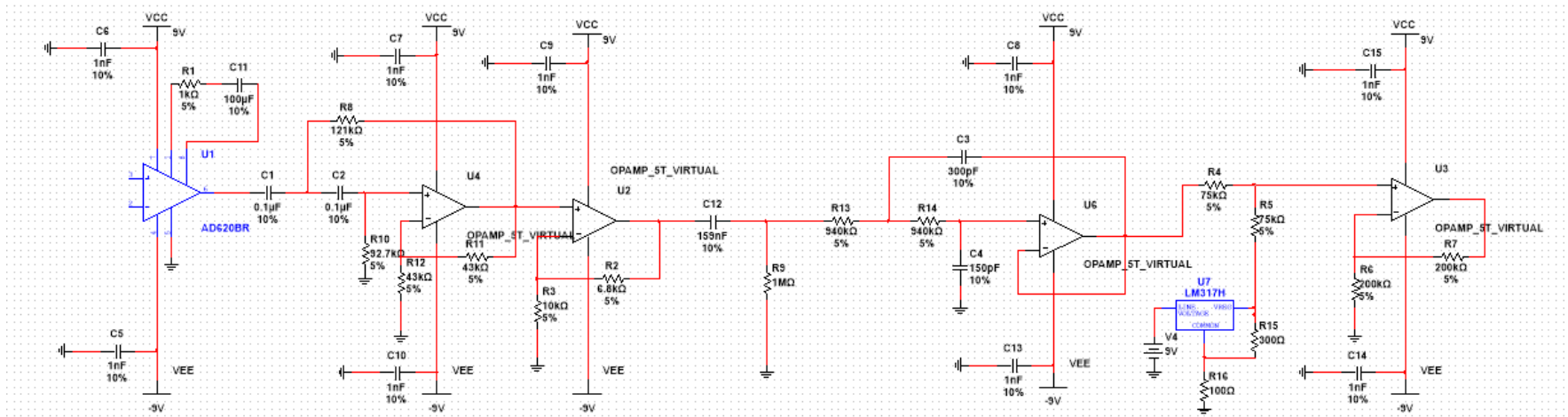
Figure 5.50: Schematic of the front end for wireless EMG design

This circuit was implemented on a breadboard; after verifying that the frequency response and gain were correct, the board was used on a person to collect EMG data. The electrodes were connected on the skin over a person's biceps muscles as described in Background section 2.3.2 and shown in Figure 2.9. The two active electrodes on the bicep were connected at the inputs of the instrumentation amplifier (pins 2 and 3 in Figure 5.50). We gathered data at rest and then at three levels of force: light, medium, and high contraction. The output of our analog front end went through the ADC of one TI CC26X2R1and then traveled wirelessly via Bluetooth to another TI CC26X2R1 which communicated with the serial port of a laptop. The transmission is further explained in section 5.3.6. Then, an application on MATLAB, designed by WPI graduate student He Wang could show us the data in real time. We recorded data lasting 15 seconds and found the following results:

Figure 5.51 shows the raw data gathered at rest. The plot shows a large amount of 60 Hz noise when the biceps were at rest.
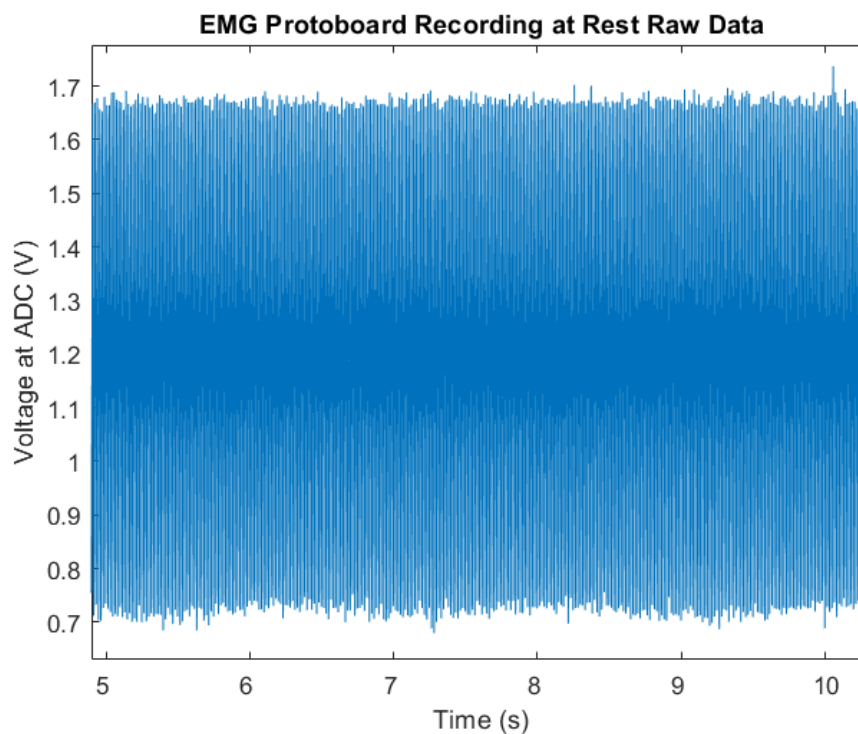
Figure 5.51: EMG protoboard recording at rest, raw data

A 60 Hz notch filter was added to the recorded data in MATLAB which resulted in Figure 5.52. The notch filter significantly decreased noise and the amplitude of the signal.
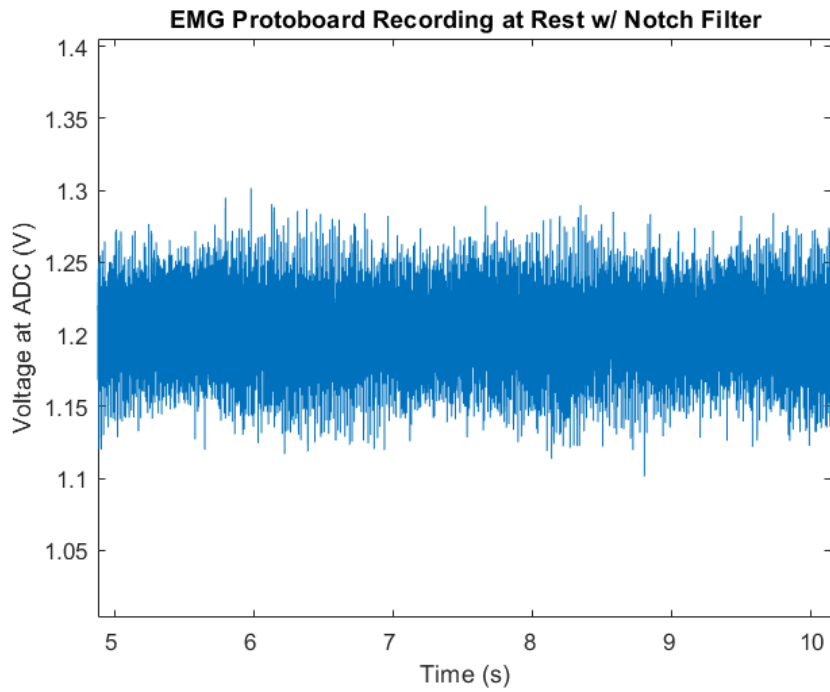
Figure 5.52: EMG protoboard recording at rest w/ notch filter

The next signal recorded was the biceps using light force, which is light relative to the medium and high force used later. Figure 5.53 shows the raw data when light force was used.
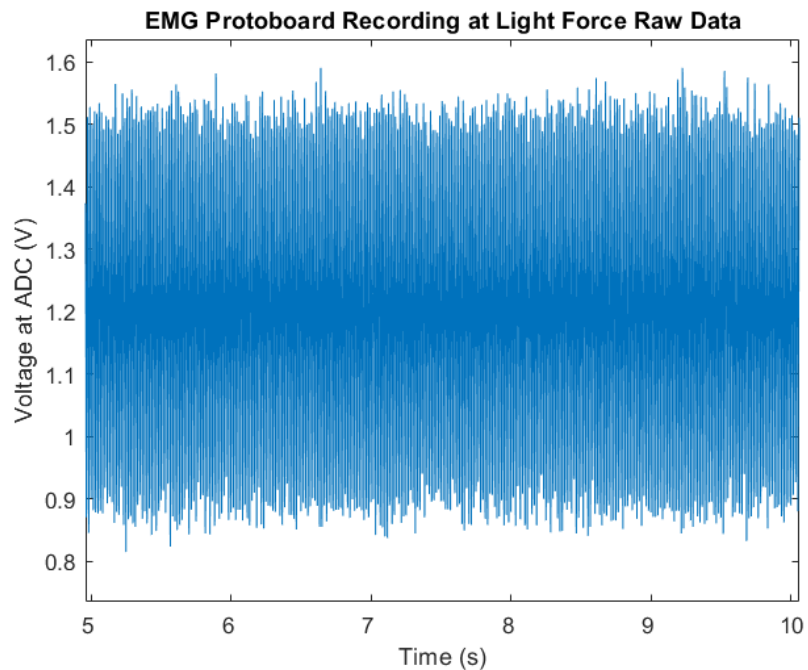
Figure 5.53: EMG protoboard recording at light force raw data

These raw data were similarly noisy and a notch filter was applied in MATLAB which yielded the result shown in Figure 5.54.
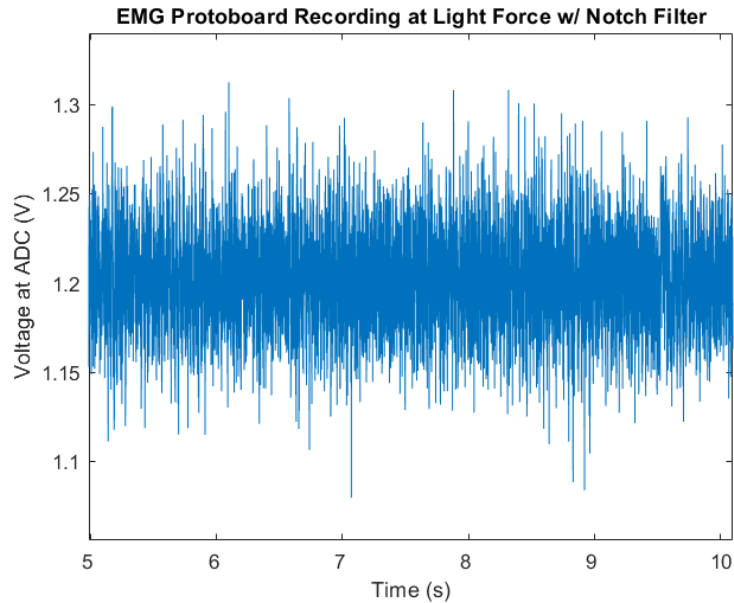
Figure 5.54: EMG protoboard recording at light force w/ notch filter

Comparing the light force and rest recordings, the recordings were overlapped with the light force behind the rest recording. Figure 5.55 shows the result of this comparison. Because of the large amount of noise from the rest recording, the light force recording barely peaks out from behind the rest recording.
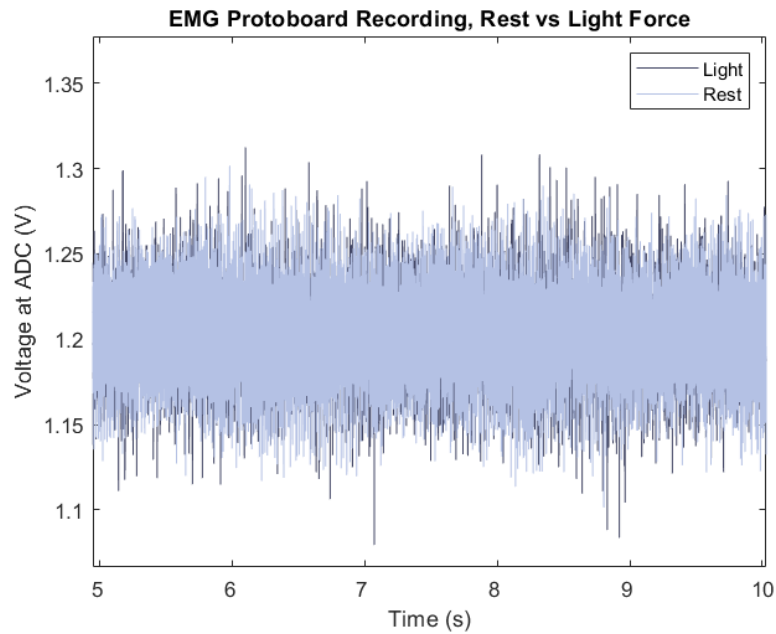
Figure 5.55: Rest vs Light Force

The next figure shows the raw recording when medium force was used.
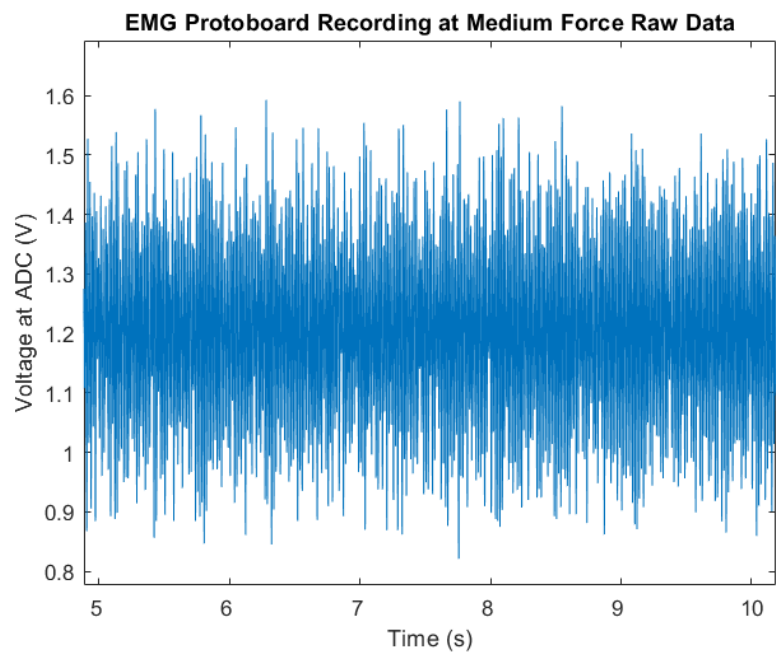
Figure 5.56: EMG protoboard recording at medium force raw data

The result of the notch filter, implemented in MATLAB is shown in Figure 5.57.
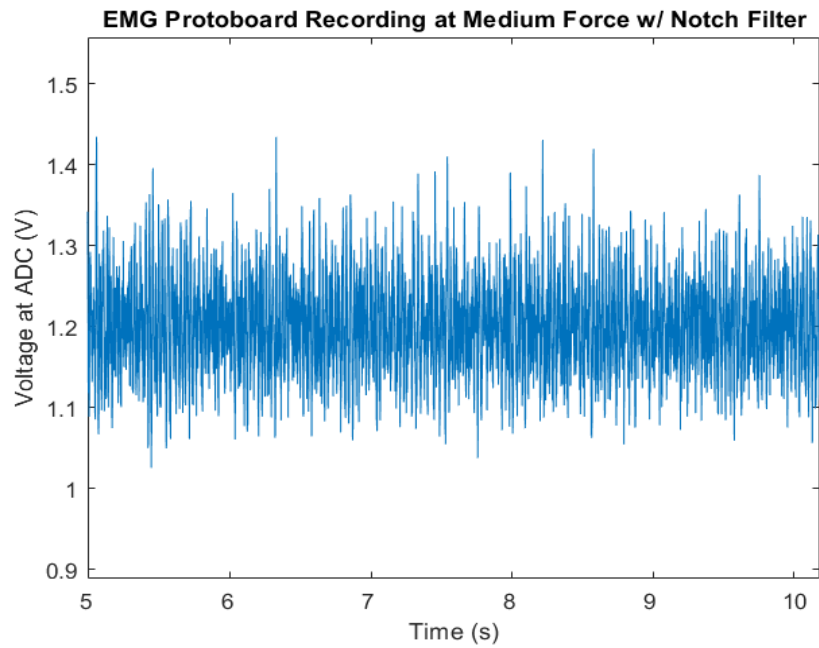
Figure 5.57: EMG protoboard recording at medium force w/ notch filter

Similar to Figure 5.55, this next Figure shows the light force recording overlaid upon the medium force recording. It more clearly shows that the Medium force has a larger amplitude than the Light force.
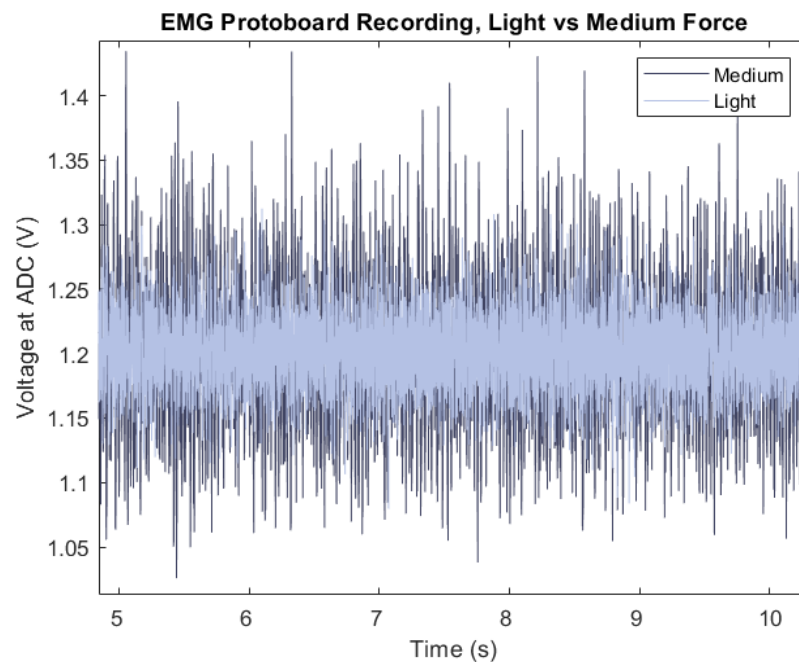
Figure 5.58: Light vs Medium

Next, Figure 5.59 shows the raw data from the recording of EMG when using high force.
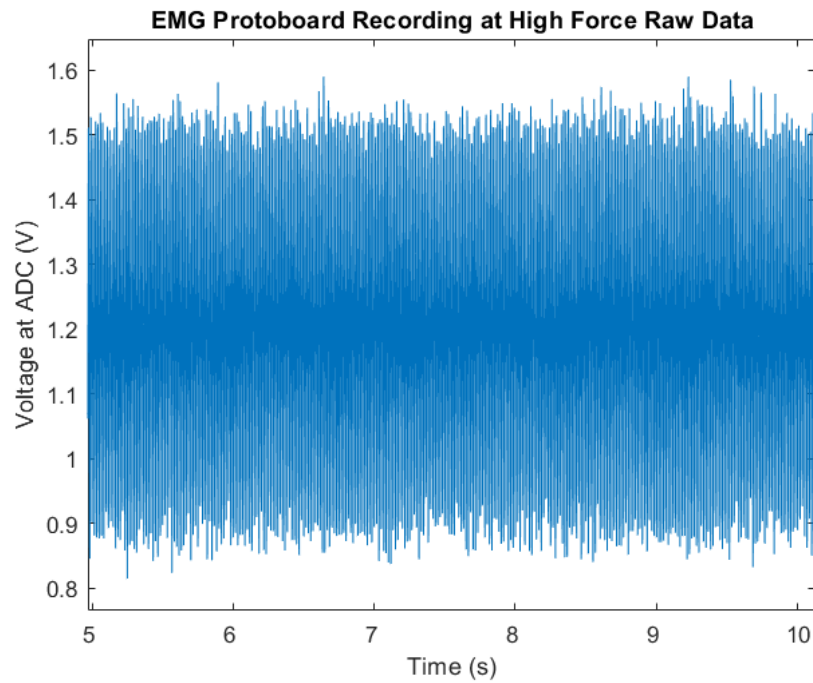
Figure 5.59: EMG protoboard recording at high force raw data

After the notch filter was applied, the result is shown in Figure 5.60.
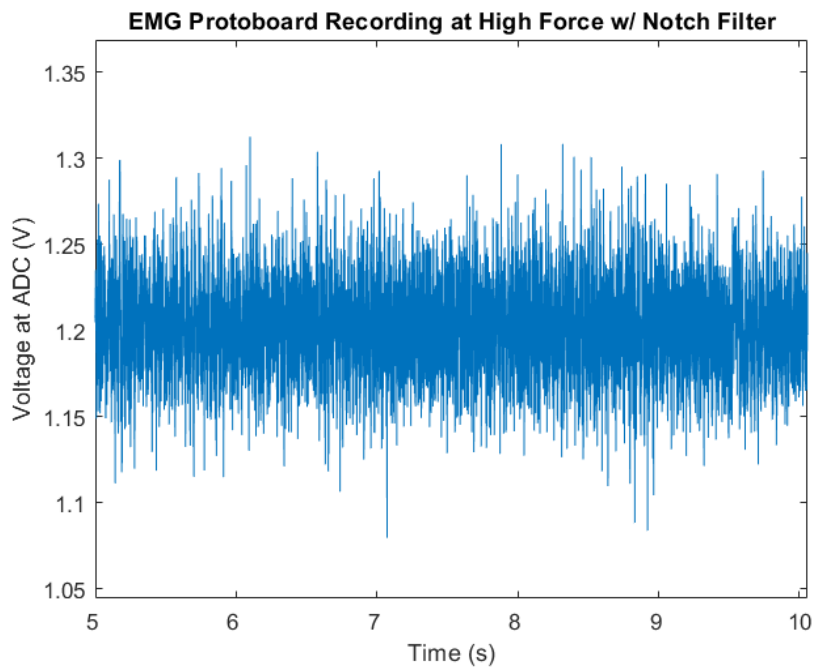
Figure 5.60: EMG protoboard recording at high force w/ notch filter

When compared to the medium force, the high force has a higher amplitude as shown in Figure 5.61. The difference between Medium and high force is more subtle compared to the difference between low and medium. However, it is more clear than the difference between low force and at rest.
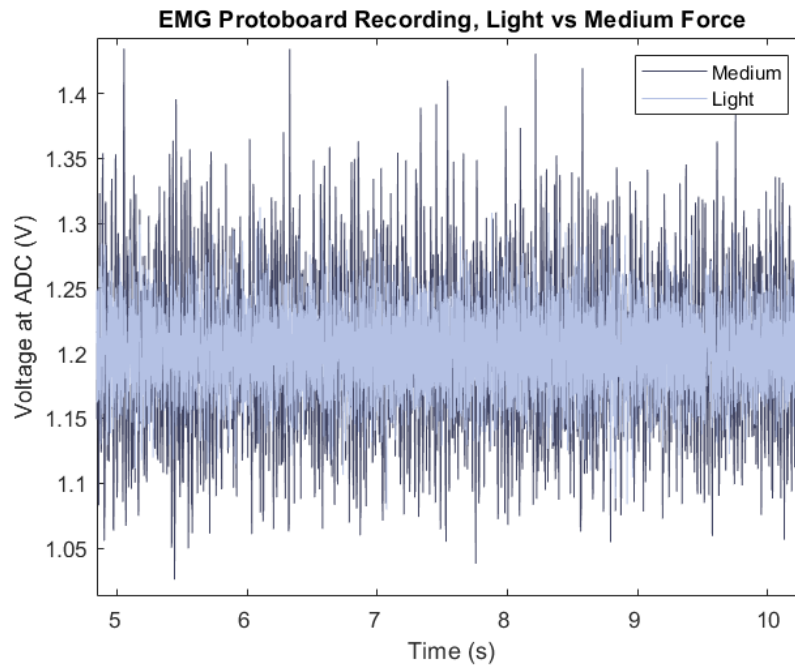
Figure 5.61: High vs Medium

Lastly, the signals were all placed over each other in descending order starting with the high force recording and ending with the rest recording. This result is shown in Figure 5.62.
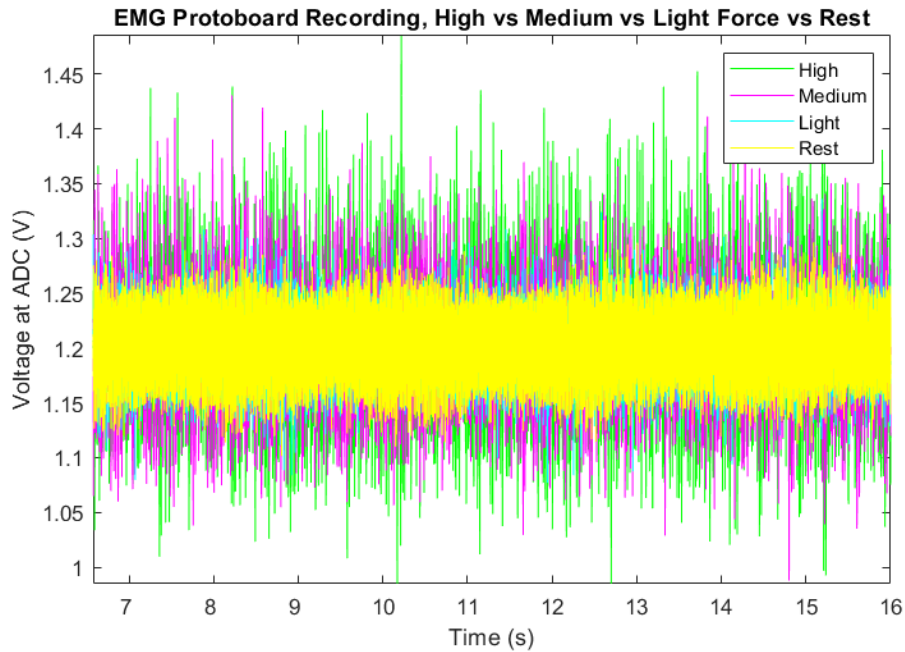
Figure 5.62: High, Medium, Light, Rest EMG recordings (after notch filtering)

5.2.7 Wireless EMG PCB Design

A PCB design for the EMG wireless system was created using EAGLE. The schematic was then converted to a PCB. Figure 5.63 shows the schematic and Figure 5.64 shows the arrangement of the board. The board has an 8 pin header to connect the power supply, electrodes, and output of the system. In the EMG system there are three electrodes. Two are connected to the negative and positive inputs of the instrumentation amplifier while the third electrode (reference electrode) is simply connected to ground. Decoupling capacitors are placed near the supply.
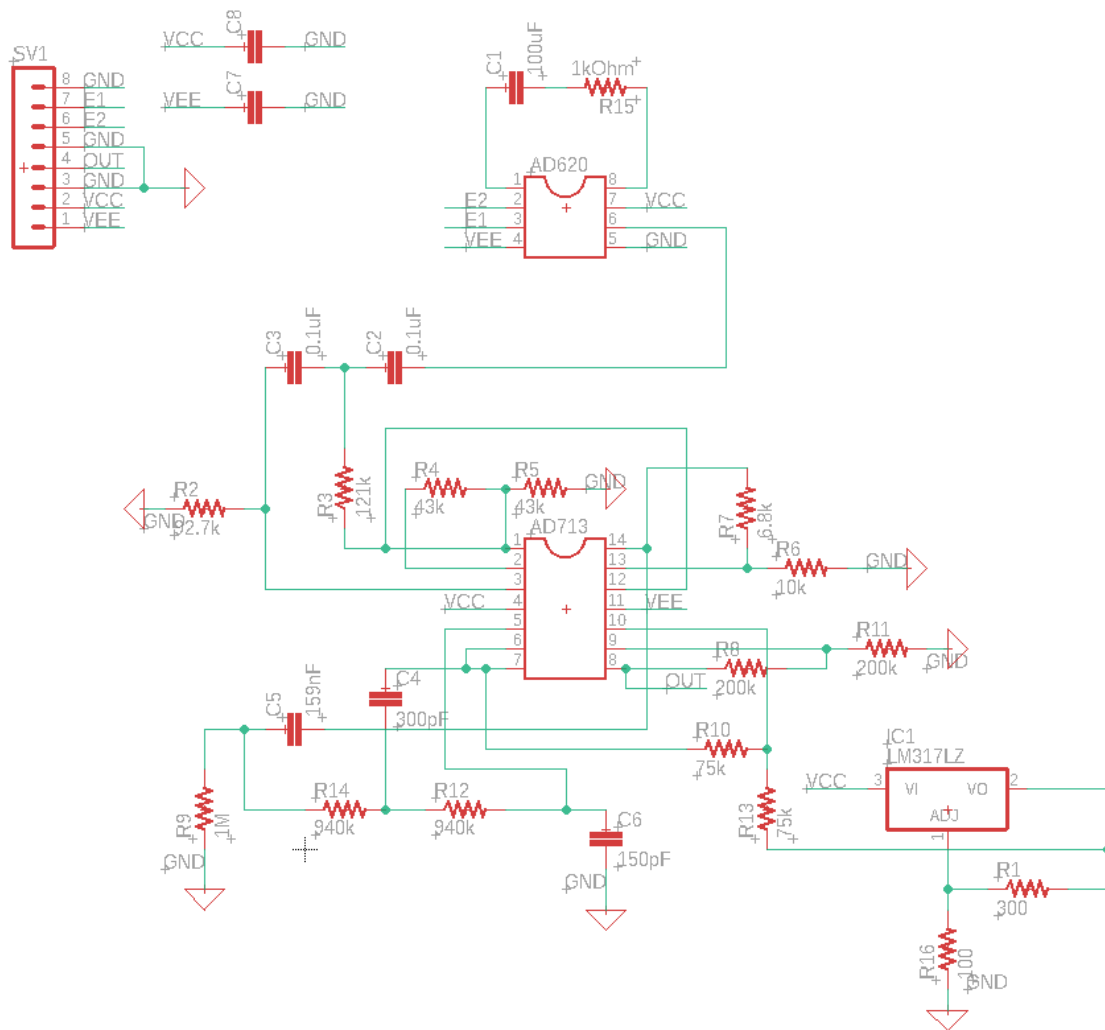
Figure 5.63: Schematic of Wireless EMG circuit for PCB Design

The board has a ground plane on the top and bottom. Both sides of the board were utilized for routing with some routing going between layers as needed through the use of vias. The main ICs of the board are the AD620, the AD713, and a voltage regulator. The rest of the components consist of standard resistors and capacitors.
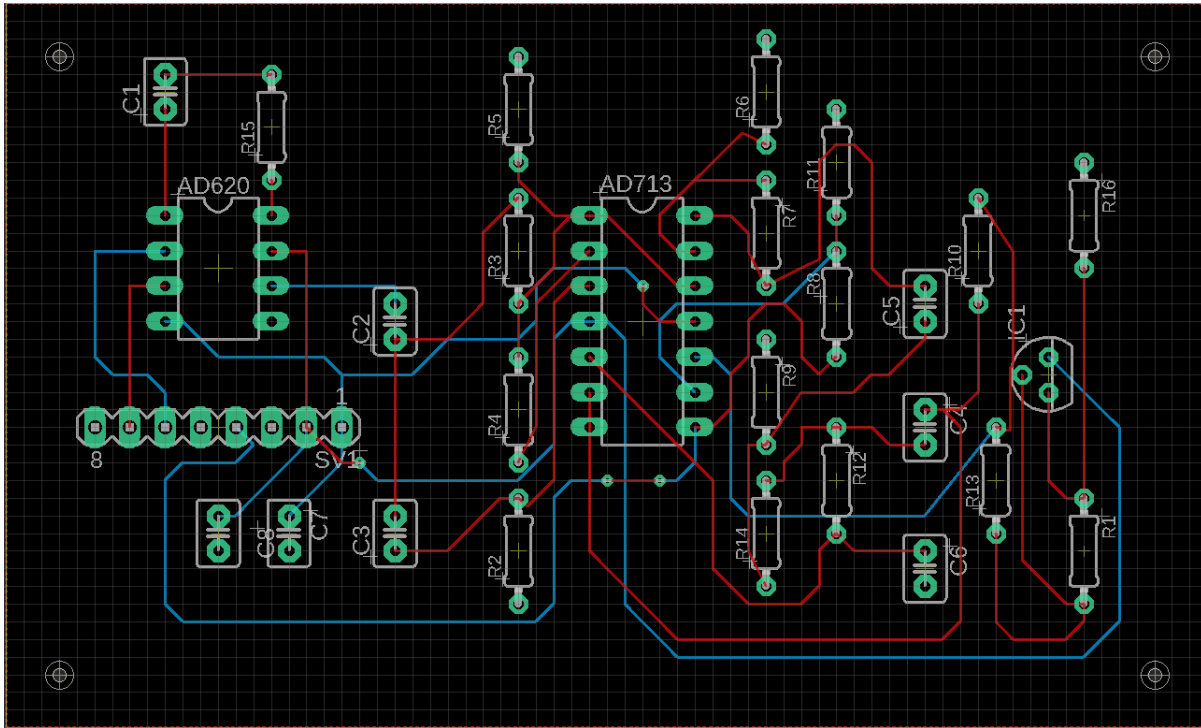
Figure 5.64: PCB Board Design of Wireless EMG circuit

Once the board was routed, the board was sent to be built through OSH Park (Lake Oswego, OR). Figures 5.65 and 5.66 show the top and bottom of the PCB, respectively. The board size is 3.39 x 2.05 inches.
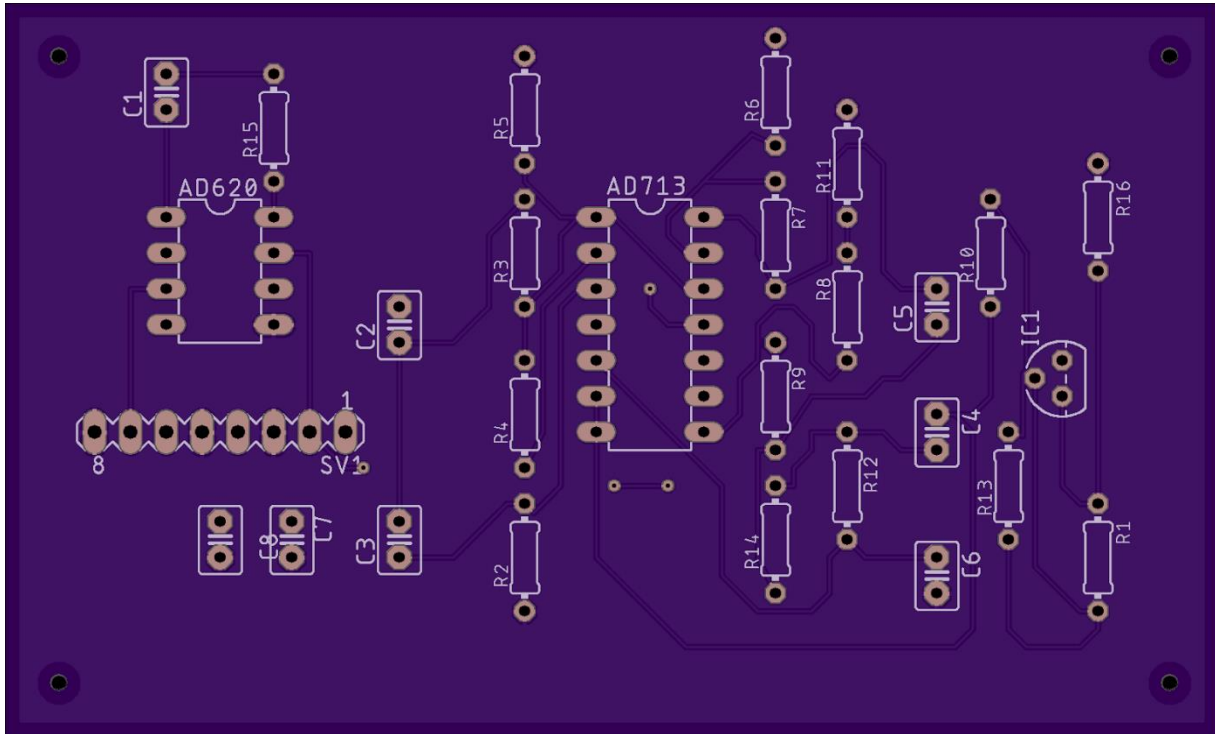
Figure 5.65: Wireless EMG PCB top layer
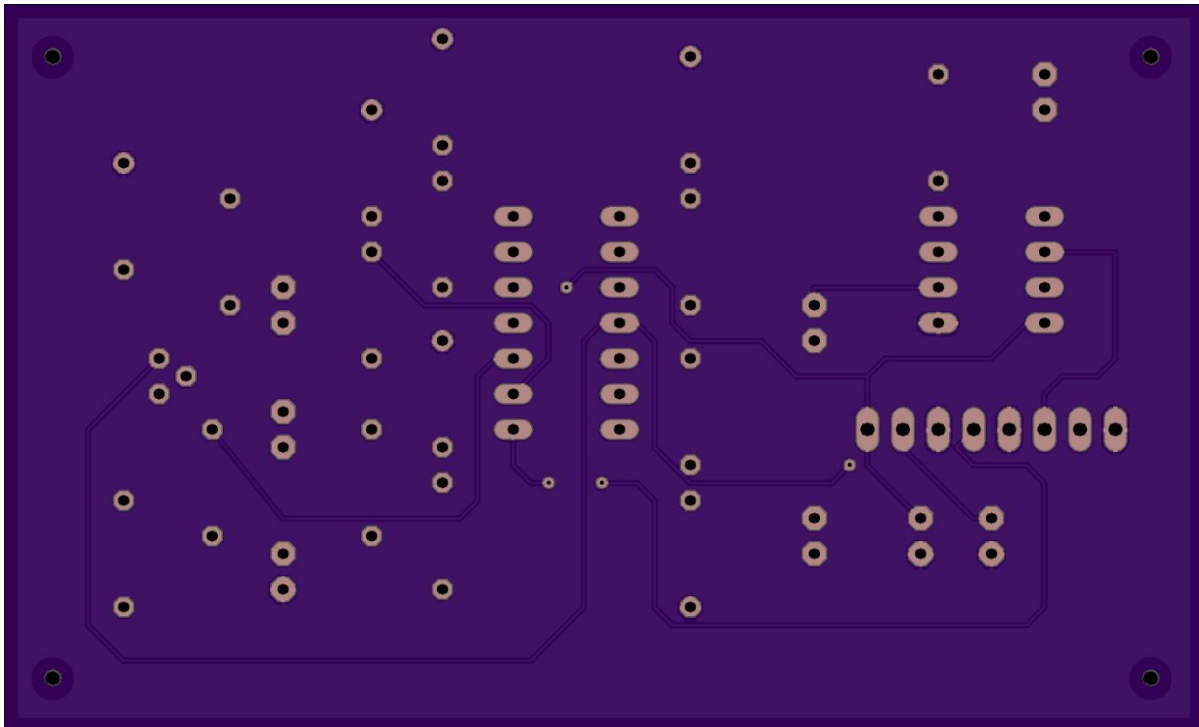
Figure 5.66: Wireless EMG PCB bottom layer

Table 5-4: Component specification for Wireless EMG Implementation

Name	Component	Application	Image
AD713	Quad Operational Amplifier (14-pins)	Highpass/ lowpass filtering, selectable gain, and level shifter	
AD620	Instrumentation Amplifier (8-pins)	Amplification	
LM317LZ	Adjustable Voltage Regulator (3-pins)	1.6 V Voltage reference for level shifter	
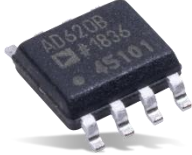
Figures 5.67 and 5.68 show the wireless EMG PCB before and after being populated, respectively. The results for the EMG PCB were unsuccessful. Problems were found with the ground plane of the board. In addition, the soldering is suspected of altering the connections. Overall, the instrumentation amplifier worked correctly. The selectable gain stage also worked as expected. The high pass stage had a correct magnitude frequency response but no gain. Upon further inspection, the schematic used for the PCB board incorrectly implemented the negative feedback loop at pins 1 and 2 of the AD713. R4 and R5 in Figure 5.65 are not supposed to be in series. Meanwhile, the low pass stage and level shifter had an incorrect flat output at -5V even though the voltage regulator was outputting the correct voltage. Since the selectable gain, high pass filter, low pass filter, and level shifter are on the same AD713 quad amp, it did not make sense that only half of it is working since they share the same power source.
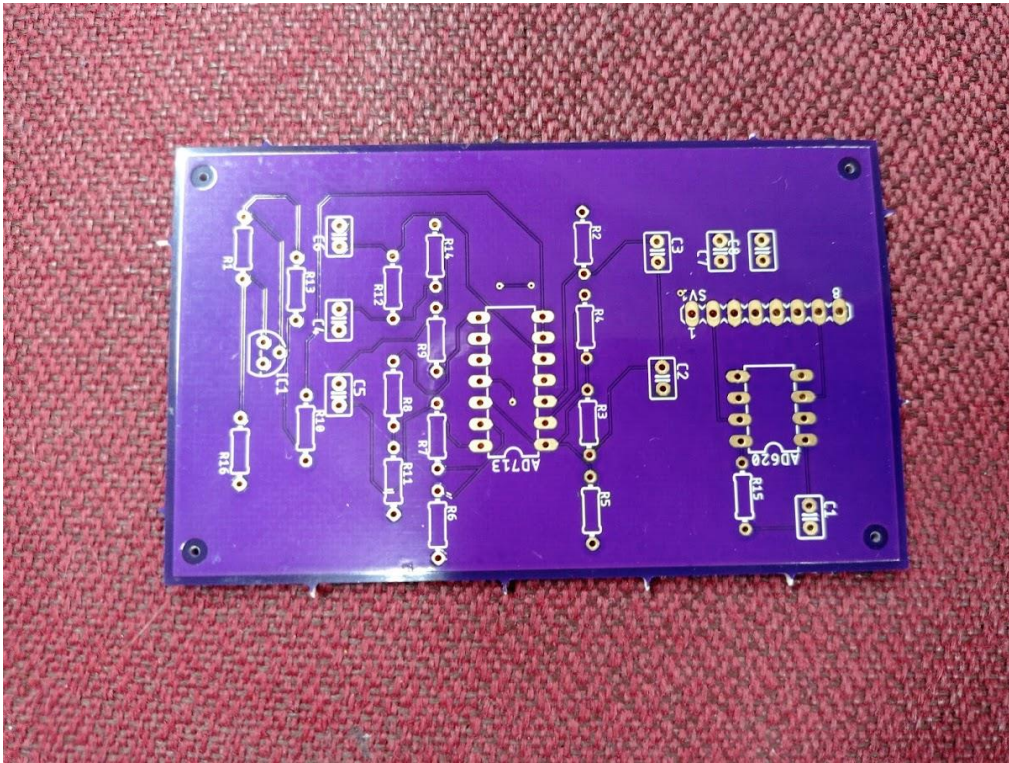
Figure 5.67: Wireless EMG Printed Circuit Board PCB
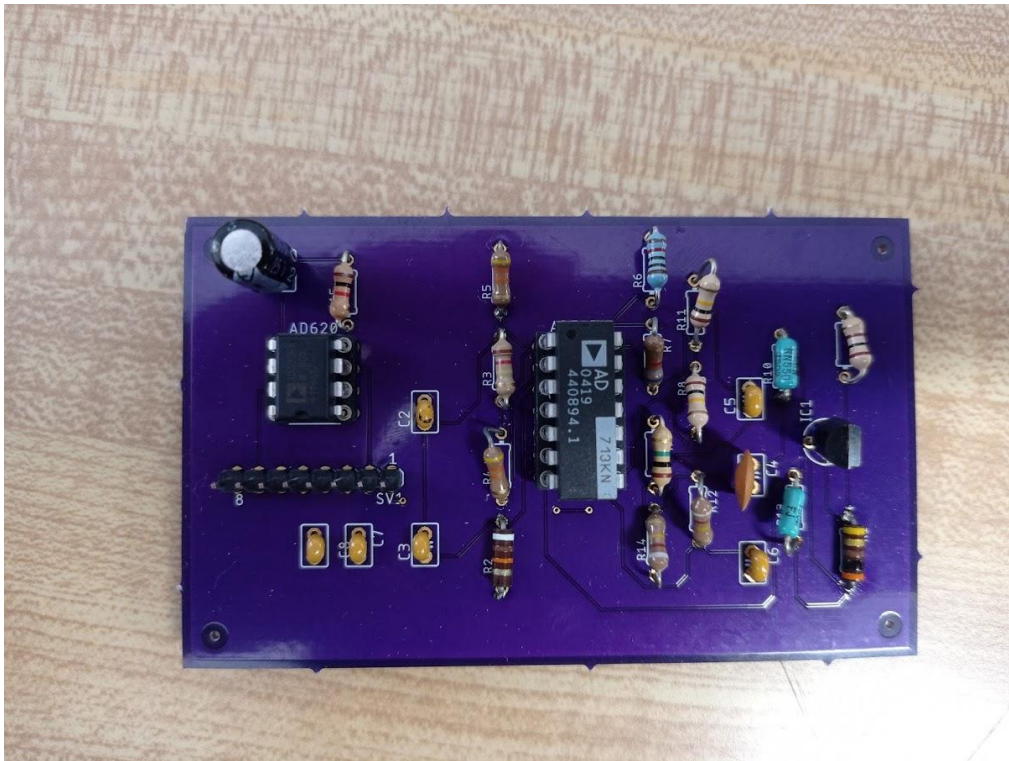
Figure 5.68: Populated Wireless EMG PCB

5.3. Wireless ECG System Design Implementation

5.3.1 Wireless ECG Instrumentation Amplifier

The implementation of the instrumentation amplifier shown in Figure 5.69 was the first step completed for the wireless ECG circuit, following the two-electrode system for the measurement design. Resistors R1 and R2 are used to create a common reference for the two-electrode design. The values of R1 and R2 were chosen to be 1 MΩ in order to limit the current going to ground as we want them to represent a high input impedance. The AD620 instrumentation amplifier was selected for this circuit as it has a wide range of power supply voltage of ± 2.3 V to 18 V providing the required voltage for the circuit and is available in a DIP package for ease of use on a breadboard.
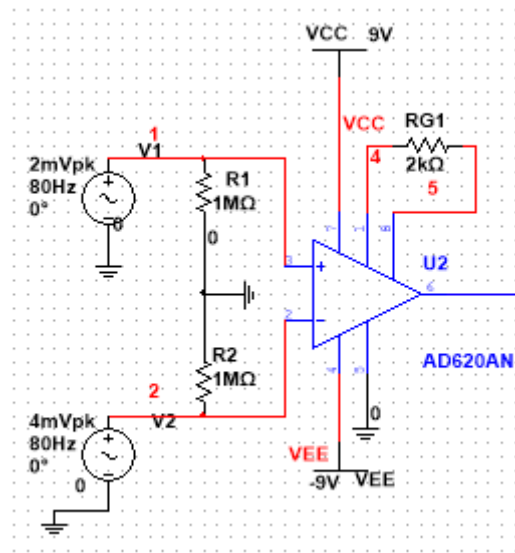
Figure 5.69: Circuit Diagram of Instrumentation Amplifier for ECG circuit

The decoupling capacitors values were chosen according to the data sheet of the AD620 component by Analog Devices, in order to eliminate noise generated by any AC signal. The most gain of the ECG circuit design was added in the first stages of the system. Specifically, in the instrumentation amplifier stage, the gain was intended to be as high as possible to magnify the signal without saturating the amplifier output. However, the use of a 9 V bipolar supply was a

limitation. The maximum voltage supply the battery provides is ± 9 V minus the ± 0.7 V due to the diode drop within the AD620 thus, the maximum available output voltage range for the AD620 is:

$$\pm\ 9\ V - \pm\ 0.7\ V = \pm\ 8.3\ V$$

In order to calculate the allowed maximum gain when using a voltage supply of ± 8.3 V, the DC offset voltage generated by the electrode skin contact needed to be considered. In our case, the ECG maximum offset is designed for 300 mV and it is added to the maximum voltage difference of the electrode voltage input that is 2 mV for ECG. The maximum gain for the instrumentation amplifier is

$$8.3\ V\ /\ 302\ mV = 27.48\ V/V$$

The gain for the AD620 was determined to be 25.7 V/V to be close to the maximum allowable gain but safe at the same time to prevent saturation. The resistor RG1=2 kΩ shown in Figure 5.69, is used to acquire this gain using the following equation given in the AD620 data sheet:

$$A = (1+ 49.4\ k\Omega\ /RG1\ )$$

5.3.2 Wireless ECG Filters Design

The design of the filters is similar to those aforementioned in the wired and wireless EMG circuits. The wireless systems use a set of two second order Butterworth filters implemented in Sallen-Key topology and the values for the ECG circuit were similarly determined by using the MATLAB function "butter_hi_design" and "butter_lo_design" provided to us by Professor Clancy.

High Pass Filter

The output of the instrumentation amplifier is the input of the high pass filter. The high pass filter is used to remove the low frequency components such as motion artifacts created by the contact of the electrodes to the patient's skin. The Sallen-Key filter topology for this second order Butterworth high pass filter is shown in Figure 5.70 The ECG signal can be obtained over the frequency range of 0.05 Hz - 150 Hz for an accurate representation of the biopotential signal and to provide the appropriate information of the heart's condition. For simplicity, the cutoff frequency was chosen to be at 0.5 Hz for the high pass filter, which is adequate for the heart rate to be recorded, while being less susceptible to motion artifact.
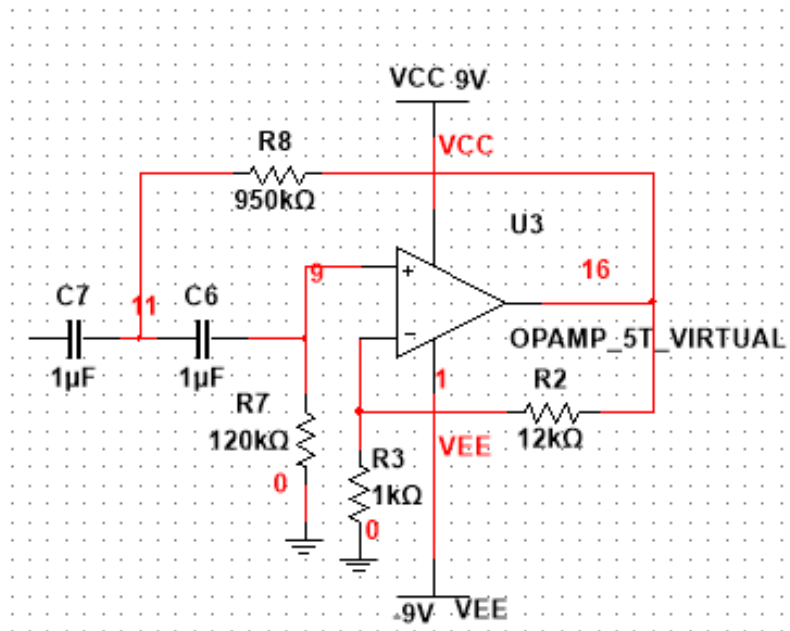
Figure 5.70: Circuit Diagram of Butterworth second order High Pass for ECG circuit.

To implement the Sallen-Key topology, the values 1 µF for the capacitors and 0.5 Hz for the cutoff frequency were inputted to the function "butter_hi_design". The resulting values were chosen to be C7=1 µF, C6=1 µF, R7=120 kΩ and R8=950 kΩ as shown in Figure 5.70.

The gain of the high pass filter was decided to be as high as possible but not saturate the system, By adding the most gain in the first two stages will filter the DC offset at the low pass filter stage. The resistors R2 and R3 shown in Figure 5.70 were utilized in the following equation to obtain the gain of the high pass filter:

$$A = (1 + R2/R3)$$

The ECG signal is expected to be around 2 mV maximum in peak amplitude, thus after being amplified by the gain of the instrumentation amplifier, the expected output of the instrumentation amplifier would have a peak magnitude of 50 mV. The voltage gain of the high pass filter was determined to be 13 using the following resistors R2=12 kΩ and R3 =1 kΩ.

Low Pass Filter

The Sallen-Key topology for the Butterworth, second order low pass filter shown in Figure. 5.71 was also determined using the MATLAB function "butter_lo_design" providing us with the

values of R9=100 kΩ, R10=100 kΩ, C8=22 nF and C5=10 nF and a desired cutoff frequency of 100 Hz.
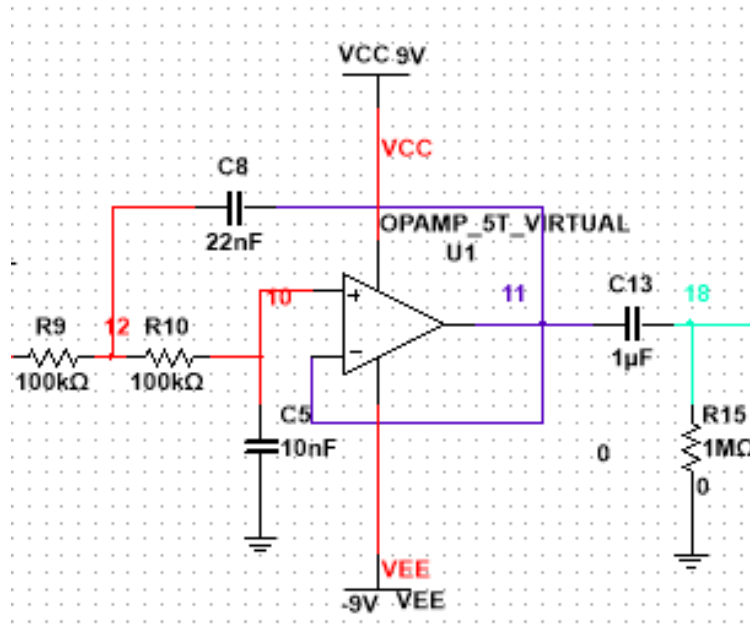
Figure 5.71: Circuit Diagram of Butterworth second order Low Pass for ECG circuit.

The gain of the low pass filter was chosen to be 1. A passive capacitor-resistor filter is added at the output of the low pass filter to eliminate any offset generated by the IC while filtering. A capacitor C13=1 µF and a resistor R15=1 MΩ shown in Fig. 5.71 connected in series, create a high pass filter with a cutoff of 0.159 Hz as explained in the Background section 2.4.3. This circuit eliminates any DC components, with limited influence on the desired passband.

The combined high pass and low pass filters create a bandpass filter ideally allowing frequencies ranging from 0.5 Hz to 100 Hz to pass through. The circuits diagrams of the filters were originally designed in NI Multisim using an input of an AC voltage source of 2 mV peak amplitude and 80 Hz frequency. The simulated magnitude response of the filters was generated using the "Bode Plotter" generator in Multisim. The resulting graph can be seen in Figure. 5.72

.
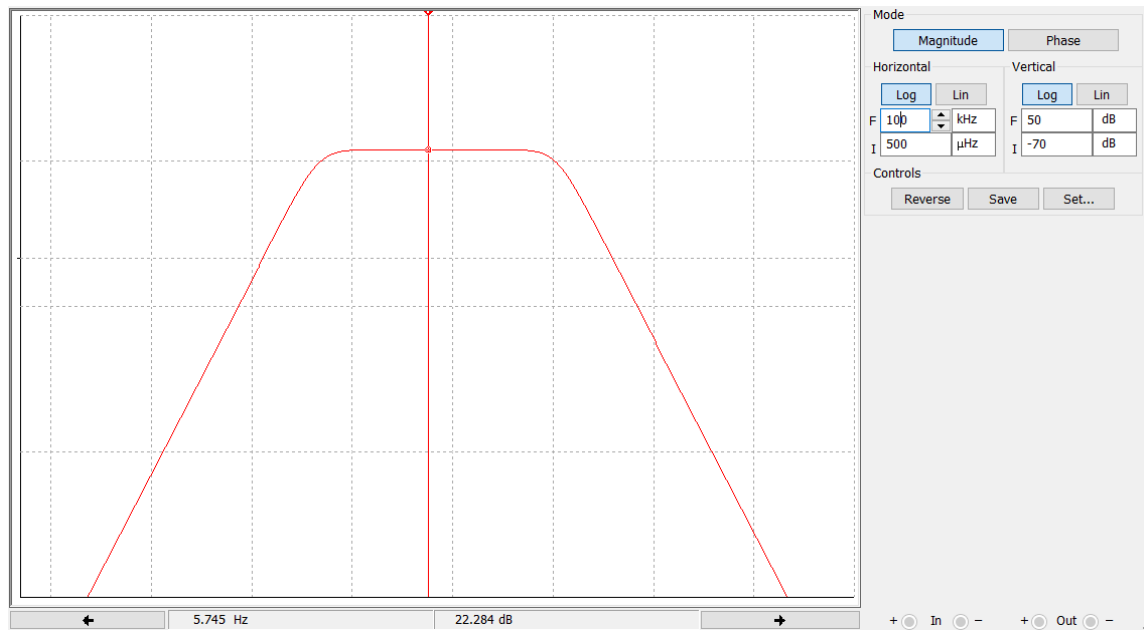
Figure 5.72: Simulated magnitude response for Wireless ECG filters.The horizontal axis is the frequency from 500 µHz to 100 kHz. The vertical axis is the magnitude of the output signal from -70 dB to 50 dB. Both axes are on a logarithmic scale

The maximum amplitude the filter reached the bandpass is 22.284 dB. Based on the   -3 dB drop the cutoff frequency for the high pass is measured to be 0.454 Hz at 19.284 dB and 105.3 Hz at 19.84 dB for the low pass filter. These results shown in Figure 5.72 satisfy the desired cutoff frequencies in the ideal design.

The next testing was for the filters to be built on a breadboard. The circuit was powered by using two 9 V batteries connected in series and the BitScope BS10 "Micro" Oscilloscope and Analyzer was used as a function generator and as an oscilloscope. For the low pass filter, the L1 pin of the Bitscope was used as the waveform generator and along with channel A pin used as an oscilloscope channel, were connected to the non inverting input of the AD713 operational amplifier used to construct the filter. Frequencies ranging from 5 Hz to 3000 Hz were used to test the system and the peak to peak amplitude of the inputted waveform (1 V) was compared to the amplitudes of the output waveform. Dividing the peak to peak amplitude of the output by the amplitude of the input, the gain at each frequency was computed and then converted to dB using the equation mentioned in section 5.1.1 Wired EMG Filter Design. Next, the Bitscope could not be used to test the high pass filter since the cutoff frequency was at 0.5 Hz and the minimum frequency provided by the Bitscope was 5 Hz. The Tektronix TDS 210 Two Channel Digital Real-

Time Oscilloscope and the Tektronix CFG253 3 MHz Function Generator were used instead. Similar to the low pass filter, the magnitude response of the high pass was generated, however the input voltage used was 100 mV and the frequencies ranged from 400 mHz to 3000 Hz.

As expected, Figure 5.73 shows that the magnitude response of the theoretical and simulated designs are matched closely. The components used in the simulation were ideal components so that we can compare our design to the theoretical design. The black line in Figure 5.73, shows the experimental data gathered for the filters. The resulting data provided us with sufficient accuracy and an acceptable frequency range to move forward with testing the rest of the circuit.

.
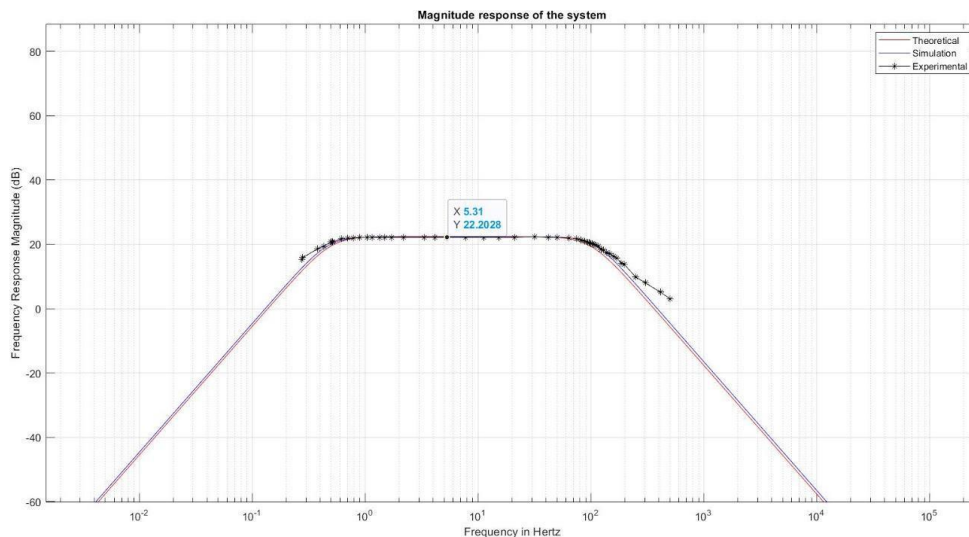
Figure 5.73: Theoretical, Simulated and Experimental Magnitude Response for ECG filters

5.3.3 Wireless ECG Selectable Gain

The selectable gain stage of this ECG acquisition system is utilized to provide extra amplification if needed with respect to the amplitude of the biopotential signal. The ECG signal may differ from person to person and in this case the selectable gain stage will offer the appropriate amplification. We set the initial gain to be 2 in this test case using the resistors R13=1 kΩ and R14=1 kΩ shown in Figure 5.74. The equation below was used to acquire the desired gain:

$$A = (1 + R13/R14)$$
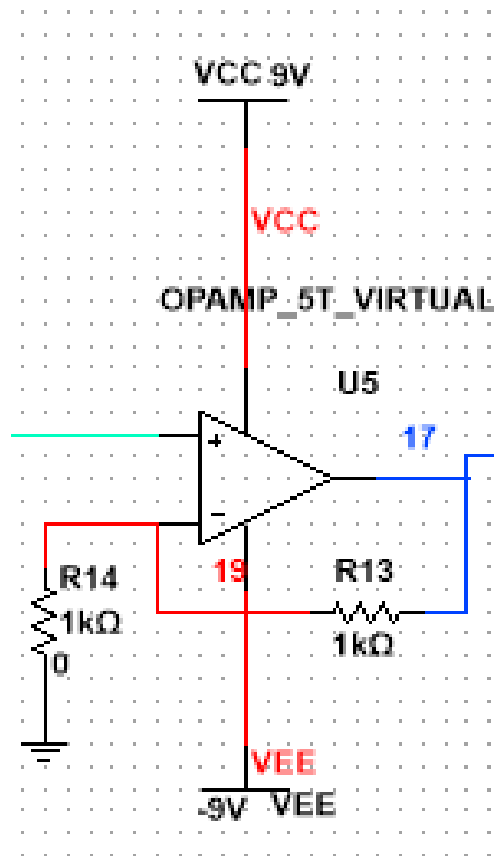
Figure 5.74: Circuit Diagram of Selectable Gain Amplifier for ECG circuit.

The amplitude of the ECG signal input at the instrumentation amplifier is expected to be around 2 mV and will then be amplified by a gain of 25.7 resulting in 0.0514 V output. The signal will then go through the Butterworth high pass filter and will be amplified by a gain of 13 resulting in a 0.668 V output. The Butterworth low pass filter has a gain of 1, so the amplitude of the ECG signal at the output of the low pass filter will not be affected.

Thus, the input of the selectable gain stage will be 0.668 V and, following an amplification by a gain of 2, the resulting output will be around 1.336 V. The selectable gain can be adjusted by replacing the resistor R13 to add more gain or short it out depending on the peak to peak voltage of the acquired signal.

5.3.4 Wireless ECG Power Supply

The ECG wireless system, similar to the wireless EMG system, required two 9 V batteries to be powered. The exact configuration as well as the details and requirements, were mentioned in section 5.2.4 Wireless EMG Power Supply.

5.3.5 Wireless ECG Level Shifter

The design and implementation of the level shifter stage for the ECG circuit is similar to the circuit constructed for the EMG circuit and the differences are explained in section 5.2.5.

5.3.6 Wireless Bluetooth Transmission and Real Time Data Display

The wireless devices that were designed and built required data transmission from a peripheral microcontroller to a central which will be connected to a computer to record and display the data that was obtained. The TI CC26X2R1 boards that we decided to use are optimized for low power wireless communications and contain the Bluetooth 5 LE protocol. The algorithms that were imported on the MCUs were written by WPI graduate students Jianan Li and He Wang and were provided to us to use for the purpose of this project. The programming of the master and the peripheral boards required two different scripts to achieve communication based on instruction from the TI website describing how to achieve Bluetooth transmission. In addition, He Wang also provided us with a graphical user interface (GUI), designed in MATLAB and listed in Appendix C, that was utilized for real-time data display. Once the central board is connected to the computer, BTool (a Texas Instruments software tool) is used to form a connection to the peripheral board. Later, the peripheral board connects to the output of the ECG circuit as well as the reference point (ground) of the system. Since there is an established connection, the function of the GUI consists of routing the data collected by BTool and graphing the results in real time. The application also allowed us to record the displayed data for further processing and analysis.

5.3.6 Testing Full Wireless ECG System

The final ECG circuit is analogous to the EMG circuit explained in section 5.2.6 Testing Full EMG System. The implementation of the systems mostly differ in the values used in resistors and capacitors that provide the cutoff frequencies and the appropriate gain, as well as the electrodes used as inputs to the instrumentation amplifiers. The five stages of the front end of the ECG circuit are shown in Figure. 5.75.

The last step for testing the implemented ECG circuit on the breadboard, was to acquire ECG data using an ECG simulator and later electrodes attached to skin. Since the magnitude responses of the filters, the gain of all the stages as well as the expected outputs using a sine wave input were achieved, the TechPatient CARDIO ECG Simulator device was used next. The use of a simulator ensured that the function of each of the stages was correct since there was no noise generated by the skin-electrode contact and a clear representation of an ECG would be displayed. The output of our analog circuit was then connected to the analog pin DIO23 of the TI CC26X2R1 peripheral board (its ADC input pin) which sampled and transmitted the signal to the master TI CC26X2R1 via Bluetooth as described earlier in the previous section. The data transferred are displayed on the computer using the application designed by He Wang and was granted to us in order to graph the obtained signal in real time shown in Figure 5.76.
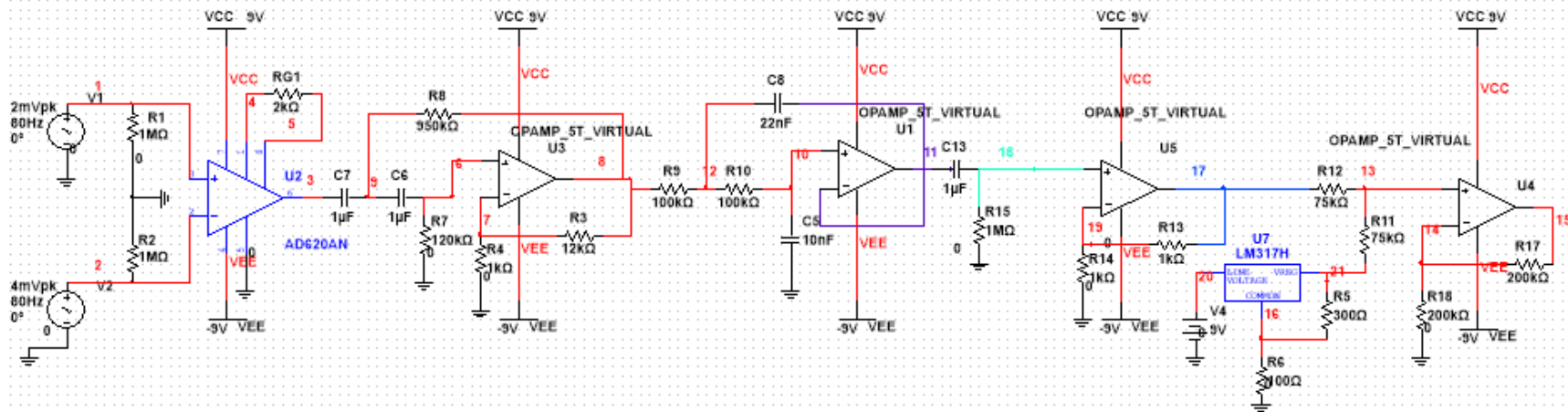
Figure 5.75: Circuit Diagram of the front end for wireless ECG design

The simulator device provides a 12-lead signal. However, since the designed system utilizes two electrodes, only the right and left arms connections were used, mimicking Lead I. The ECG signal was successfully obtained as seen in Figure 5.76; thus the accuracy of the circuit was verified and we proceeded to testing the circuit by attaching the electrodes on skin.
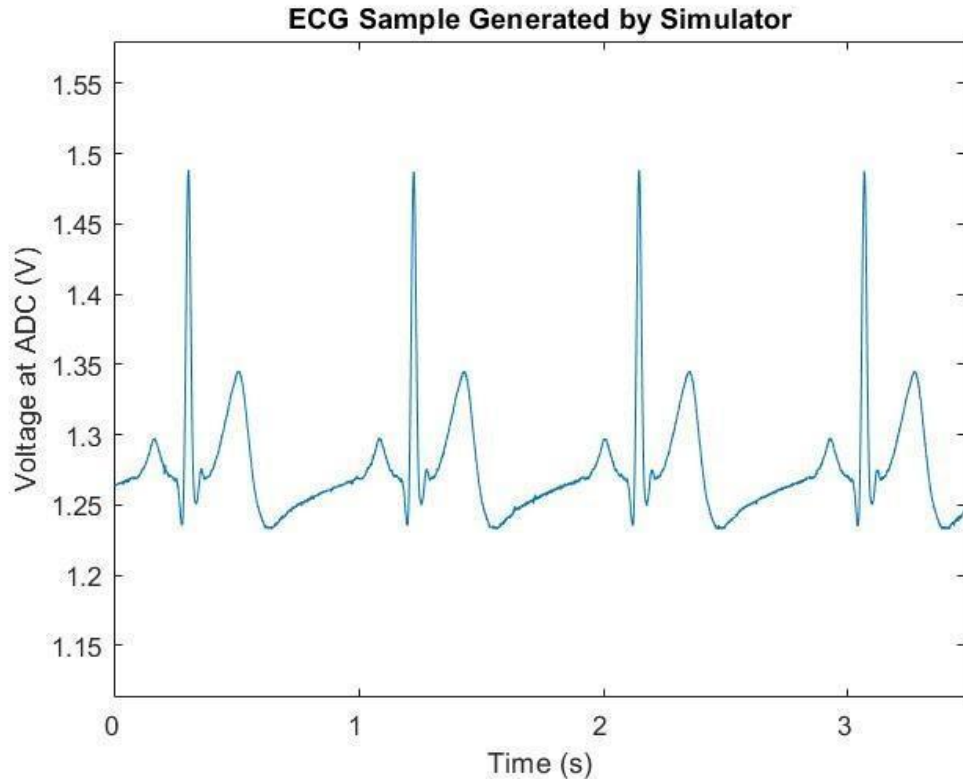
Figure 5.76: Wireless ECG Signal Recorded from the TechPatient CARDIO ECG Simulator.

Following the sample generated by the simulator device using Leal I, the electrodes were attached on a person's chest connecting the inverting input of the instrumentation amplifier to the right arm and the non-inverting input to the left arm. The implementation of Lead I was chosen as the electrodes are located closer to the heart, thus a high signal to noise ratio is expected. However, as observed in Figure 5.77, the signal can be partially detected, yet the presence of noise is prominent.

While testing, the decline of the noise was significant when the attachment between the electrodes and skin was secured by pressing on the electrodes against the skin. And, the noise appears to be periodic at 60 Hz frequency. Therefore, power line noise was suspected to have an

impact on the signal. Consequently, a digital notch filter was applied in real-time in MATLAB using a custom function "LogPlot_noNotch". Indeed, most of the noise was eliminated as seen in Figure 5.78. The denoised signal can be identified as an ECG as the QRS complex is visible, more information about the ECG characteristics as mentioned in the Background chapter, section 2.2.1 ECG Signal Characteristics.
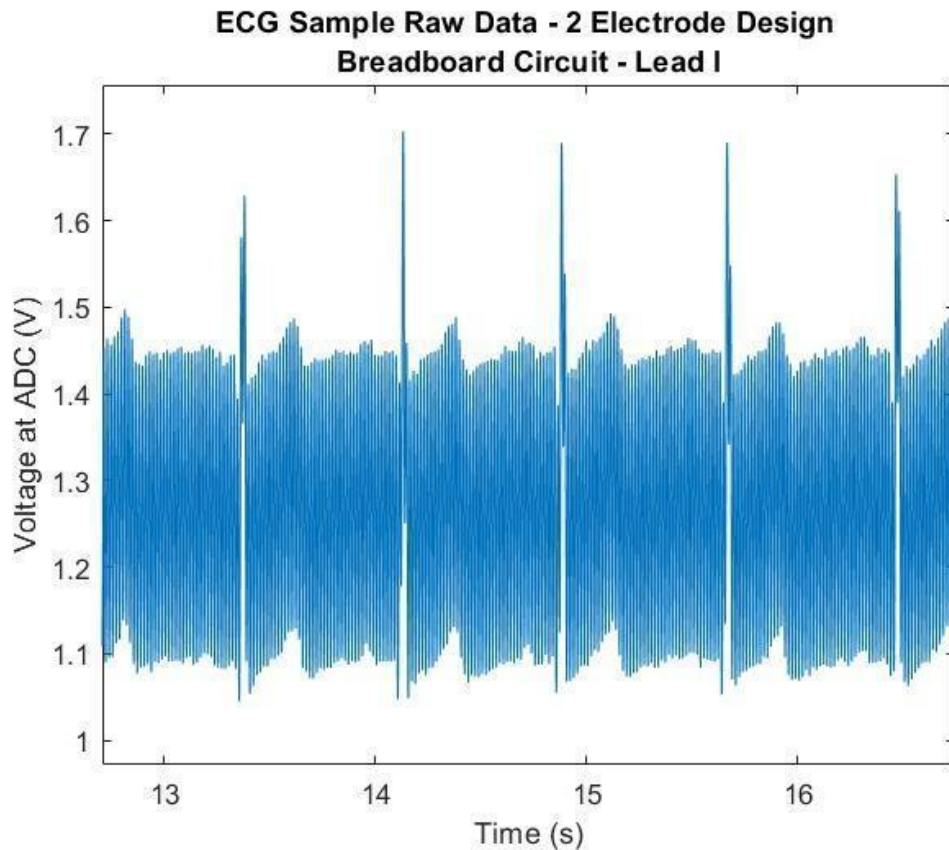
Figure 5.77: Wireless ECG Sample Raw Data - 2 Electrode Design Breadboard Circuit Lead I
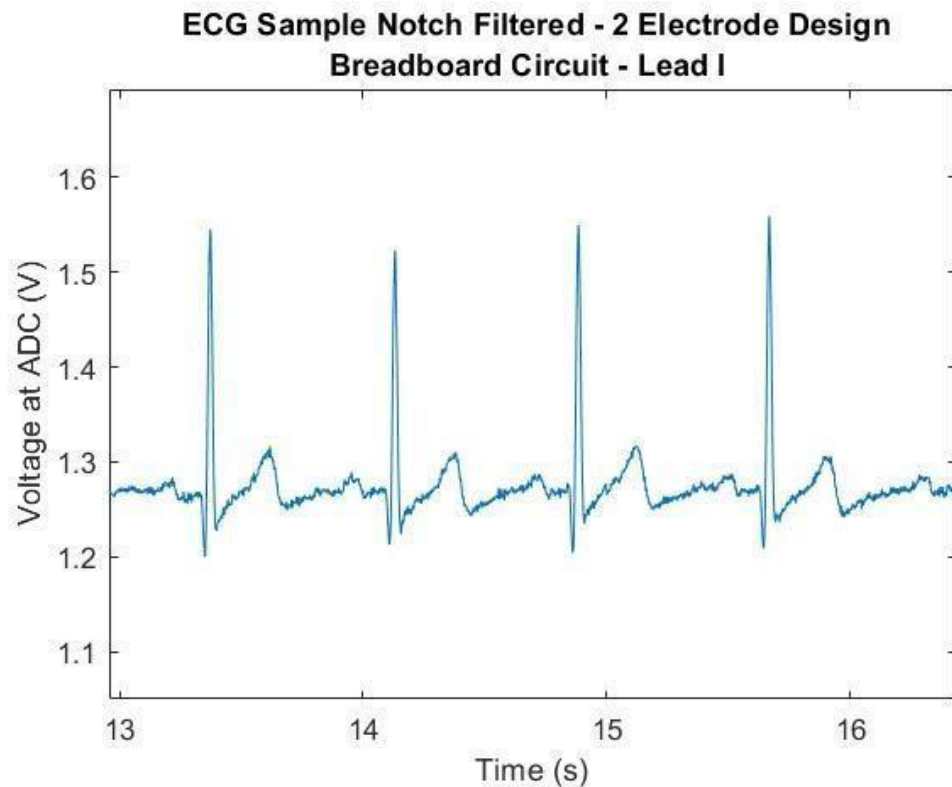
Figure 5.78: Wireless ECG Sample Notch Filtered - 2 Electrode Design on Breadboard Circuit Lead I

5.3.8 Wireless ECG PCB Board

The PCB design for the ECG system includes all the stages as shown in the Multisim circuit diagram in Figure 5.75. Like the previous PCB designs for the EMG circuit, the circuit was recreated in EAGLE and then converted to the PCB layout shown in Figure 5.79 with dimensions of 66.04 mm x 83.82 mm. The values, as well as the components are based on the breadboard implementation of the two-electrode ECG circuit. However, there is one difference in this PCB design that allowed us to implement a three-electrode ECG design as well to eliminate the noise as much as possible. The addition of part S1 shown on the lower left of Figure 5.79, is an EAGLE package of a 4-pin slider switch which connects the one end of each of two 1 MΩ resistors to ground. The 1 MΩ resistors that are mentioned, constitute resistors R1 and R2 shown in Figure 5.75. These two resistors are connected to the center tap of the two batteries which are connected in series, establishing a connection to the system's reference point.

The three-electrode design that is explained in section 2.3.2 Three-Electrode Design of the Background chapter, requires a third electrode attached to the skin to create a reference point.

Thus, in order to use it, the 1 MΩ resistors R1 and R2 need to be floating to allow the third electrode to create the reference point. To do so, two small jumper wires can be manually connected to the two holes when using the two-electrode design.
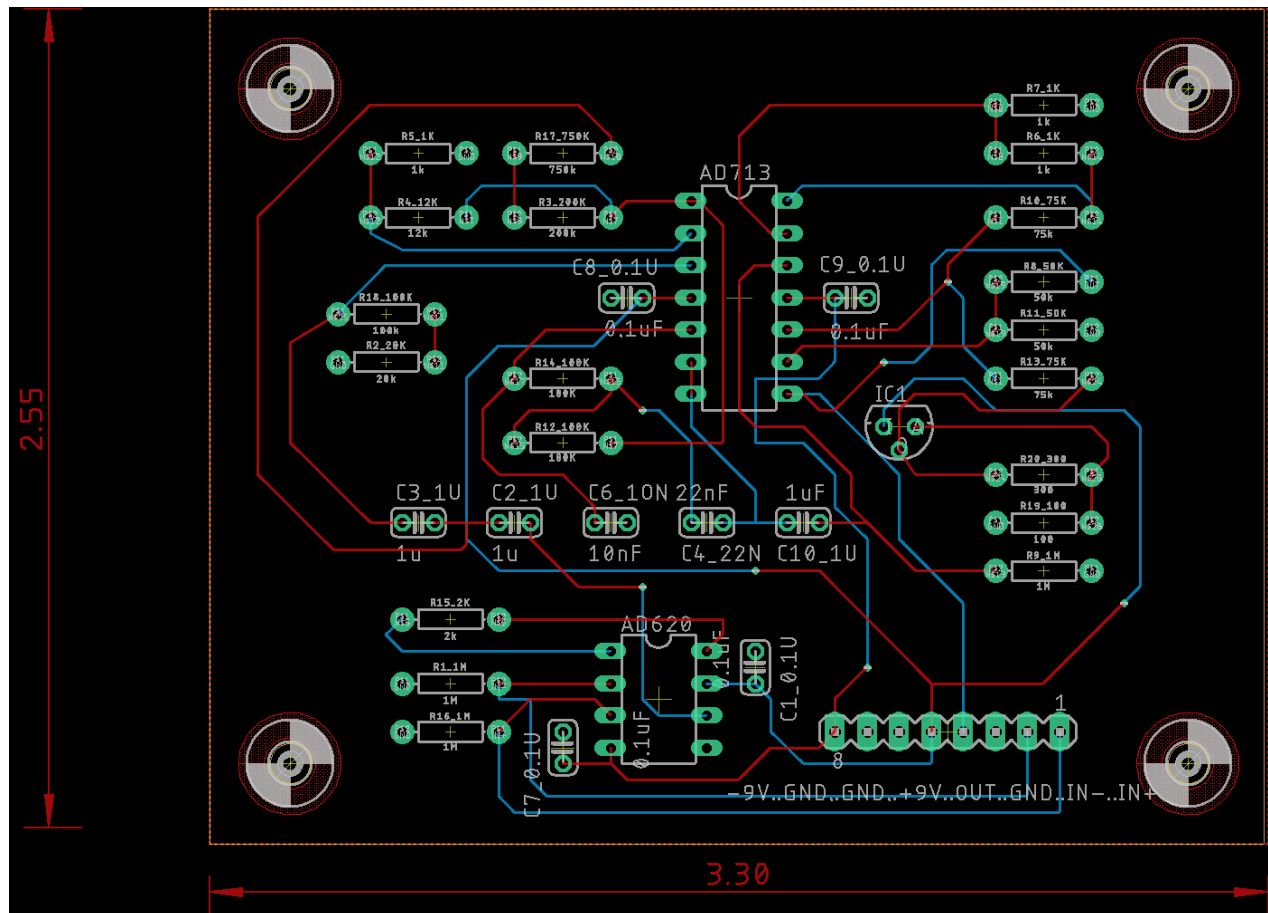
Figure 5.79: PCB Board Design of Wireless ECG circuit

The integrated circuit component specifications for the ECG circuit are identical to those components used for the EMG PCB design listed in Table 5-4 of section 5.2.7. The components' packages and the footprints that were selected for this design specifically for resistors, capacitors and DIP sockets are equivalent to the wired EMG's selection explained in section 5.1.5 Wired EMG System Components Selection.
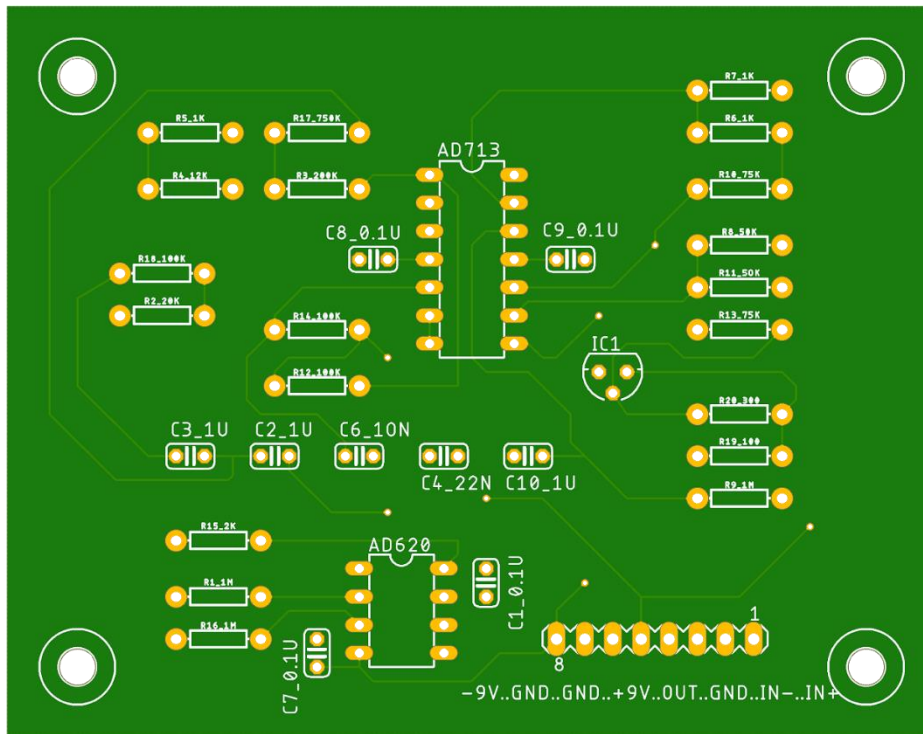
Figure 5.80: PCB Top Layer of Wireless ECG PCB Design
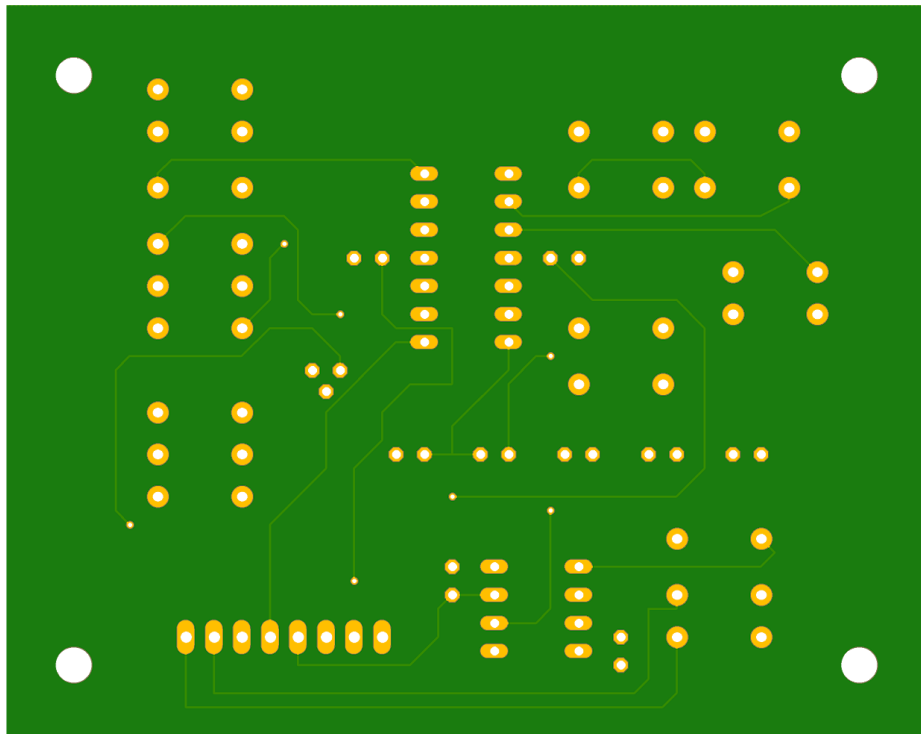
Figure 5.81: PCB Bottom Layer of Wireless ECG PCB Design

The following packages are used in the ECG design to complete the requirements of the circuit. As mentioned at the beginning of this section, a code switch package shown in Figure 5.82 is used to implement the three-electrode design.
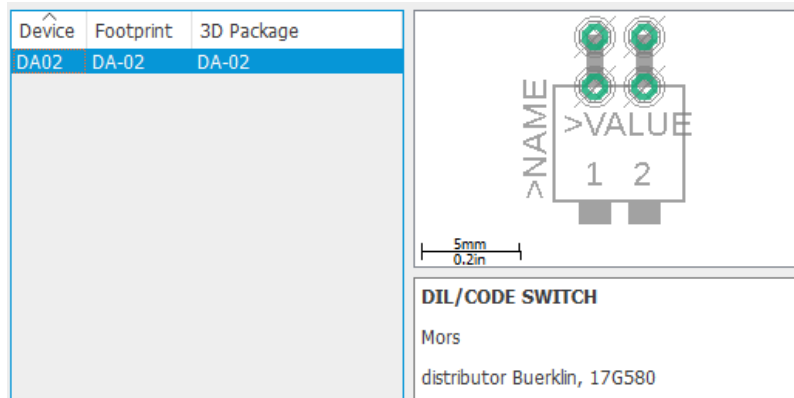
Figure 5.82: EAGLE Package Specification for Code Switch.

The DIP packages for the ICs were used in this design for convenience when soldering and testing. DIP sockets for the ICs are used to allow for replacement of components that might be damaged.
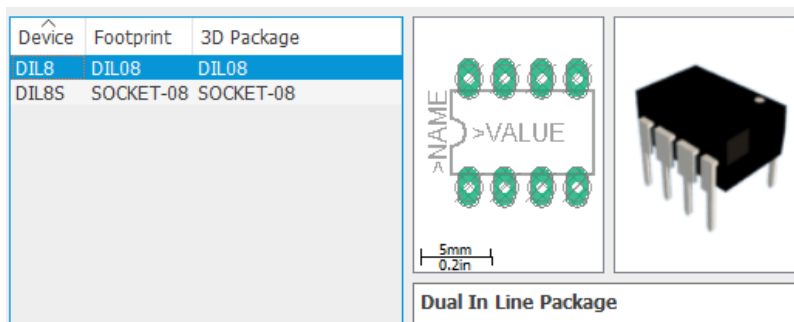
Figure 5.83: EAGLE Package Specification for AD620 Instrumentation Amplifier.

The pin headers were appropriate to connect the board to the power supply, connect the inputs of the electrodes to the instrumentation amplifier as well as provide an output pin of the system. Multiple pins were used as ground to ensure that all the peripherals used are connected to the reference point of the system.
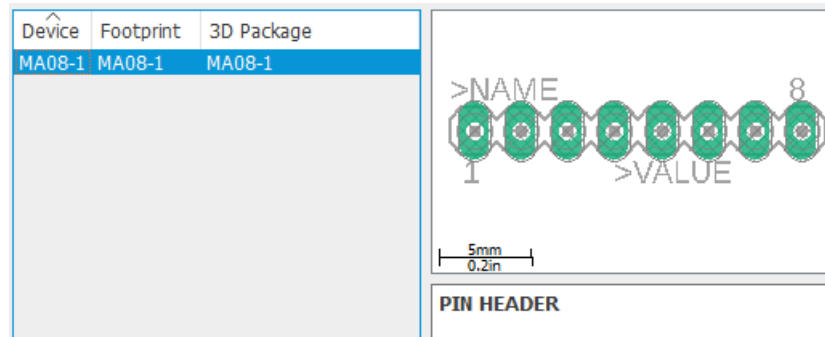
Figure 5.84 EAGLE Package Specification for 8 Pin Header

5.3.9 Wireless ECG PCB Assembly and Testing

The fabrication and considerations that provide a more accurate and possibly more reliable product as discussed in section 5.1.6, implemented for the EMG wired's design, were accordingly applied to develop the ECG circuit. The final product with all of the required components is shown in Figure 5.85.

Figure 5.85: The finished PCB for the ECG Wireless Circuit

Next, the PCB underwent testing to ensure accuracy and verify that it operates as expected. First, the gain of the instrumentation amplifier was tested within a range of 1 Hz to 3000 Hz to. A sine wave input of amplitude 200 mV was used for testing and the AD620 maintained a constant gain of 25.38 against the ideal expected gain of 25.7. The outcome was considered appropriate and we proceeded to testing the filters.

The magnitude response of the filters was generated following the same procedure that was used for testing the breadboard designs. The magnitude response of all the stages the system went through before being printed on a PCB are displayed in Figure 5.86. The response of the PCB is not ideal, as the cutoff frequency of the low pass filter seemingly lowered. Indeed, while testing the cutoff frequencies of the system confirmed to have dropped to 0.450 Hz for the high pass and 95 Hz for the low pass. These changes might be an impact of the tolerances of the resistors and capacitors as well as the thermal conditions of the ICs.
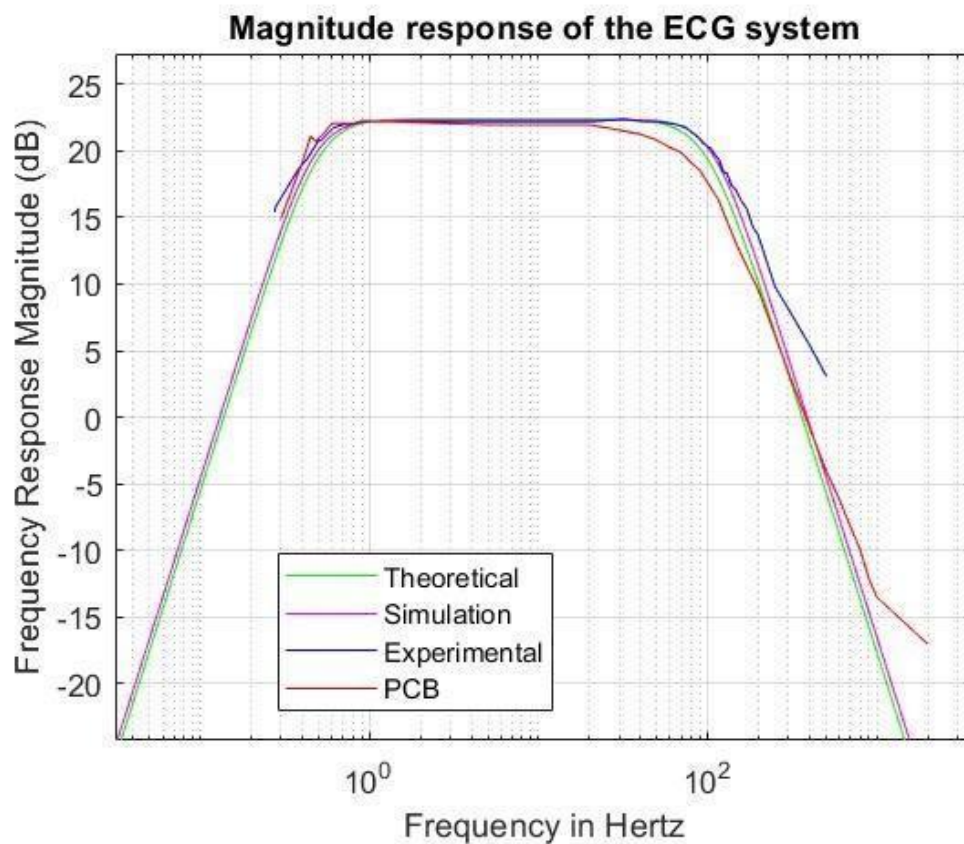
Figure 5.86: Magnitude Responses of Theoretical, Simulated, Experimental and PCB data gathered from filters.

Lastly, the PCB was tested with the two and the three-electrode design. The electrodes were placed on the chest acquiring ECG signal from Lead 1 as previously implemented for the breadboard circuit. As expected, the power line noise when using the two-electrode design was present as seen in Figure 5.87.
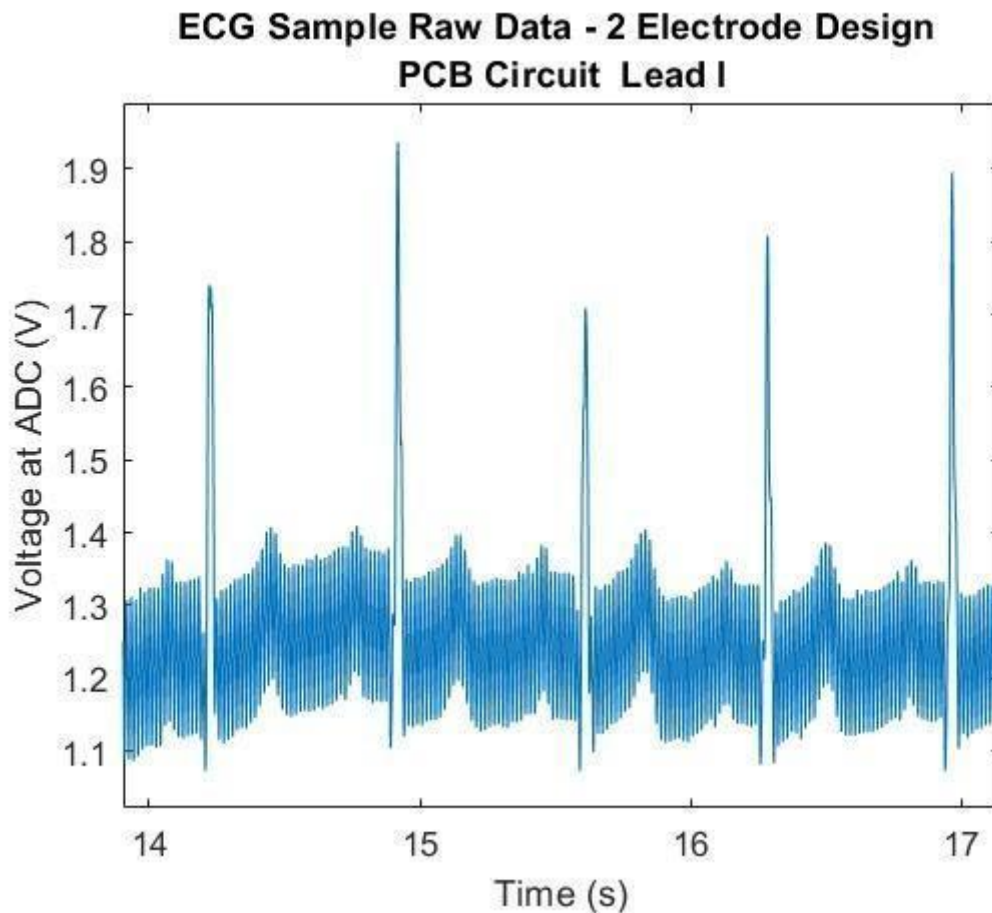
Figure 5.87: Wireless ECG Sample Raw Data - 2 Electrode Design PCB Circuit Lead I

The digital notch filter was applied in MATLAB to the raw ECG data to obtain a clear representation of the signal as seen in Figure 5.88. The outcome is similar to the data gathered using the breadboard circuit providing a detectable QRS complex verifying the ECG signal.

To conclude, the PCB was tested by using the three-electrode design to compare the level of noise generated. The resistors that connect the inputs to the reference point are now

disconnected, and a third electrode is connected to ground and to the right leg to provide the reference point. The raw data that were obtained using the third electrode is significantly denoised as you can observe in Figure 5.89. In this case, not only the QRS complex is recognizable, but each of the peaks are more distinct and sharp.
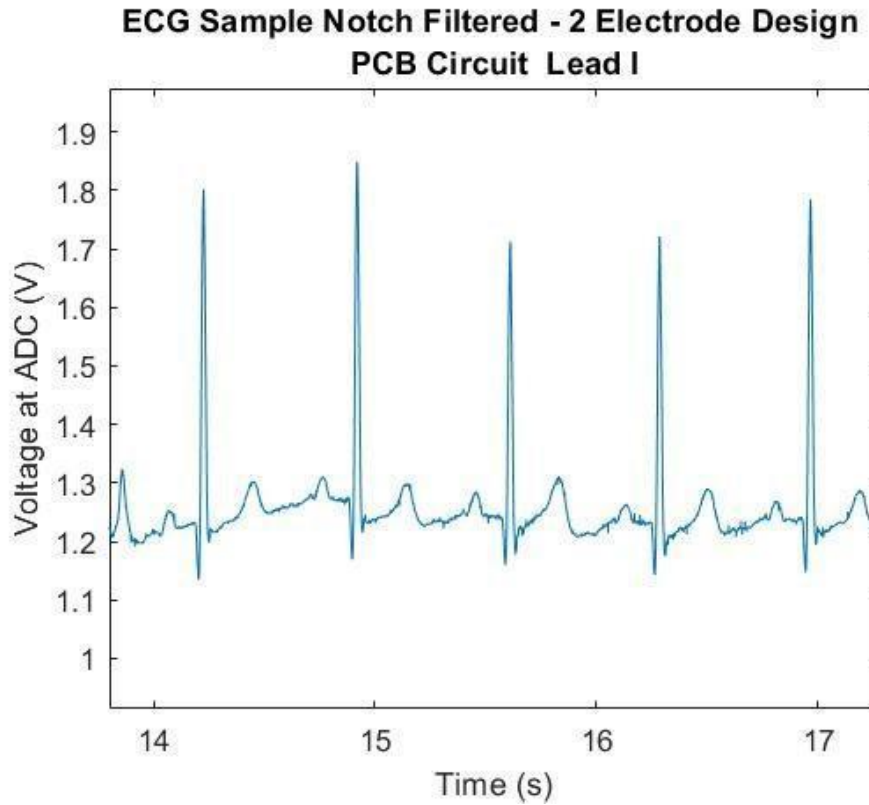
Figure 5.88: Wireless ECG Sample Notch Filtered- 2 Electrode Design PCB Circuit Lead I
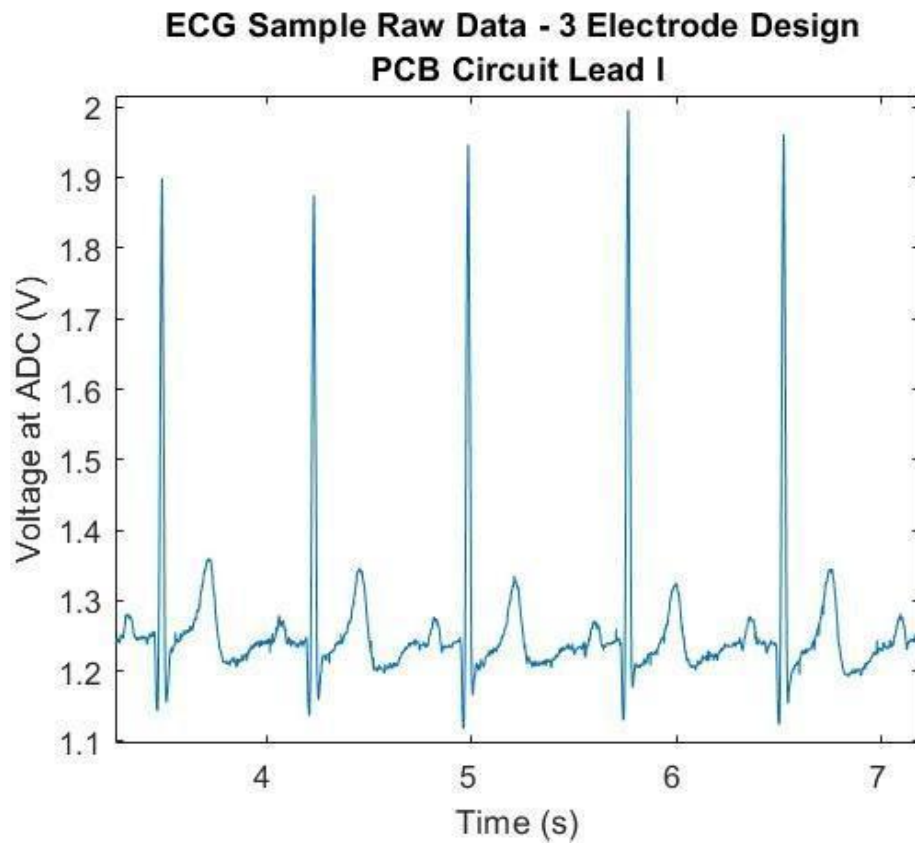
Figure 5.89: Wireless ECG Sample Raw Data - 3 Electrode Design PCB Circuit Lead I

6 Discussion

Originally, this project was meant to be focused completely on the wired EMG system. However, due to the COVID 19 pandemic, the majority of the project was completed off-campus and had group members in different states and countries. In order to preserve the learning and academic experience for all involved, a wireless team was created where one person worked on wireless EMG and the other worked on wireless ECG. The main difference between the wired and wireless systems is the simplicity. The wireless system is a single channel system employing second-order filtering instead of fourth-order. In addition, the wireless team had the additional challenge of wireless transmission. The wireless EMG and ECG systems had various aspects of their design in common, sharing design stages that the wired EMG system didn't have. However, their signal characteristics are different such that each system has different filtering needs.

Overall, the creation of the different systems—wired EMG, wireless EMG, and wireless ECG—created a project where every member had goals and tasks that could be completed separately and independent of one another. At the same time, the similarities in design between the various systems made it easy to collaborate and help each other.

Wired System

The goals for the wired EMG were defined as developing a 4-channel EMG acquisition system with a 16–24-bit resolution ADC module, isolated power supply, and 5V power to the ADC. Also, a CMRR of 80-100 dB at 60 Hz, selectable gain, current consumption of ≤ 350 mA, and overall a relatively small system in size and weight. The final design was tested with the equipment available in the lab and with a less expensive 12-bit resolution ADC module. The completed wired EMG system is shown below.
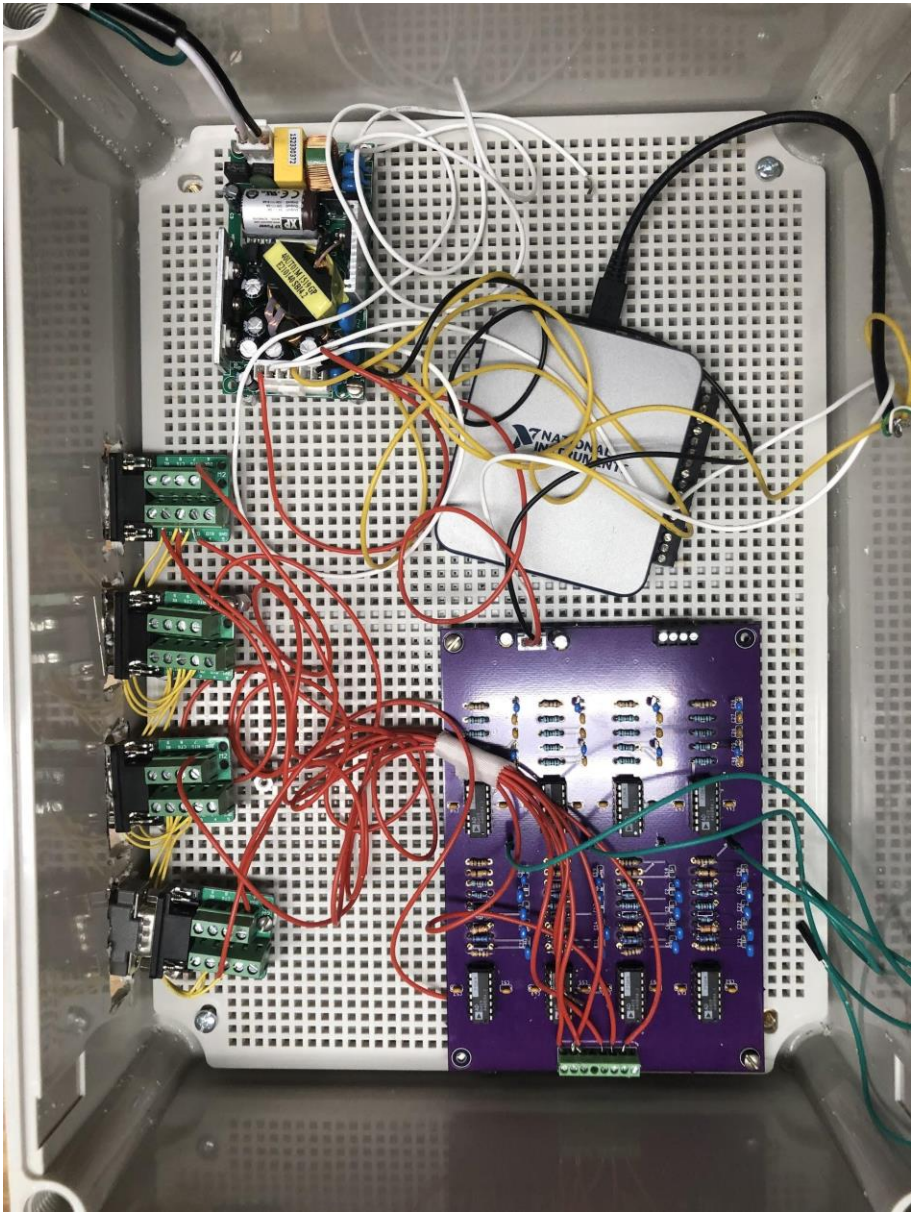
Figure 6.1: Wired EMG Acquisition System (without top)
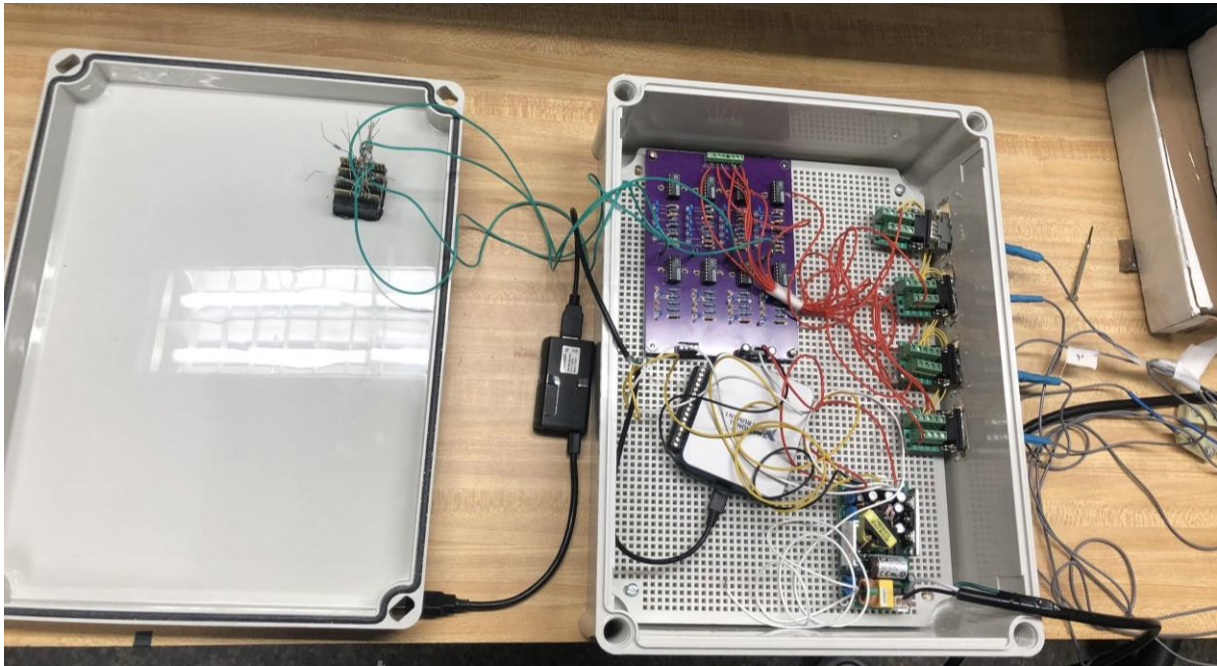
Figure 6.2: Completed Wired EMG Acquisition System (with top)

Figure 6.3: Wired EMG Acquisition System (Electrodes)

Limitations

Certain limitations were placed on the project due to the COVID-19 Pandemic. The two students who were able to be on campus completed the wired EMG system. The other two members worked remotely on two wireless systems, one EMG and one ECG. The goals were altered to adapt to the current situation where the overall accomplishment was getting data and testing the functionality. The wired EMG, was able to be tested using electrodes and a prosthetic arm to fulfill the end goal of a working product.

Future Work

Future implementations for the Wired EMG system include developing the 16-channel system. This would involve an additional 3 PCB's of the 4-channel system and switching the ADC module to accommodate the increase in channels. The NI USB-6210 ADC will replace the 8 input ADC. Another implementation is developing an enclosure specifically for the system 16-channel system that can hold all of the components.

Wireless Systems

The goals for the wireless systems included the design and implementation of EMG and ECG acquisition systems and the wireless transmission of the data via Bluetooth between two microcontrollers. Our goals also included the design and print of a custom printed board along with post signal processing for at least one of the systems.

After a period of design and simulation, the wireless systems were both built on breadboards. The two systems were found to be working properly and the wireless transmission between a central and a peripheral TI CC26X2R1 board was achieved. The final output for both designs were displayed in real time on a MATLAB graphical user interface that allowed us to detect an ECG signal as well as identify the change in the signal amplitude of an EMG signal when there was a muscle flexion.
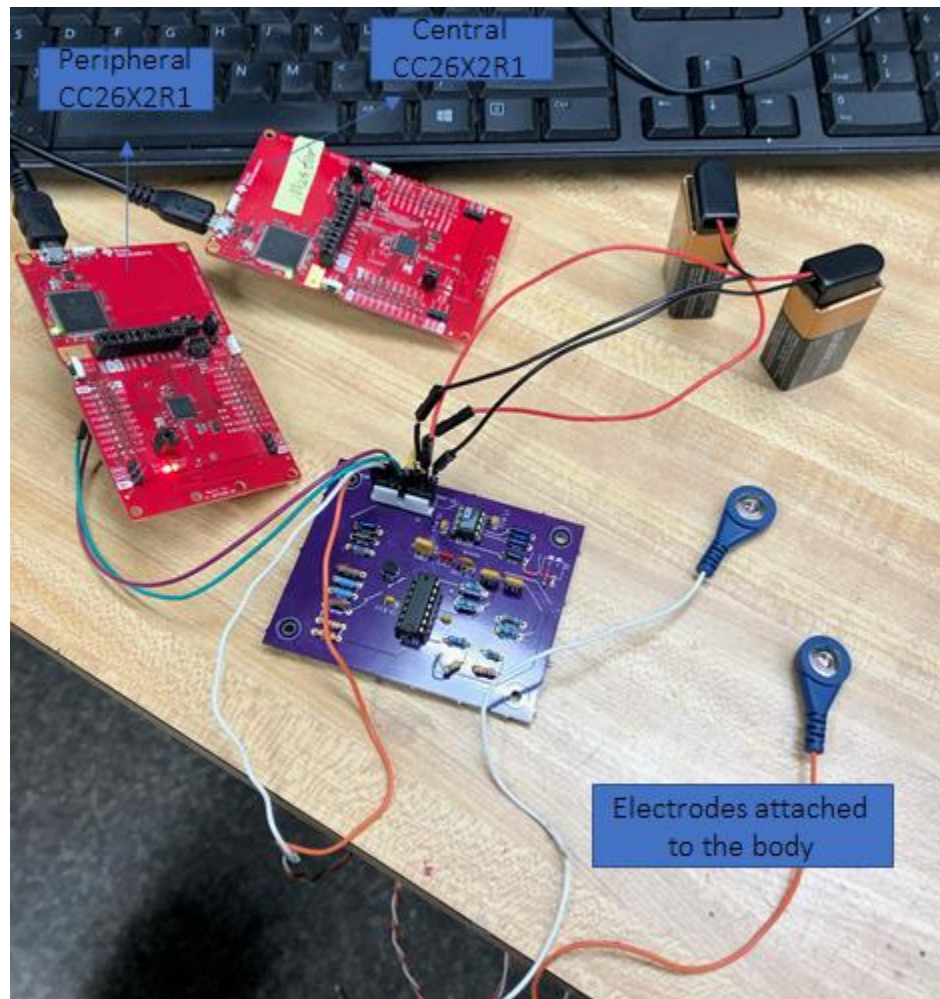
Figure 6.4: Wireless ECG Acquisition Assembled System

An attempt at a PCB for both the EMG and ECG systems were made. Ultimately, the ECG PCB was successful, while the EMG PCB was not. The goal of making one of these systems a PCB was met. The fully assembled wireless ECG system is shown in Figure 6.4 where the peripheral board, connected to the output of the PCB, transmits the acquired data to the central board wirelessly. The peripheral microcontroller, in its development board for our prototype, is intended to be battery powered in a fielded device.

Standards

The subteam that completed the first half of the project remotely worked towards designing and developing an EMG and an ECG wireless acquisition system. The research and design process

was obtained based on design requirements as well as specific standards and ethics to ensure the testing process is safe and accurate.

The data samples collected by the ECG system using the graphical user interface were later processed by applying a notch filter on MATLAB to eliminate the noise generated by a 60 Hz power line hum in the results.

The MCUs that were used for the wireless systems, the CC2640R2F, are wireless and support Bluetooth 5.1 Low Energy protocol at 2.4 GHz. The boards were used as a master and a slave using the Bluetooth Low Energy (BLE) Profile which allowed us to send the desired data between the two connected devices. BLE was appropriate for our project, since we do not require very high data rates, yet low consumption was an important factor as our systems use batteries.

Creating each of the three circuit boards relied on physical board layer information exchanged using a standard Gerber file format. Connection of the master MCU to a PC relied on real-time connection over a standard USB port. Electronic circuit simulation in Multisim relied on their implementation of the PSpice standard.

Limitations

The biggest challenge faced by the wireless team was the fact that we were forced to work remotely by the pandemic. This greatly affected the timeline of the project. Throughout the first half of the project, the wireless teams did not have access to lab equipment to test either prototype. Eventually, the wireless team received Bitscopes via mail but this tool had issues with precision, due to the fact that the inputs to our sensing circuits are meant to receive very small signals. Upon both members of the wireless team arriving back to campus, it was easier to test the boards and see that they were working correctly. However, when it came to the PCB design, the team realized early on that there would only be enough time for one attempt, since we had to wait for OSHPark to make the board and send it to us. This is the main factor for attempting the PCB design for both systems so that we would have a better chance of at least one working. This ended up being a good idea because even though the EMG PCB was created first, the ECG PCB was the one that ended up working. In addition, this was the first PCB ever designed by members of the team. Therefore, there was a lot of room for error in the PCB design.

148

Future Work

Despite the challenges faced, we were able to meet the goals for this project. When considering the scope we would set for the wireless team, a few reach goals were discussed. One of the possibilities included a very small PCB design where the board could be designed to be smaller than a couple centimeters sided square. The boards we created are more a couple inches on each side as we were not actively trying to create a very small board. A smaller design would be convenient for placing on human test subjects, and there would be less noise from large lengths of wire. Moreover, another possibility is a more accurate wireless EMG system. The wired EMG system had more channels and higher order filters, but it was not designed to be used with the wireless system. If one's goal was to have a more accurate wireless system, parts of the wired EMG front end and wireless ECG front end could be combined to achieve that goal.

Conclusion

Ultimately, the goals of this report for both the wired and wireless teams were accomplished. This project was able to deliver the design and prototype for a wired EMG system, a wireless EMG system, and a wireless ECG system. In addition, successful PCBs were designed and printed for the wired EMG and wireless ECG system. Moreover, a successful transmission of data between a peripheral and central node was implemented for the wireless systems. This data transmission can be displayed in real time using MATLAB. These deliverables were made possible through research and design based on design specifications laid out early in the project.

References

1. ASET - The Neurodiagnostic Society (1997, August) Invasive Electrode Techniques Retrieved from https://www.aset.org/files/public/Invasive_Electrode_Techniques.pdf

2. Bai, Y. W., Cheng, C. Y., Lu, C. L., & Huang, Y. S. (2005, May). Design and implementation of an embedded remote ECG measurement system. In 2005 IEEE Instrumentationand Measurement Technology Conference Proceedings (Vol. 2, pp. 1401-1406). IEEE.

3. Bermudez Follow, N. (2011, June 23). Cardiac Electrophysiology. Retrieved September 13, 2020, from https://www.slideshare.net/TeleClinEd/cardiac-electrophysiology

4. Biel, L., Pettersson, O., Philipson, L., & Wide, P. (2001, June). ECG Analysis: A New Approach in Human Identification. Retrieved September 13, 2020, from https://ieeexplore.ieee.org/stamp/stamp.jsp?tp=

5. Bitscope. (2020). BitScope Micro: BS05. Retrieved February 14, 2021, from https://bitscope.com/product/BS05/

6. Cadogan, M. (2019). [Image of three electrode system] [Image]. Line in the Fast Lane. Retrieved from https://litfl.com/ecg-lead-positioning/

7. Company-Bosch, E., & Hartmann, E. (2003, November). ECG Front-End Design is Simplified with MicroConverter®. Retrieved October 05, 2020, from https://www.analog.com/en/analog-dialogue/articles/ecg-front-end-design-simplified.html

8. Davis, M. (15, April 2020). How the Heart Works: Diagram, Anatomy, Blood Flow. Retrieved September 13, 2020, from https://www.medicinenet.com/heart_how_the_heart_works/article.htm

9. DayCounter Inc. (2019). Sallen-Key Low Pass Butterworth Filter Calculator. Retrieved November 29, 2020, from https://daycounter.com/Filters/Sallen-Key-LP-Calculator.phtml

10. Duskalov, I. K., Dotsinsky, I. A., & Christov, I. I. (1998). Developments in ECG acquisition, preprocessing, parameter measurement, and recording. IEEE Engineering in Medicine and Biology Magazine, 17(2), 50-58.

11. Francis, J. (2016). ECG monitoring leads and special leads. Indian pacing and electrophysiology journal, 16(3), 92-95.

12. Hampton, J. R., & Hampton, J. (May, 2019). Part 1: The ECG made very easy indeed. In *The ECG made easy* (9th ed., pp. 1-7). Amsterdam: Elsevier.

13. Hsieh, H. Y., Luo, C. H., Ye, J. W., & Tai, C. C. (2019). Two-electrode-pair electrocardiogram with no common ground between two pairs. Review of Scientific Instruments, 90(11), 114703.

14. Jones, S. A. (7, December 2009). *ECG notes: Interpretation and management guide* (2nd ed., pp. 1-30). Philadelphia, PA: F.A. Davis.

15. Konrad, P. (2005). Signal Origin and Acquisition. In *The ABC of EMG: A Practical Introduction to Kinesiological Electromyography* (pp. 9-11). Noraxon.

16. M. Konar, R. Sahu and S. Kundu, "Improvement of the Gain Accuracy of the Instrumentation Amplifier Using a Very High Gain Operational Amplifier," 2019 Devices for Integrated Circuit (DevIC), Kalyani, India, 2019, pp. 408-412, doi: 10.1109/DEVIC.2019.8783414.

17. Kumar, A. (2020, January 08). 10 Lead ECG Placement [Digital image]. Retrieved March 28, 2021, from https://www.biometriccables.in/blogs/blog/three3-five5-ten10-lead-ecg-cable-electrode-placement

18. Mangukiya, Y., Purohit, B., & George, K. (2017). Electromyography(EMG) sensor controlled assistive orthotic robotic arm for forearm movement. 2017 IEEE Sensors Applications Symposium (SAS), 1-4.

19. Muhammad Zahak Jamal (2012, October). Signal Acquisition Using Surface EMG and Circuit Design Considerations for Robotic Prosthesis, Computational Intelligence in Electromyography Analysis - A Perspective on Current Applications and Future Challenges, Ganesh R. Naik, IntechOpen, DOI: 10.5772/52556. Available from: https://www.intechopen.com/books/computational-intelligence-in-electromyography-analysis-a-perspective-on-current-applications-and-future-challenges/signal-acquisition-using-surface-emg-and-circuit-design-considerations-for-robotic-prosthesis

20. National Instruments. (2020). Multifunction I/O Device Product. Retrieved November 26, 2020, from https://www.ni.com/en-us/shop/hardware/products/multifunction-io-device.html?modelId=124893

21. Novosel, D., Noll, G., & Lüscher, T. F. (1999). Corrected formula for the calculation of the electrical heart axis. Croatian Medical Journal, 40, 77-79.

22. Pu, X., Wan, L., Sheng, Y., Chiang, P., Qin, Y., & Hong, Z. (2012, November). A wireless 8-channel ECG biopotential acquisition system for dry electrodes. In *2012 IEEE International Symposium on Radio-Frequency Integration Technology (RFIT)* (pp. 140-142). IEEE

23. Rehman, I. (2020, July 10). Anatomy, Thorax, Heart. Retrieved September 13, 2020, from https://www.ncbi.nlm.nih.gov/books/NBK470256/

24. Reisner, Andrew T., Clifford,Gari D, and Mark, Roger G. Course materials for HST.582J / 6.555J / 16.456J, Biomedical Signal and Image Processing, Spring 2007. MIT OpenCourseWare (http://ocw.mit.edu), Massachusetts Institute of Technology.Downloaded on [4 October 2020].

25. Samuel, O. W., Zhou, H., Li, X., Wang, H., Zhang, H., Sangaiah, A. K., & Li, G. (2018). Pattern recognition of electromyography signals based on novel time domain features for amputees' limb motion classification. Computers & Electrical Engineering, 67, 646-655.

26. Sedra, A. S., Smith, K. C., Carusone, T. C., & Gaudet, V. (2020). *Microelectronic circuits* (p. 79). New York, NY, NY: Oxford University Press.

27. Sörnmo, L., & Laguna, P. (2005). Bioelectrical signal processing in cardiac and neurological applications. Elsevier Academic Press.

28. Sparkfun. (2021). Sparkfun/sparkfun-eagle-libraries. Retrieved February 15, 2021, from https://github.com/sparkfun/SparkFun-Eagle-Libraries

29. Thakor, N. V., & Webster, J. G. (1980). Ground-free ECG recording with two electrodes. IEEE Transactions on Biomedical Engineering, (12), 699-704.

30. Tompkins, W. J. (2006). Electrocardiography. In *Biomedical digital signal processing: C-language examples and laboratory experiments for the IBM PC* (pp. 24-53). New Delhi: Prentice-Hall.

31. Weiss, L., Weiss, J., Gaudino, W., & Gustafson, K. (2004). Chapter 5: Electromyography. In *Easy EMG*. Butterworth-Heinemann.

32. XP Power. (2020). ECP40 Series Power Product Range. Retrieved November 26, 2020, from https://www.xppower.com/product/ECP40-Series

33. Yamamoto, A. Y., Nakamura, T., & Kitaoka, K. (2000, May). Automatic interference controller device for eliminating the power-line interference in biopotential signals. In Proceedings of the 17th IEEE Instrumentation and Measurement Technology Conference [Cat. No. 00CH37066] (Vol. 3, pp. 1358-1362). IEEE.

34. Yazicioglu, R. F., Hoof, C. V., & Puers, R. (2009). Introduction to Biopotential Acquisition. In *Biopotential readout circuits for portable acquisition systems* (pp. 5-18). Dordrecht: Springer.

35. Yoo, J., Yan, L., Lee, S., Kim, H., & Yoo, H.-J. (2009). A Wearable ECG Acquisition System With Compact Planar-Fashionable Circuit Board-Based Shirt. *IEEE Transactions on Information Technology in Biomedicine*, *13*(6), 897–902. https://doi.org/10.1109/TITB.2009.2033053

Appendix

Appendix A: MATLAB Files

butter_hi_design.m (Written by E.A.Clancy) (Select components and plot the frequency response of the high pass filter)

```
function H = butter_hi_design(f, Fc, A, Stage1, Stage2, Stage3, Stage4, Stage5)
%
% H = b_hi_des(f, Fc, A, Stage1[, Stage2[, Stage3[, Stage4[, Stage5]]]])
%
%   Helps design an electronic circuit to build even-order, high-pass
% Butterworth filters of orders 2, 4, 6, 8, 10.  Plots the magnitude of
% the resulting frequency response.
%   See [Thomas Kugelstadt, "Chapter 16: Active
% Filter Design Techniques," Literature Number SLOA088, Texas Instruments
% Incorporated, Post Office Box 655303, Dallas, Texas  75265, 2001.
% Excerpted from "Op Amps for Everyone," Literature Number SLOD006A,
% Texas Instruments.  Available on the Internet at: http://www.ti.com].
%
% f:     Frequency axis (Hertz) for all calculations and plotting (vector).
% A:     Overall circuit gain (>=1).  Applied in 1st stage.
% Fc:    Desired cutoff frequency in Hertz (scalor).
% StageX: Up to 5 StageX arguments (one per stage) are permitted.  For each stage,
%         StageX is a vector of 1-4 elements, corresponding to C1, C2,
%         R1 and R2, respectively.  C1 must be supplied (in Farads) and
%         is the first vector element.  If a second argument is supplied,
%         then it is C2 (in Farads).  If C2 is not supplied, it is set
%         equal to C1.  If
%         a third argument is supplied, it is R1 (Ohms).  If not supplied,
%         it is set as required to form a Butterworth filter.  If a fourth
%         argument is supplied, it is R2 (Ohms).  If not supplied, it is
%         set as required to form a Butterworth filter.
%
% H: Resulting (complex-valued) frequency response corresponding to the
%    frequency axis f.
%
% USAGE RECOMENDATIONS:  To build a filter, initially call script with only
%   C1 and C2 specified for each stage.  Use the recommended
%   R1 and R2 values to find R1's and R2's that are manufactured.  Call the
%   script a second time with all values to see the resultant nominal frequency
%   response.

% Table of ai values.  For even-order Butterworth, all bi values equal 1.
aiTable = [1.4142   NaN   NaN   NaN   NaN;  % For 1-stage filter.
```

```
          1.8478 0.7654   NaN   NaN   NaN;  % For 2-stage filter.
          1.9319 1.4142 0.5176   NaN   NaN;  % For 3-stage filter.
          1.9616 1.6629 1.1111 0.3902   NaN;  % For 4-stage filter.
          1.9754 1.7820 1.4142 0.9080 0.3129]; % For 5-stage filter.

% Determine the number of stages.
Nstage = nargin - 3;
if Nstage<1 | Nstage>5, error('Must have 1-5 stages.'); end
if A<1, error('"A" must be >= 1.'); end

% Extract/develop parameters for each stage and build the frequency response.

H = ones( 1, length(f) );  % Initialize frequency response to unity.
w = 2*pi*f;           % Convert to radian frequency.
MagBig = A;            % Cascade passband gain.

for S = 1:Nstage

  if S>1, A = 1; end  % Set gain to one after first stage.

  % Prepare to parse parameter vector.
  eval(['Param = Stage' int2str(S) ';']);  % Copy parameters to a scratch vector.
  if length(Param)<1, error(['Stage ' int2str(S) ' parameter list < 1.']); end;
  if length(Param)>4, error(['Stage ' int2str(S) ' parameter list > 4.']); end;
  ai = aiTable(Nstage,S);

  % Parse parameter vector.
  % C1.
  C1 = Param(1);
  % C2.
  if length(Param)>1,  C2 = Param(2);  else,  C2 = C1; end
  % R1.
  if length(Param)>2,  R1 = Param(3);
  elseif A==1
   R1 = ( C1+C2 ) / ( 2*pi*Fc*ai*C1*C2 );
  else
   a = ((2*pi*Fc)^2) * C1*C2*C2*(1-A);
   b = -ai * 2*pi*Fc * C1*C2;
   c = C1 + C2;
   R1 = ( -b - sqrt(b*b - 4*a*c) ) / (2*a);
  end
  % R2.
  if length(Param)>3,  R2 = Param(4);
  else,  R2 = 1 / ( ((2*pi*Fc)^2)*R1*C1*C2 ); end
```

```
  % Print component values.
  fprintf('Stage %d: C1=%e F, C2=%e F, R1=%e Ohms, R2=%e Ohms\n', S, C1, C2, R1, R2);

  % Update frequency response.
  a = ( R2*(C1+C2) + R1*C2*(1-A) ) ./ (R1*R2*C1*C2);
  b = 1 ./ (R1*R2*C1*C2);
  Hstage = A ./ (  1 + ( a./(j*w) ) + ( b./(-w.*w) )  );
  H = H .* Hstage;
end

% Now, plot the frequency response magnitude.
plot( f, abs(H) )
xlabel('Frequency in Hertz')
ylabel('Frequency Response Magnitude')

L1 = find( abs(H) >= (MagBig*sqrt(2)/2) );
hold on, plot([f(L1(1)) f(L1(1))], [0 MagBig], 'm'), hold off
Thing = sprintf('Cut-off at %0.2f Hz, Passband Gain = %0.2f', f(L1(1)), MagBig);
text( max(f)/5, max(abs(H))/3, Thing);
title('Butterworth High-Pass Filter');

figure(gcf);

return
```

butter_lo_design.m(Written by E.A.Clancy) (Select components and plot the frequency response of the low pass filter)

```
function H = butter_lo_design(f, Fc, A, Stage1, Stage2, Stage3, Stage4, Stage5)
%
% H = b_lo_des(f, Fc, A, Stage1[, Stage2[, Stage3[, Stage4[, Stage5]]]])
%
%   Helps design an electronic circuit to build even-order, low-pass
% Butterworth filters of orders 2, 4, 6, 8, 10.  Plots the magnitude of
% the resulting frequency response.
%   See [Thomas Kugelstadt, "Chapter 16: Active
% Filter Design Techniques," Literature Number SLOA088, Texas Instruments
% Incorporated, Post Office Box 655303, Dallas, Texas  75265, 2001.
% Excerpted from "Op Amps for Everyone," Literature Number SLOD006A,
% Texas Instruments.  Available on the Internet at: http://www.ti.com].
%
% f:     Frequency axis (Hertz) for all calculations and plotting (vector).
% A:     Overall circuit gain (>=1).  Applied in 1st stage.
% Fc:    Desired cutoff frequency in Hertz (scalor).
% StageX: Up to 5 StageX arguments (one per stage) are permitted.  For each stage,
%          StageX is a vector of 1-4 elements, corresponding to C1, C2,
```

```
%          R1 and R2, respectively.  C1 must be supplied (in Farads) and
%          is the first vector element.  If a second argument is supplied,
%          then it is C2 (in Farads).  If C2 is not supplied, it is set
%          equal to C1.  If
%          a third argument is supplied, it is R1 (Ohms).  If not supplied,
%          it is set as required to form a Butterworth filter.  If a fourth
%          argument is supplied, it is R2 (Ohms).  If not supplied, it is
%          set as required to form a Butterworth filter.
%
% H: Resulting (complex-valued) frequency response corresponding to the
%    frequency axis f.
%
% USAGE RECOMENDATIONS:  To build a filter, initially call script with only
%   C1 and C2 specified for each stage.  Use the recommended
%   R1 and R2 values to find R1's and R2's that are manufactured.  Call the
%   script a second time with all values to see the resultant nominal frequency
%   response.

% Table of ai values.  For even-order Butterworth, all bi values equal 1.
aiTable = [1.4142   NaN   NaN   NaN   NaN;  % For 1-stage filter.
          1.8478 0.7654   NaN   NaN   NaN;  % For 2-stage filter.
          1.9319 1.4142 0.5176   NaN   NaN;  % For 3-stage filter.
          1.9616 1.6629 1.1111 0.3902   NaN;  % For 4-stage filter.
          1.9754 1.7820 1.4142 0.9080 0.3129]; % For 5-stage filter.

% Determine the number of stages.
Nstage = nargin - 3;
if Nstage<1 | Nstage>5, error('Must have 1-5 stages.'); end
if A<1, error('"A" must be >= 1.'); end

% Extract/develop parameters for each stage and build the frequency response.

H = ones( 1, length(f) );  % Initialize frequency response to unity.
w = 2*pi*f;            % Convert to radian frequency.
MagBig = A;             % Cascade passband gain.

for S = 1:Nstage

 if S>1, A = 1; end  % Set gain to one after first stage.

 % Prepare to parse parameter vector.
 eval(['Param = Stage' int2str(S) ';']);  % Copy parameters to a scratch vector.
 if length(Param)<1, error(['Stage ' int2str(S) ' parameter list < 1.']); end;
 if length(Param)>4, error(['Stage ' int2str(S) ' parameter list > 4.']); end;
 ai = aiTable(Nstage,S);
```

```
% Parse parameter vector.
% C1.
C1 = Param(1);
% C2.
if length(Param)>1,  C2 = Param(2);  else,  C2 = C1; end
% R1.
if length(Param)>2,  R1 = Param(3);
else
  a = ((2*pi*Fc)^3) * C2 * ( C1 + (1-A)*C2 );
  b = -ai * C2 * ((2*pi*Fc)^2);
  c = 2*pi*Fc;
  R1 = ( -b - sqrt(b*b - 4*a*c) ) / (2*a);
end
% R2.
if length(Param)>3,  R2 = Param(4);
else,  R2 = 1 / ( ((2*pi*Fc)^2)*R1*C1*C2 ); end

% Print component values.
fprintf('Stage %d: C1=%e F, C2=%e F, R1=%e Ohms, R2=%e Ohms\n', S, C1, C2, R1, R2);

% Update frequency response.
a = C1*(R1+R2) + (1-A)*R1*C2;
b = R1 * R2 * C1 * C2;
Hstage = A ./ (  1 + ( a*j*w ) - ( b*w.*w )  );
H = H .* Hstage;
end

% Now, plot the frequency response magnitude.
plot( f, abs(H) )
xlabel('Frequency in Hertz')
ylabel('Frequency Response Magnitude')

L1 = find( abs(H) <= (MagBig*sqrt(2)/2) );
hold on, plot([f(L1(1)) f(L1(1))], [0 MagBig], 'm'), hold off
Thing = sprintf('Cut-off at %0.2f Hz, Passband Gain = %0.2f', f(L1(1)), MagBig);
text( max(f)/5, max(abs(H))/3, Thing);
title('Butterworth Low-Pass Filter');

figure(gcf);

return
```

Theoretical.m (Construct the frequency response of the prototype)
```
sim = readmatrix("ideal op-amp.txt");
```

```
experiment = readmatrix("Exp.xlsx");
f = logspace(0,6,10000); % Frequency in log scale
H2 = butter_hi_design(f, 15, 4, [68e-9 68e-9 90e3 280e3],[68e-9 68e-9 410e3 60e3]);
%Theoretical high pass filter
H4 = butter_lo_design(f, 800, 1, [1.84e-9 2.15e-9 100e3 100e3],[0.76e-9 5.2e-9 100e3 100e3]);
%Theoretical low pass filter
totalH = H2.*H4
fsim = sim(:,1); % frequency range of the simulation
gainsim = sim(:,2);  % frequency response of the simulation
fexp = experiment(:,2); % frequency range of the experiment
fmag = experiment(:,6);% frequency response of the experiment
figure(gcf), clf

semilogx(f, 20*log10(abs(totalH)),'r',fexp,fmag,'k',fsim,gainsim,'b')
grid on
xlabel('Frequency in Hertz');
ylabel('Frequency Response Magnitude (dB)');
title('Magnitude response of the system');
legend('Theoretical','Experimental','Simulation')
%print -djpeg -r300 butter_plt1.jpg
```

Daq_init.m (Initialize the ADC to sample a signal and plot it on MATLAB)
```
clear all;
dq = daq("ni");
dq.Rate = 10000; % The sampling rate is 10000 Hz
addinput(dq,"Dev1","ai0","Voltage");
data = read(dq,seconds(0.01)); % The sampling time is 0.01 second
figure(1);
plot(data.Time,data.Variables);
ylabel("Voltage(V)")
```

PCB_Testing.m (Construct the frequency response of the PCB)
```
sim = readmatrix("ideal op-amp.txt");
experiment = readmatrix("pcb testing.xlsx");
f = logspace(0,6,10000); % Frequency in log scale
H2 = butter_hi_design(f, 15, 4, [68e-9 68e-9 90e3 280e3],[68e-9 68e-9 410e3 60e3]);
%Theoretical high pass filter
H4 = butter_lo_design(f, 800, 1, [1.84e-9 2.15e-9 100e3 100e3],[0.76e-9 5.2e-9 100e3 100e3]);
%Theoretical low pass filter
totalH = H2.*H4;
fsim = sim(:,1); % frequency range of the simulation
gainsim = sim(:,2); % frequency response of the simulation
exp1f = experiment(:,2); % frequency range of the experiment
exp1mag = experiment(:,6); % frequency response of channel 1
```

```
exp2mag = experiment(:,11);% frequency response of channel 2
exp3mag = experiment(:,16);% frequency response of channel 3
exp4mag = experiment(:,21);% frequency response of channel 4
figure(gcf), clf

semilogx(f,
20*log10(abs(totalH)),'r',exp1f,exp1mag,'k',fsim,gainsim,'b',exp1f,exp2mag,'g',exp1f,exp3mag,'c
',exp1f,exp4mag,'m')
grid on
xlabel('Frequency in Hertz');
ylabel('Frequency Response Magnitude (dB)');
title('Magnitude response of the system');
legend('Theoretical','Channel 1','Simulation','Channel 2','Channel 3','Channel 4')
axis ([10^0 10^4 -50 50])
%print -djpeg -r300 butter_plt1.jpg
```

LogPlot_noNotch.m (Graphs the recorded data of wireless devices and implements notch filter)

```
clear;
clc;
%% Please change path to your own before using
path = '"C:\Users\athen\OneDrive\Desktop\C TERM 2021
Couses\MQP\TESTING_ECG_results"';
fid = fopen('Sample_pcb_test_chest_last_3ele2.bin','r');
data = fread(fid,'single','ieee-be');
fclose(fid); % Close files
NNfft = 256;
% [Smm_sCal,f] = pwelch(data, NNfft, round(0.75*NNfft), NNfft, 2);
% figure(1);
% plot(f*900,Smm_sCal);
%% Notch
%
 Fz =  [50 60 70 80 120:60:840];
 Bw = [8.2 10.2 8.2 8.2 8.2*ones(1,13)];

%Fz = [60 120 180];
%Bw = [10 5 5];


SampFreq = 1800;
for i = 1:length(Fz)
   [b, a] = iirnotch(2*Fz(i)/SampFreq, 2*Bw(i)/SampFreq);
   data = filtfilt(b,a,data);
end
figure(2);
```

```matlab
ax = gca;

plot(((data*3.3)/4096));

ylabel('Voltage at ADC (V)');
xlabel('Time (s)');
title('ECG Sample Generated by Simulator');

tick_scale_factor = 1800;
xlim([1 36000]);
ylim([1 2]);
ticks=[0 1800 3600 5400 7200 9000 10800 12600 14400 16200 18000 19800 21600 23400
25200 27000 28800 30600 32400 34200 36000];
xticks(ticks)
ax.XTickLabel = ax.XTick / tick_scale_factor;


% figure(3);
%[Smm_sCal,f] = pwelch(data, NNfft, round(0.75*NNfft), NNfft, 2);
% plot(f*900,Smm_sCal);
```

Appendix B: Instrumentation Amplifier Frequency Magnitude Response MATLAB

```matlab
function iamp_stage_v01

% Components.
Rg = 750;
R1 = 24.7E3;
Cg = 10E-6;
% Frequency values at which to evaluate.
f = 0:0.01:200;
w = 2*pi*f;

fdata = [5,10,20,50,100,140,180,200];

mag_data =
[13.72340426,27.51937984,44.8,61.47540984,61.40684411,62.40310078,61.64122137,62.8906
25];

phase_data = [64.8,64.8,51.84,21.6,21.6,0,0,0];
% Frequency response.
H = 1 + ( 2*R1 ./ (Rg + (1./(1j*w*Cg))) );

figure(1)
% Plot magnitude only.
plot(fdata,mag_data,':b.')
title('Ideal and recorded magnitude response')
hold on

plot(f, abs(H),'k')
% Passband gain line.
Hpass = 1 + ( 2*R1 ./ Rg );
hold on, plot([f(1) f(end)], [Hpass Hpass], 'k--'), hold off

box('off')
xlabel('Frequency (Hz)')
ylabel('Magnitude Response')
title('Wireless EMG I-Amp Circuit')

legend('Recorded data','Ideal')
Return
```

Appendix C: Graphical User Interface Used for Real Time Display

classdef EMG < matlab.apps.AppBase

```
    % Properties that correspond to app components
    properties (Access = public)
        UIFigure                matlab.ui.Figure
        UIAxes                  matlab.ui.control.UIAxes
        StartButton             matlab.ui.control.Button
        StopButton              matlab.ui.control.Button
        PathEditFieldLabel      matlab.ui.control.Label
        PathEditField           matlab.ui.control.EditField
        InitiateButton          matlab.ui.control.Button
        SlaveAddressEditFieldLabel  matlab.ui.control.Label
        SlaveAddressEditField   matlab.ui.control.EditField
        StateTextAreaLabel      matlab.ui.control.Label
        StateTextArea           matlab.ui.control.TextArea
        RecordSwitchLabel       matlab.ui.control.Label
        RecordSwitch            matlab.ui.control.Switch
        COMEditFieldLabel       matlab.ui.control.Label
        COMEditField            matlab.ui.control.NumericEditField
        FilenameEditFieldLabel  matlab.ui.control.Label
        FilenameEditField       matlab.ui.control.EditField
        Label                   matlab.ui.control.Label
        EditField               matlab.ui.control.EditField
        EditField_2Label        matlab.ui.control.Label
        EditField_2             matlab.ui.control.EditField
        EditField_3Label        matlab.ui.control.Label
        EditField_3             matlab.ui.control.EditField
        EditField_4Label        matlab.ui.control.Label
        EditField_4             matlab.ui.control.EditField
        EditField_5Label        matlab.ui.control.Label
        EditField_5             matlab.ui.control.EditField
        TimeSEditFieldLabel     matlab.ui.control.Label
        TimeSEditField          matlab.ui.control.NumericEditField
        Switch                  matlab.ui.control.Switch
    end


    properties (Access = private)
        EMGTimer % EMGTimer
        s%serial port
```

```
        first_tag = 0;
        unfinishedTail = [];
        BUFFER_SIZE = 8000;
        xLimits = [0 8000];
        yLimits = [0 2000];
        buffer1 = zeros(8000,1);%%plotting buffer
        A_tt = [];
        fid        %%file ID for data saved
%       h
        PlotLine        % Line object
        DurTime %%%%Duriation time
    end
    methods (Access = private)
        function  HCI_CMD(app,command)
            dec_t=hex2dec(command);
            fwrite(app.s,char(dec_t)');
            pause(0.5);
            while (app.s.BytesAvailable ~= 0)%%app.s.BytesAvailable
                [A_t,~] = fread(app.s,get(app.s,'BytesAvailable'));
                h=dec2hex(A_t);
                h_disp='';
                for i=1:length(h)
                    h_disp=[h_disp h(i,:) ' '];
                end
                app.StateTextArea.Value = [app.StateTextArea.Value;  h_disp];
                pause(0.5);
            end
        end
        function EMGTimerFcn(app, ~, event)
            while (app.s.BytesAvailable == 0)
                pause(0.001)
            end
            [app.A_tt,~] = fread(app.s);
            h=dec2hex(app.A_tt); %Weird stuff seems to happen on the first transmission.  Find an
identifiable ECG transmission to avoid weirdness.
            if(isempty(app.unfinishedTail) )
                firstHeadIndex = 1;
                while(~strcmp(h(firstHeadIndex,:),'04'))
                    firstHeadIndex = firstHeadIndex + 1;
                end
                h = h(firstHeadIndex:end, :);
            end
            [parsedStream, app.unfinishedTail] = parseLiveLogECG_noNotch(app.unfinishedTail,
h);
            decStream = hex2dec(parsedStream)
```

```matlab
%          decStream = parsedStream;


         if strcmp(app.RecordSwitch.Value , 'On')
            fwrite(app.fid,decStream,'single','ieee-be');
            if strcmp(app.Switch.Value , 'On')
               if app.DurTime >= 2000*app.TimeSEditField.Value
                  app.DurTime = 0;
                  StopButtonPushed(app, event);
%                  stop(app.EMGTimer);
               end
             app.DurTime = app.DurTime + length(parsedStream);
            end

         end
         app.buffer1 = [app.buffer1;decStream];
         if(length(app.buffer1)>app.BUFFER_SIZE)
            app.buffer1 = app.buffer1(end -(app.BUFFER_SIZE-1):end);
         end
%          plot(app.UIAxes,app.buffer1(:));
            app.PlotLine.YData= app.buffer1;
%            set(app.UIAxes,'xdata',app.buffer1);
%              set(app.h,'XData',app.buffer1);
%            drawnow;

      end

   end



   % Callbacks that handle component events
   methods (Access = private)

      % Code that executes after component creation
      function startupFcn(app)
         app.DurTime = 0;%%%initate
         app.PlotLine = plot(app.UIAxes,0:7999,zeros(1,8000));
         % Create timer object
         app.EMGTimer = timer(...
            'ExecutionMode', 'fixedSpacing', ...      % Run timer repeatedly
            'Period', 0.06, ...                    % Period is 0.06 seconds
            'BusyMode', 'queue',...              % Queue timer callbacks when busy
            'TimerFcn', @app.EMGTimerFcn);   % Callback that runs every period
      end
```

```matlab
    % Button pushed function: StartButton
    function StartButtonPushed(app, event)
        %
        %WRITE FOR ADCREAD = 01:00 for connection 0
        %%file save
        filepath = [app.PathEditField.Value '\' app.FilenameEditField.Value '.bin'];
        app.fid = fopen(filepath,'a');
%          fclose(app.fid);
        app.StateTextArea.Value = [app.StateTextArea.Value ; 'Write for ADC Read'];
        ADCREAD = [ '01';'92';'FD';'06';'00';'00';'32';'00';'01';'00'];
        dec_t=hex2dec(ADCREAD);
        fwrite(app.s,char(dec_t)');
        app.StateTextArea.Value = [app.StateTextArea.Value ;'End write for ADC read'];
        app.StartButton.Enable = 'off';
        app.StopButton.Enable = 'on';
        if strcmp(app.EMGTimer.Running, 'off')
            % Start timer
            start(app.EMGTimer);
        end
    end

    % Button pushed function: StopButton
    function StopButtonPushed(app, event)
        %%%
        stop(app.EMGTimer);
        app.StateTextArea.Value = [app.StateTextArea.Value ; 'Write for ADC stop'];
        ADCSTOP = [ '01';'92';'FD';'06';'00';'00';'32';'00';'00';'00'];
        dec_t=hex2dec(ADCSTOP);
        fwrite(app.s,char(dec_t)');
        app.StateTextArea.Value = [app.StateTextArea.Value ;'End write for ADC stop'];
        % Stop timer
        app.unfinishedTail = [];
        fclose('all');
        app.StartButton.Enable = 'on';
        app.StopButton.Enable = 'off';

    end

    % Button pushed function: InitiateButton
    function InitiateButtonPushed(app, event)
        try
            fclose(instrfind);%closes all current ports
        catch
        end
```

```matlab
        %%
        port = ['COM' num2str(app.COMEditField.Value)];
        app.s = serial(port);
        set(app.s,'BaudRate',921600,'Timeout',10,'FlowControl','none','Parity','none',
'InputBufferSize', 2048);
        fopen(app.s);

        %HCI reset
        app.StateTextArea.Value =[app.StateTextArea.Value ;'HCI Reset command'];
        %HCI_reset = [ '01';'1D';'FC';'01';'00'];%
        HCI_reset = [ '01';'03';'0C';'00'];
        HCI_CMD(app,HCI_reset);
        app.StateTextArea.Value = [app.StateTextArea.Value ; 'End HCI Reset Command'];

        %GAP_initialize
        app.StateTextArea.Value = [app.StateTextArea.Value ;'GAP Initialize Command'];
        %GAP_initialise=['01';'00';'FE';'08';'08';'00';'00';'00';'00';'00';'00';'00'];
        GAP_initialise=['01';'00';'FE';'26';'08';'03';'00';'00';'00';'00';'00';'00';'00'
            '00';'00';'00';'00';'00';'00';'00';'00';'00';'00';'00';'00';'00'
            '00';'00';'00';'00';'00';'00';'00';'00';'00';'00';'00';'00';'01'
            '00';'00';'00'];
        HCI_CMD(app,GAP_initialise);
        app.StateTextArea.Value = [app.StateTextArea.Value ;'End Gap Initialize Command'];

        %check interval
%        app.StateTextArea.Value = [app.StateTextArea.Value ;'Interval Commands'];
%        TGAP_CONN_EST_INT_MIN = [
'01';'61';'FE';'02';'01';'02'];%TGAP_CONN_EST_INT_MIN = [ '01';'31';'FE';'01';'15'];
%        HCI_CMD(app,TGAP_CONN_EST_INT_MIN);
%        TGAP_CONN_EST_INT_MAX = [
'01';'61';'FE';'02';'01';'03'];%TGAP_CONN_EST_INT_MAX = [ '01';'31';'FE';'01';'16'];
%        HCI_CMD(app,TGAP_CONN_EST_INT_MAX);
%        TGAP_CONN_EST_LATENCY = [
'01';'61';'FE';'02';'01';'04'];%TGAP_CONN_EST_LATENCY = [ '01';'31';'FE';'01';'1A'];
%        HCI_CMD(app,TGAP_CONN_EST_LATENCY);
%        TGAP_CONN_EST_SUPERV_TIMEOUT = [
'01';'61';'FE';'02';'01';'05'];%TGAP_CONN_EST_SUPERV_TIMEOUT = [
'01';'31';'FE';'01';'19'];
%        HCI_CMD(app,TGAP_CONN_EST_SUPERV_TIMEOUT);
%        app.StateTextArea.Value = [app.StateTextArea.Value ;'End Interval Commands'];
%        %change interval to 20ms
%        app.StateTextArea.Value = [app.StateTextArea.Value ;'change Interval Commands'];
%        TGAP_CONN_EST_INT_MIN_C = [ '01';'60';'FE';'04';'01';'02';'0C';'00'];
%        HCI_CMD(app,TGAP_CONN_EST_INT_MIN_C);
```

```
%          TGAP_CONN_EST_INT_MAX_C = [ '01';'60';'FE';'04';'01';'03';'0C';'00'];
%          HCI_CMD(app,TGAP_CONN_EST_INT_MAX_C);
%          TGAP_CONN_EST_LATENCY_C = [ '01';'60';'FE';'04';'01';'04';'00';'00'];
%          HCI_CMD(app,TGAP_CONN_EST_LATENCY_C);
%          TGAP_CONN_EST_SUPERV_TIMEOUT_C = [ '01';'60';'FE';'04';'01';'05';'D0';'07'];
%          HCI_CMD(app,TGAP_CONN_EST_SUPERV_TIMEOUT_C);
%          app.StateTextArea.Value = [app.StateTextArea.Value ;'End change Interval
Commands'];

        %Establish Connection
          app.StateTextArea.Value = [app.StateTextArea.Value ;'Establish Connection'];
          GAP_EstablishLinkRequest= ['01'; '09'; 'FE'; '09'; '00'; '00'; '00'; app.EditField.Value;
app.EditField_2.Value; app.EditField_3.Value; app.EditField_4.Value; app.EditField_5.Value;
app.SlaveAddressEditField.Value];
          %GAP_EstablishLinkRequest= ['01'; '62'; 'FE'; '0A'; '00';  app.EditField.Value;
app.EditField_2.Value; app.EditField_3.Value; app.EditField_4.Value; app.EditField_5.Value;
app.SlaveAddressEditField.Value; '01'; '00';'00'];
%          GAP_EstablishLinkRequest= ['01'; '09'; 'FE'; '09'; '00'; '00'; '00'; 'E8'; '39';
'83'; '0E'; '6C'; '54'];
          HCI_CMD(app,GAP_EstablishLinkRequest);
%            if (length(app.StateTextArea.Value{end}) < 30)
%                app.InitiateButton.BackgroundColor = [0.9412 0.3098 0.3098];
%            end
          app.StateTextArea.Value = [app.StateTextArea.Value ;'End Establish Connection'];
          %set connection interval to 15ms
          HCIExt_SetConnetion_15 = [
'01';'11';'FE';'0A';'00';'00';'0C';'00';'0C';'00';'00';'00';'D0';'07'];
          HCIExt_SetConnetion_60 = [
'01';'11';'FE';'0A';'00';'00';'30';'00';'30';'00';'00';'00';'D0';'07'];
          HCI_CMD(app,HCIExt_SetConnetion_15);
          app.StateTextArea.Value = [app.StateTextArea.Value ;'change Connection 1 interval
to 15ms'];
%          %SET DATALENGTH  for connection 0
%          app.StateTextArea.Value = [app.StateTextArea.Value ;'SET_DATALENGTH'];
%          ATT_ExchangeMTUReq = [ '01';'22';'20';'06';'00';'00';'FB';'00';'48';'08'];
%          HCI_CMD(app,ATT_ExchangeMTUReq);
%          app.StateTextArea.Value = [app.StateTextArea.Value ;'End
SET_DATALENGTH'];

          %SET ATT_ExchangeMTUReq = 251 for connection 0
          app.StateTextArea.Value = [app.StateTextArea.Value ;'ExchangeMTUReq'];
          ATT_ExchangeMTUReq = [
'01';'02';'FD';'04';'00';'00';'FB';'00'];%ATT_ExchangeMTUReq = [
'01';'02';'FD';'04';'00';'00';'FB';'00'];
          HCI_CMD(app,ATT_ExchangeMTUReq);
```

```
            %DISCOVER ALL UUID for connection 0
            app.StateTextArea.Value =[app.StateTextArea.Value ;'Discover UUIDs'];
            UUID = [ '01';'90';'FD';'02';'00';'00'];
            HCI_CMD(app,UUID);
            DiscoverAllChar = [ '01';'84';'FD';'06';'00';'00';'01';'00';'FF';'FF'];
            HCI_CMD(app,DiscoverAllChar);
            app.StateTextArea.Value =[app.StateTextArea.Value ;'End Discover UUIDs'];
            %%%%read gua default value
%              for i = 1:5
%                  app.StateTextArea.Value =[app.StateTextArea.Value ;'read gua default value'];
%                  GUA = ['01';'8C';'FD';'06';'00';'00';'37';'00';'00';'00'];
%                  HCI_CMD(app,GUA);
%                  app.StateTextArea.Value =[app.StateTextArea.Value ;'End read gua default
value'];
%              end
         app.InitiateButton.Enable = 'off';
         app.StartButton.Enable = 'on';
       end


       % Value changed function: RecordSwitch
       function RecordSwitchValueChanged(app, event)
          value = app.RecordSwitch.Value;

       end
    end

    % Component initialization
    methods (Access = private)

       % Create UIFigure and components
       function createComponents(app)

          % Create UIFigure and hide until all components are created
          app.UIFigure = uifigure('Visible', 'off');
          app.UIFigure.Position = [100 100 639 483];
          app.UIFigure.Name = 'UI Figure';

          % Create UIAxes
          app.UIAxes = uiaxes(app.UIFigure);
          title(app.UIAxes, 'EMG')
          xlabel(app.UIAxes, 'Time')
          ylabel(app.UIAxes, 'Volt')
          app.UIAxes.XLim = [0 8000];
          app.UIAxes.YLim = [0 4000];
          app.UIAxes.Box = 'on';
```

```
app.UIAxes.YTick = [0 500 1000 1500 2000 2500 3000 3500 4000];
app.UIAxes.XGrid = 'on';
app.UIAxes.YGrid = 'on';
app.UIAxes.Position = [11 57 610 306];

% Create StartButton
app.StartButton = uibutton(app.UIFigure, 'push');
app.StartButton.ButtonPushedFcn = createCallbackFcn(app, @StartButtonPushed, true);
app.StartButton.Enable = 'off';
app.StartButton.Position = [165 375 100 22];
app.StartButton.Text = 'Start';

% Create StopButton
app.StopButton = uibutton(app.UIFigure, 'push');
app.StopButton.ButtonPushedFcn = createCallbackFcn(app, @StopButtonPushed, true);
app.StopButton.BusyAction = 'cancel';
app.StopButton.Enable = 'off';
app.StopButton.Position = [276 375 100 22];
app.StopButton.Text = 'Stop';

% Create PathEditFieldLabel
app.PathEditFieldLabel = uilabel(app.UIFigure);
app.PathEditFieldLabel.HorizontalAlignment = 'right';
app.PathEditFieldLabel.Position = [51 443 30 22];
app.PathEditFieldLabel.Text = 'Path';

% Create PathEditField
app.PathEditField = uieditfield(app.UIFigure, 'text');
app.PathEditField.Position = [96 443 505 22];
app.PathEditField.Value = 'C:\Users\athen\OneDrive\Desktop\C TERM 2021
Couses\MQP\HE WANG_CODE_BOTH_UPDATES\EMG-ECG_wireless-
main\Matlab_code_no_notch\test_results_no_notch';

% Create InitiateButton
app.InitiateButton = uibutton(app.UIFigure, 'push');
app.InitiateButton.ButtonPushedFcn = createCallbackFcn(app, @InitiateButtonPushed,
true);
app.InitiateButton.Position = [57 375 100 22];
app.InitiateButton.Text = 'Initiate';

% Create SlaveAddressEditFieldLabel
app.SlaveAddressEditFieldLabel = uilabel(app.UIFigure);
app.SlaveAddressEditFieldLabel.HorizontalAlignment = 'right';
app.SlaveAddressEditFieldLabel.Position = [219 410 83 22];
app.SlaveAddressEditFieldLabel.Text = 'Slave Address';
```

```
% Create SlaveAddressEditField
app.SlaveAddressEditField = uieditfield(app.UIFigure, 'text');
app.SlaveAddressEditField.Position = [309 410 25 22];
app.SlaveAddressEditField.Value = 'B0';

% Create StateTextAreaLabel
app.StateTextAreaLabel = uilabel(app.UIFigure);
app.StateTextAreaLabel.HorizontalAlignment = 'right';
app.StateTextAreaLabel.Position = [35 34 34 22];
app.StateTextAreaLabel.Text = 'State';

% Create StateTextArea
app.StateTextArea = uitextarea(app.UIFigure);
app.StateTextArea.Editable = 'off';
app.StateTextArea.Position = [84 7 524 51];

% Create RecordSwitchLabel
app.RecordSwitchLabel = uilabel(app.UIFigure);
app.RecordSwitchLabel.HorizontalAlignment = 'center';
app.RecordSwitchLabel.Position = [548 402 44 22];
app.RecordSwitchLabel.Text = 'Record';

% Create RecordSwitch
app.RecordSwitch = uiswitch(app.UIFigure, 'slider');
app.RecordSwitch.ValueChangedFcn = createCallbackFcn(app,
@RecordSwitchValueChanged, true);
app.RecordSwitch.Position = [553 423 33 14];

% Create COMEditFieldLabel
app.COMEditFieldLabel = uilabel(app.UIFigure);
app.COMEditFieldLabel.HorizontalAlignment = 'right';
app.COMEditFieldLabel.Position = [156 410 33 22];
app.COMEditFieldLabel.Text = 'COM';

% Create COMEditField
app.COMEditField = uieditfield(app.UIFigure, 'numeric');
app.COMEditField.Position = [192 410 24 22];
app.COMEditField.Value = 11;

% Create FilenameEditFieldLabel
app.FilenameEditFieldLabel = uilabel(app.UIFigure);
app.FilenameEditFieldLabel.HorizontalAlignment = 'right';
app.FilenameEditFieldLabel.Position = [37 410 58 22];
app.FilenameEditFieldLabel.Text = 'File name';
```

```
% Create FilenameEditField
app.FilenameEditField = uieditfield(app.UIFigure, 'text');
app.FilenameEditField.Position = [107 410 50 22];
app.FilenameEditField.Value = 'Sample';

% Create Label
app.Label = uilabel(app.UIFigure);
app.Label.HorizontalAlignment = 'right';
app.Label.Position = [482 410 10 22];
app.Label.Text = ':';

% Create EditField
app.EditField = uieditfield(app.UIFigure, 'text');
app.EditField.Position = [496 410 25 22];
app.EditField.Value = '15';

% Create EditField_2Label
app.EditField_2Label = uilabel(app.UIFigure);
app.EditField_2Label.HorizontalAlignment = 'right';
app.EditField_2Label.Position = [444 410 10 22];
app.EditField_2Label.Text = ':';

% Create EditField_2
app.EditField_2 = uieditfield(app.UIFigure, 'text');
app.EditField_2.Position = [458 410 25 22];
app.EditField_2.Value = 'FC';

% Create EditField_3Label
app.EditField_3Label = uilabel(app.UIFigure);
app.EditField_3Label.HorizontalAlignment = 'right';
app.EditField_3Label.Position = [406 410 10 22];
app.EditField_3Label.Text = ':';

% Create EditField_3
app.EditField_3 = uieditfield(app.UIFigure, 'text');
app.EditField_3.Position = [420 410 25 22];
app.EditField_3.Value = '69';

% Create EditField_4Label
app.EditField_4Label = uilabel(app.UIFigure);
app.EditField_4Label.HorizontalAlignment = 'right';
app.EditField_4Label.Position = [371 410 10 22];
app.EditField_4Label.Text = ':';
```

```matlab
        % Create EditField_4
        app.EditField_4 = uieditfield(app.UIFigure, 'text');
        app.EditField_4.Position = [385 410 25 22];
        app.EditField_4.Value = '22';

        % Create EditField_5Label
        app.EditField_5Label = uilabel(app.UIFigure);
        app.EditField_5Label.HorizontalAlignment = 'right';
        app.EditField_5Label.Position = [333 410 10 22];
        app.EditField_5Label.Text = ':';

        % Create EditField_5
        app.EditField_5 = uieditfield(app.UIFigure, 'text');
        app.EditField_5.Position = [347 410 25 22];
        app.EditField_5.Value = '91';

        % Create TimeSEditFieldLabel
        app.TimeSEditFieldLabel = uilabel(app.UIFigure);
        app.TimeSEditFieldLabel.HorizontalAlignment = 'right';
        app.TimeSEditFieldLabel.Position = [440 372 48 22];
        app.TimeSEditFieldLabel.Text = 'Time(S)';

        % Create TimeSEditField
        app.TimeSEditField = uieditfield(app.UIFigure, 'numeric');
        app.TimeSEditField.Position = [497 372 24 22];
        app.TimeSEditField.Value = 20;

        % Create Switch
        app.Switch = uiswitch(app.UIFigure, 'slider');
        app.Switch.Items = {'Inf', 'On'};
        app.Switch.Position = [548 375 38 17];
        app.Switch.Value = 'Inf';

        % Show the figure after all components are created
        app.UIFigure.Visible = 'on';
    end
end

% App creation and deletion
methods (Access = public)

    % Construct app
    function app = EMG

        % Create UIFigure and components
```

```matlab
        createComponents(app)

        % Register the app with App Designer
        registerApp(app, app.UIFigure)

        % Execute the startup function
        runStartupFcn(app, @startupFcn)

        if nargout == 0
            clear app
        end
    end

    % Code that executes before app deletion
    function delete(app)

        % Delete UIFigure when app is deleted
        delete(app.UIFigure)
    end
  end
end
```

Appendix D: Bill of Materials - Wired EMG

Table 1:
* Be sure to account for extra components incase some break or are faulty*

Category	Package	Value/ Name	PCB Designator	Qty/Unit	Manufacturer
Main Board	Osh Park	-	-	3 -(3 boards came with one order)	OSH Park
Resistors	¼ Watt Rating	1 MΩ	R1, R16, R19, R20, R31, R38, R39, R50, R57, R58, R69, R76	12	Vishay Dale (Digikey)
Resistors	¼ Watt Rating (Through hole)	91 kΩ	R3, R22, R41 R60	4	Yageo (Digikey)
Resistors	¼ Watt Rating (Through hole)	10 kΩ	R4, R24, R43, R62 (Additional resistors used for selectable gain switch)	8	Vishay Dale (Digikey)
Resistors	¼ Watt Rating (1%) (Through hole)	280 kΩ	R2, R21, R40, R59	4	Yageo (Digikey)
Resistors	¼ Watt Rating (Through hole)	412 kΩ	R7, R26, R45, R64	4	Stackpole Electronics Inc (Digikey)
Resistors	¼ Watt Rating (Through hole)	62 kΩ	R6, R25, R44, R63	4	Yageo (Digikey)

Resistors	¼ Watt Rating (Through hole)	300 kΩ	R8, R32, R51, R70(Additional resistors are used for selectable gain)	8	Yageo (Digikey)
Resistors	¼ Watt Rating (Through hole)	100 kΩ	R10, R11, R12, R13, R27, R28, R29, R30, R46, R47, R48, R49. R65, R66, R67, R68 (Additional resistors are used for selectable gain)	20	TE Connectivity Passive Product (Digikey)
Resistors	¼ Watt Rating	43 kΩ	Used for Selectable Gain Switch	4	Yageo (Digikey)
Resistors	¼ Watt Rating (Through hole)	20 kΩ	Used for Selectable Gain Switch	4	Vishay Dale (Digikey)
Resistors	¼ Watt Rating (Through hole)	30 kΩ	R5, R23, R42, R61	4	Yageo (Digikey)
Capacitors	50 V	68 nF	C1, C2, C3, C4, C11, C12, C13, C14, C21, C22, C23, C24, C31, C32, C33,C34	16	KEMET (Digikey)
Capacitors	50 V	1 μF	C5, C20, C30, C40	4	KEMET (Digikey)
Capacitors	50 V	2.15 nF	C5, C20, C30, C40	4	KEMET (Digikey)
Capacitors	50 V	1.84 nF	C6, C15, C25, C35	4	TDK Corporation (Digikey)
Capacitors	50 V	5.2 nF	C7, C16, C26, C36	4	KEMET (Digikey)

Capacitors	50 V	0.76 nF	C8, C17, C27, C37,	4	TDK Corporation (Digikey)
Capacitors	50 V	159 nF	C9, C10, C18, C19, C28, C29, C38, C39	8	KEMET (Mouser)
Capacitors	Electrolytic Decoupling	100 µF	C41,C42	2	Sparkfun
IC's	14-Lead DIP	AD713NJ	IC1, IC2, IC3, IC4, IC5, IC6, IC7, IC8	8	Analog Devices
DIP Sockets	14		IC1, IC2, IC3, IC4, IC5, IC6, IC7, IC8	8	
Switches	DSP9111AK2	Thumbwheel switch decimal	J4, J5, J6, J7	4	APEM Inc (Digikey)
Connectors	VHR-3N (3.96 mm)	3-Pin Rectangular Connector	J1	1	JST Sales America
Connectors	VHR-6N (3.96 mm)	3-Pin Rectangular Connector	J3	1	JST Sales America
Screw terminals	3.5mm pitch	Screw Terminal Block	J4	3	Sparkfun
Connectorsand Wires Kit	Wires Kit	-	-	1	Pulsivo Store (Amazon)
Enclosure	Junction Box	15x11x5.1	-	1	Qilipsu (Amazon)
Crimping Tool Kit	Connectors Kit	JST Connectors for AWG 2620	-	1	Qibaok (Amazon)

Appendix E: Bill of Materials - Wireless Systems

* Be sure to account for extra components incase some break or are faulty*

Category	Package	Value/ Name	Qty/Unit	Manufacturer
Main Boards	Osh Park	-	2 sets of 3 -(3 boards came with one order)	OSH Park
Resistors	¼ Watt Rating	1 MΩ	4	WPI ECE Shop
Resistors	¼ Watt Rating (Through hole)	940 kΩ	1	WPI ECE Shop
Resistors	¼ Watt Rating (Through hole)	10 kΩ	1	WPI ECE Shop
Resistors	¼ Watt Rating (Through hole)	1 kΩ	4	WPI ECE Shop
Resistors	¼ Watt Rating (Through hole)	20 kΩ	1	WPI ECE Shop
Resistors	¼ Watt Rating (Through hole)	12 kΩ	1	WPI ECE Shop
Resistors	¼ Watt Rating (Through hole)	2 kΩ	1	WPI ECE Shop
Resistors	¼ Watt Rating (Through hole)	750 kΩ	1	WPI ECE Shop
Resistors	¼ Watt Rating (Through hole)	91 kΩ	1	WPI ECE Shop
Resistors	¼ Watt Rating (Through hole)	6.8 kΩ	1	WPI ECE Shop
Resistors	¼ Watt Rating (Through hole)	121 kΩ	1	WPI ECE Shop

Resistors	¼ Watt Rating (Through hole)	200 kΩ	3	WPI ECE Shop
Resistors	¼ Watt Rating (Through hole)	75 kΩ	4	WPI ECE Shop
Resistors	¼ Watt Rating (Through hole)	50 kΩ	2	WPI ECE Shop
Resistors	¼ Watt Rating (Through hole)	100 kΩ	3	WPI ECE Shop
Resistors	¼ Watt Rating	43 kΩ	2	WPI ECE Shop
Resistors	¼ Watt Rating (Through hole)	300 Ω	2	WPI ECE Shop
Resistors	¼ Watt Rating (Through hole)	100 Ω	2	WPI ECE Shop
Capacitors	50 V	0.1 µF	8	WPI ECE Shop
Capacitors	50 V	1 µF	3	WPI ECE Shop
Capacitors	50 V	159 pF	2	WPI ECE Shop
Capacitors	50 V	10 nF	1	WPI ECE Shop
Capacitors	50 V	22 nF	1	WPI ECE Shop
Capacitors	Electrolytic Decoupling	100 µF	1	WPI ECE Shop
IC's	14-Lead DIP	AD713JN	2	Analog Devices
Instrumentation Amplifier	8-Lead DIP	AD620	2	Analog Devices
Voltage Reference	3-Lead DIP	LM317LZ	2	STMicroelectronics (DigiKey)
DIP Socket	14		2	WPI ECE Shop
DIP Socket	8		2	WPI ECE Shop
Connectors	Connector Header Through Hole 4	MTA Connectors	4	WPI ECE Shop

Appendix F: Link for Wired EMG Testing With Prosthetic Hand

https://drive.google.com/file/d/1ETDdx-nJUngXdmqdILdZLk6MVo2k4CHp/view?usp=sharing